A General Methodology for Inferring Failure Propagation Process from Post-disaster Disruptions Data

Xiangyang Guan

A dissertation
submitted in partial fulfillment of the
requirements for the degree of

Doctor of Philosophy

University of Washington
2018

Reading Committee:
Cynthia Chen, Chair
Ying Chen
Michael Gabbay

Program Authorized to Offer Degree:
Civil and Environmental Engineering

University of Washington

Abstract

A General Methodology for Inferring Failure Propagation Process
from Post-disaster Disruptions Data

Xiangyang Guan

Chair of the Supervisory Committee:
Cynthia Chen, Professor
Department of Civil and Environmental Engineering

Cascading failures, where failures propagate from an initially small portion of a system to a much larger portion or even the entire system, are ubiquitous phenomenon in a number of natural, social and technical systems, and have seen instances in the formation of large-scale disasters such as the recent devastations caused by Hurricanes Harvey, Irma and Maria. Understanding and ultimately controlling the dynamics of cascading failures are critical for securing the functionality of those systems, and ensuring the wellbeing of the people and the society. This, however, is a challenging task due to the complexities in the cascading failure dynamics.

In this dissertation, a novel methodology to model, infer and reconstruct cascading failure dynamics is proposed, tested and validated. A survival-analysis-based formulation is derived to mathematically describe how external factors and failure propagations give rise to observed failure outcomes, and maximum likelihood estimation is employed to estimate the model parameters. With the estimated parameters, cascading failure dynamics, including the temporal-spatial patterns of failure spreading and node-to-node failure propagation patterns, are reconstructed. This approach is applied to four simulation studies: (a) cascading failures in

interdependent power and transportation networks in New York City (NYC) during Hurricane Sandy; (b) a hypothetical influenza epidemic in NYC; (c) a congestion cascade scenario in the Sioux-Falls benchmark network; and (d) cascading power outages in the Wood-Wollenberg 6-bus benchmark system. The inference results returned by the proposed approach and simulation results are compared for each simulation study. All comparisons in the simulation studies return consistent patterns between the inferred cascading failure dynamics and simulated cascading failure dynamics, suggesting the accuracy, robustness and generalizability of the proposed methodology.

This dissertation demonstrates strong potential of broad impact both within and beyond the domain of civil engineering. The civil infrastructure systems like transportation and power are constantly under the threat of cascading failures. A methodology for understanding the cascading failure dynamics, especially the node-to-node failure propagation patterns that have been overlooked in existing research, will open a channel to more efficiently enhancing the resilience of infrastructure systems against malfunctioning and assisting emergency response to effectively contain the impact of disruptive events such as natural disasters, terrorist attacks and internal performance fluctuations. More broadly, cascading failures are also observed in a number of other disciplines such as information science, social science, epidemiology, biology and physics. Researchers in those disciplines are faced with similar challenges in learning cascading failure dynamics. The present research constructs a universal methodological framework for understanding and controlling cascading failures, which is applicable to a broad range of systems studied by researchers from various disciplines. It thus will potentially facilitate the inter-disciplinary communications that will foster more efficient and high-impact research in each of

the individual fields.

TABLE OF CONTENTS

Page

LIST OF FIGURES

LIST OF TABLES

ACKNOWLEDGMENTS

This dissertation documents a body of two research projects funded by the National Science Foundation (NSF) under award number CMMI # 1536340 and the National Institutes of Health (NIH) under award number 1R01GM108731-01A1. The funding support from NSF and NIH is greatly appreciated.

I would like to thank my advisor Professor Cynthia Chen. Her knowledge, expertise, professionalism, wisdom and sense of responsibility inspired and guided me through my Ph.D. study. The help and insights she provided to my research are invaluable and indispensable for me to finish my Ph.D. study. Through working with her in the last five years, I learned not only how to do research well, but also how to think about and solve a problem in general.

I also want to express my sincere thanks to my dissertation committee, Professor Cynthia Chen, Professor Michael Gabbay, Professor Thomas Richardson and Professor Ying Qing Chen. The constructive and insightful advice from them provides great help to me in designing and conducting my doctoral research. They created a friendly, independent and collaborative research atmosphere which I enjoyed throughout my Ph.D. study.

I also want to thank my family and friends. Their company and encouragement have always been a motivation for me to move forward.

Dedicated to my parents，

Tongxin Guan and Jinxiu Hou

Section 1
Introduction and Motivation

1.1. Cascading failures: a real threat

Cascading failures are incidents in which failures of certain nodes (e.g. an infrastructure facility that provides lifeline service to a community) increase the susceptibility of other nodes, resulting in a spreading process of failures from an initial small set of nodes to a much larger set. It is a both old and new concept. The earliest account of cascading failures goes back to the investigation report of the 1965 Northeast blackout [1, 2], when they were first observed in the power grid. The blackout took place when faulty tripping of a heavily loaded transmission line in Ontario, Canada initialized a cascade of failures in which the power flow shifted from failed transmission lines to working lines, overloaded the working lines and lead to additional failures. The failed transmission lines also cut the path for the generated power in Ontario to travel north, and as a result the power surged south into the state of New York, causing the power grid in New York to become overloaded. Failed transmission lines due to overloading made the Northeastern power grid in the U.S. fragmented into isolated “islands”. Imbalance between power generation and consumption in each of the islands ultimately shut down the power systems in the islands. About 30 million people in Ontario, New York, Connecticut, Rhode Island, Massachusetts, Vermont, New Hampshire, New Jersey and Pennsylvania were without power for up to 13 hours due to the blackout [2]. Then the story repeated itself in August 14, 2003, when a blackout struck the northeastern United States, affecting 50 million people in the states of Ohio, Michigan, Pennsylvania, New York, Vermont, Massachusetts, Connecticut, New Jersey and the Canadian province of Ontario [3]. Later investigation of the blackout reveals this disaster as a consequence of cascading failures: the initial incident was just a power line tripping due to touching trees in northeast Ohio; however, the

unbalanced grid and redistribution of power flow led to overloaded transmission lines and further failures, first locally in northeast Ohio and then propagating to a major proportion of the Eastern Interconnection [4]. Similar cascading failures, which resulted from load redistributions and imbalanced power grid, are also blamed for the large-scale blackouts in the U.S. on August 10, 1996, October 10, 1993 and February 29, 1984, each with more than two million people affected [5, 6]. In fact, researchers found that the formation process of all large-scale blackouts involves cascading failures which progress rapidly [6].

Cascading failures were also recorded in other infrastructure systems besides the power grid. On January 15, 1990, an AT&T phone call switch located in New York City (NYC) experienced internal failure. It recovered shortly but sent wrong signals to switches linked to it. Those switches receiving the signal were shut down, and continued the process to send wrong signals to switches further connected to them. The consequence was a nation-wide failure of AT&T phone network that crashed 114 switching nodes for 9 hours with a loss of at least $60 million [7-9]. Another example of cascading failures that underlie our everyday life is the propagation of congestions [10-13]. In transportation for example, a completely congested road network (a.k.a. gridlock) typically stems from congestion at a single intersection or highway segment, e.g. at the bottleneck [14-16]. The congestion on the bottleneck link propagates either through extending queues upstream from link to link [15, 17, 18] or by prompting rerouting of vehicles which renders other links overloaded and congested [19-21], and ultimately could develop into an region-wide gridlock. All the cases of cascading failures described above share one commonality: such failures propagate within a single network under a process governed by certain mechanisms such as faulty control or flow redistribution. We term these cases as *Type I* cascading failures.

It is only recently that another type of cascading failures started to attract scientists' attentions when the 2003 blackout in Italy was revisited. It is a matter of fact that, firstly the power grids are not the only infrastructures affected in the blackouts, which also stressed or disabled systems like transportation, telecommunication and water and sewage systems [5]; and secondly the cascading failures in the power grids alone would not have caused large-scale blackouts such as the one in Italy on September 28, 2003 [22, 23]. Since Buldyrev et al. [24] first described the 2003 Italy blackout as the consequence of cascading failures between the power network and the Internet network, a number of studies [24-32] have established a new frontier: cascading failures in a multi-network system. It focuses on one particular scenario of cascading failures: if two or more networks are mutually dependent on each other, failure of a small portion of nodes in one network could propagate back and forth among the networks, and eventually leads to failure of the entire system. We term this scenario as *Type II* cascading failures. Though recent advances in this field are directed toward developing theoretical/mathematical models instead of capturing the cascading failure phenomenon in real world, cascading failures in multi-network systems did substantiate themselves in a few situations. Among them are tragic disasters like Hurricane Katrina and Hurricane Sandy.

Hurricane Katrina is a notorious example in which inefficient emergency response led to the failure of multiple functions of the society in New Orleans [33, 34]. And cascading failures contributed much to it [35]. On the morning of August 29, 2005, everything seemed still under control until major levee breaches starting at approximately 9:00 am [36]. Within hours, about 80% of the city was under water with depth from 5 cm to 5 m [37]. The floods first knocked out the power supply

to the city. As of August 30, Louisiana, Mississippi and Alabama reported more than 2.4 million customers without power, primarily from extensive flooding [38]. Failures of water supply and the sewage system followed as the power outages shut down more than 1,000 drinking water facilities and 172 sewage treatment plants in the region [39]. The power outages also interrupted the operation of three major oil pipelines – the Colonial, Plantation, and Capline Pipelines – halting roughly 90% of region's oil production, which accounted for 10% of the country's gasoline supply [40]. This led to not only in New Orleans but also a nationwide fuel shortage [41]. The fuel shortage, together with a flooding-incapacitated transportation system, in turn further aggravated the power failures as refueling for the backup generators in some facilities was disabled due to inaccessibility to the refueling trucks [42, 43]. The cascading failures not only left tremendous devastation to the region, but also complicated the recovery, as inaccessible transportation slowed down the influx of repair crews for other lifelines such as the damaged power grid [44]. The story during Hurricane Sandy is similar. Characterized by its record-high storm surges, Sandy delivered massive flooding to New York City. Widespread power outages across the city were reported by the night of October 29, 2012 due to submerged power stations and broken lines taken down by the high wind [45]. Lack of power disabled the pumping system designed with the subway lines, making ways for the storm water to enter the subway tunnels [46]. Shortly after Sandy's landfall, the subway tunnels in Southern Manhattan, Long Island City, Red Hook, Hoboken, and Jersey City, as well as the eight ones that connect Queens and Brooklyn with Manhattan, were under water [45]. The collapse of power supply also affected the energy infrastructures. Two of the six refineries that serve NYC were shutdown with the other four operating at reduced capacities, sending a city-wide fuel shortage [47, 48]. The fuel shortage exacerbated tunnel flooding in the subway system, as subway crew were turning to diesel-fueled pumps in place of the electricity-

fueled pumps due to power outages [46]. Cascading failures also took place in the service restoration in the aftermath [49]. The suspended subway service, limited road accessibility and disabled ferry terminals created gridlocks on October 30 and November 1, which delayed transporting crews to repair the crippled power and subway system [45, 48, 49]. Another example of cascading failures during service restoration is that by November 1, some subway service had been restored in Manhattan and Queens, and tunnels for line 4, 5 and F were clear of flooding and ready to run. However, these segments of the subway system were not fully operational until November 3 when Con Edison brought back the power [46]. The situation became essentially a chicken-or-the-egg dilemma: improving the transportation services requires a functional power system, while restoring the power system function needs transportation services [49].

The above cases show that cascading failures of both type I and type II are recurring throughout the history, even when considerable effort has been made to enhance the safety and resilience of our infrastructures since 9/11 attacks [50]. The reasons why cascading failures are ubiquitous even in a well-protected infrastructure system are two folds. The internal factor is the increasing complexity of our infrastructure systems. In the last two decades, it is not only the sizes of the infrastructure systems that have increased, but also the connections in an infrastructure system as well as their interactions with other systems. The complexity fostered by interconnections within and between infrastructure systems leads to nonlinear and often unpredicted behaviors of the infrastructures [51]. As a result, when existing issues, usually identified through catastrophic events, are solved, new ones emerge. One example is the interdependencies between cyber infrastructures and physical infrastructures. The 2003 Italy Blackout is essentially a type II cascading failure between the power grid and the Internet communication system in Italy [24, 52].

This new failure scenario, different from the Northeast Blackout in America one and a half month ago and any other blackout before it due to the involvement of cyber infrastructures, incapacitated the traditional protection measures for power grids at that time [53]. The process of increasing complexities of our infrastructures is and will be never ending, as new components of the infrastructure systems to support electrification (e.g. fast-charging facilities) and automation (e.g. communication infrastructures) that are currently trending in the transportation society [54-56], and consequently additional interdependencies between these components and existing infrastructures, will be built. In addition to the complexities in infrastructure systems, external factors such as climate changes are also bringing challenges. It is expected that global warming will bring more furious extreme weather conditions like more powerful hurricanes [57-59]. Together with sea level rise, future hurricanes could push the coastal flooding beyond the expected and what people have prepared for [60]. Therefore, it is never secure to take that our society is safe from cascading failures, when both internal and external factors are contributing to the tremendous potential of future cascading failures. They have been and will continue to be grave threats to the wellbeing of the infrastructure systems and consequently the society that those infrastructures support.

1.2. Understanding the dynamics of cascading failures

Given the grave impacts of cascading failures on infrastructure systems and our society, understanding the formation of cascading failures, that is, how failures of an initial, small set of nodes propagate through a single network (type I) or interdependent networks (type II) is a main challenge faced in designing and managing infrastructure systems [61, 62]. Driven by the 1965 Northeast blackout, type I cascading failures have been drawing researchers' attention right since

mid-1960s [63]. These studies, focusing on the reasons and mechanisms of archived blackouts, however are mostly descriptive and observational on a case-to-case basis prior to late 1990s [64-66], in an effort toward developing preventive strategies against the recurrence of similar cases [6, 67]. The emergence of network science in late 1990s and early 2000s offers a channel for analytical studies of cascading failures. The first mathematical model of cascading failures is proposed by Parrilo et al. [68], who modeled the failure scenario of breaking the synchronous state in a power network due to frequency variations. This failure scenario is common in the power network but could encounter difficulties in its application to other systems due to the uniqueness of the performance measures and mechanisms this scenario employs to the power network [6]. The first cascading failure model that is set in a general context is devised by Watts [69]. His model, which focuses on evaluating the conditions for cascading failures to happen and the final sizes cascading failures can reach (i.e. the number of failed nodes at the end of a cascading failure process), applies to not only infrastructure networks but also all kinds of other networks [69], and thus points to the potential of a unified type I cascading model. Watts' model however, is constructed on unweighted networks, which are different from most infrastructure networks that carry flows [70-72]. Pilot efforts to model the flow redistribution dynamics in (type I) cascading failures were made by a few researchers through numerical simulations in order to understand how certain network attributes (e.g. network topologies and node capacities) affect the cascading failure outcomes such as the size and duration of a cascading failure process [11, 20, 73]. The analytical approach and its solutions regarding flow redistribution dynamics are first developed by Goh et al. using the sandpile model [74] (see also section 3.1.3).

Research of type II cascading failures is only a recent phenomenon, though the studies of

infrastructure interdependencies, which uniquely characterize type II cascading failures, have been proceeding for more than one and a half decade [75]. This line of research shares similar objectives as the research of type I cascading failures: to establish relationships between (static) network attributes and cascading failure dynamics, and more particularly to understand how network attributes affect the cascading failure process and outcome [76-80]. It is initialized by the research of Buldyrev et al. [24], who revisited the case of 2003 Italy blackout and modeled it as a process in which failures propagated back-and-forth between the interdependent power and communication networks. An analytical solution for the condition under which type II cascading failures could happen was also derived. Their work was succeeded by a number of studies which account for various interdependency layouts, the relations between network topologies and spatial factors, and the cases of more than two interdependent networks [27, 81-85]. This domain remains an active research field by the time the present dissertation is written.

The abundant research existing in understanding the dynamics of cascading failures has been successful in establishing the relationship between (static) network structures and cascading failure dynamics [85]. This relationship however, is one-way in terms of that it only addresses the question of how given network structures affect cascading failure dynamics, particularly the outcomes of the cascading events such as the cascade sizes (i.e. the number of failed nodes) and cascade durations (i.e. the time interval from the beginning to the end of a cascading event) when the networks reach equilibrium. We name the study of cascading failure outcomes based on given network structures and failure mechanisms as the **forward approach**. The forward approach is characterized by the following typical research design: a network topology, a specific failure mechanism and an initial failure condition will be assumed, and through either analytical or

numerical modeling, how they (non-linearly) affect the outcome quantities such as the sizes of cascading failures will be investigated [86]. This typically involves looking into how the outcome quantities of interest co-vary with the changing network topologies and initial failure conditions. This line of research, though granting critical insights into the linkages between (static) system properties and system behaviors, faces three challenges (see section 3.1 for a detailed account):

a) the forward approach focuses on the outcomes of cascading failures, and learning the process that leads to the outcomes is still difficult if not impossible;

b) it relies on the knowledge in network properties such as detailed network topologies, which may not be available; and

c) it requires specifying a prescribed failure mechanism that drives the cascading process, which limited its generalizability.

Existing models for cascading failures mostly take certain parameters in network structures and the initial condition at the beginning of cascading failures as the inputs, and investigate how the outputs, which are typically measures of network functionality such as the number of functional nodes or the network-level efficiency, vary with changing inputs, either through simulations or by analytically solving a system of equations [20, 77, 87-91]. The process leading from the inputs to the outputs however, is in the black box, which means how the changing inputs give rise to the corresponding outputs is not revealed. At the network level, how the network functionality evolves with time – for example, what is the path of failure propagations and how the path reorganizes itself with varying inputs – is typically overlooked; and at the node/link level, no attention has been paid to how the failures propagate from nodes to nodes, i.e. which nodes affect which other nodes and cause them to fail. The reasons for the difficulties in learning the cascading failure

process, especially the node-to-node failure propagation process during cascading failures vary. For simulation models, the cascading failure process can be investigated at each single simulation run. But for multiple runs which are required to address the stochastic nature of failure propagations [92, 93], uncertainties in the failure propagation process emerge due to 1) that there exist a great many possibilities for the initial network conditions and 2) uncertainties in the network's responses [94]. These uncertainties are frequently unquantifiable in a simulation model [78, 95]. For analytical models, solutions to the network dynamic models exist only at equilibrium conditions, when the cascading failure process is concluded and the networks are stable [96-98]. Solutions for the transient states of the networks, while the cascading process is proceeding, are not guaranteed, especially in a stochastic setting [99-103]. Insufficient understanding in cascading failure processes leaves questions like how soon the infrastructures may collapse once the cascade is initialized and which part of the network plays the most critical role in spreading the failures unanswered, which however, could be of particular interest to infrastructure research and protection practice. Similar questions also exist and are of vital importance for other types of cascading failures such as epidemics, where identifying the key players (e.g. a region or a group of people) in spreading the failures (i.e. disease infections) could make preventive actions such as vaccination more efficient in curbing the spreading of infectious diseases.

Meanwhile, real-world networks and their interdependencies are often unknown to the research community with few exceptions. The detailed physical layouts of power grids, for example, are kept secrets in many regions for commercial or security reasons, and are not publicly available or only available at a coarse scale [104]. More broadly speaking, the structures of many networks in nature are too complex to be modeled or even understood by human beings at a fine scale. One

example is human brain, in which the interconnections between neurons are not yet fully pictured at sub-cortical level [105-109]. Moreover, network structures evolve with cascading failure processes due to failed and thus removed nodes and links [110-112]. While the current state of the art typically assumes a constant network structure that remains unchanged as the initial network structure at the beginning of the cascading failures, a more rigorous modeling approach that requires retrieving the time-varying network structures at a fine temporal scale can be computationally challenging [113]. The above three reasons preclude the availability of complete information on networks structures. In existing research following the forward approach however, a prerequisite of learning the cascading failure dynamics is explicitly knowing the network structures, as this information in the simulation and analytical models is always deemed as given and serves as one of the inputs to the models. With a lack of information on network structures such as degree distributions, path lengths and clustering coefficients, the forward approach to learning cascading failure dynamics is not feasible.

In addition, the forward approach requires specifying a prescribed failure mechanism such as flow redistribution, a threshold rule or interactive games (see section 3.1) in the models. A failure mechanism refers to the fundamental forces that drive the cascading failure process, and thus determines the type and detailed formulation of the model [114]. The forward approach based on predefined failure mechanisms has three limitations. Firstly, a model devised for one specific failure mechanism has limited generalizability to others. For instance, the sandpile model for load redistributions in cascading failures of power systems [100, 115, 116] is not applicable to modeling queue spillback in the propagation of congestions in a transportation network [14, 117, 118]. This hurdle inhibits the communication between cascading failure study in different disciplines and

identifying universal patterns of cascading failures across different systems [119, 120]. Secondly, in the interdependent network context, the composing networks could be subject to various failure mechanisms and thus fit different models. To model the cascading failure process at the multi-network scale requires selecting one model or integrating multiple models of different types, which may prove to be a complex and challenging task. This could also be true for single networks, whose failures may be underlay by multiple failure mechanisms simultaneously. For example, in the formation of a gridlock in a transportation system, the mechanism of queue spillback and flow redistribution could co-exist. In this case, a forward approach that employs a single failure mechanism would be insufficient to model the cascading process even for a single network. It thus calls for a universal approach to modeling cascading failure process that is capable of reconciling different failure mechanisms. And thirdly, the failure mechanisms underlying a real-world cascading failure instance are usually not immediately known following the failures, and only knowable after a period of investigations and study [121, 122]. This could limit the mechanism-dependent forward approach from being developed into real-time tools for emergency response, which requires timely modeling efforts before a thorough understanding of the failure mechanisms is reached.

1.3. The reverse problem

The three challenges faced by the current state of the art lead the present dissertation to address the following question: without presumed network structures or failure mechanisms, and given only the observed outcomes of cascading failures, can we infer the underlying failure propagation process? In real-world cases, cascading failure outcomes can be defined and observed at different levels of details. For example, when quantifying the cascade of congestions in a transportation

network, the state of a link (i.e. a highway segment) can be evaluated either in a binary manner or in a continuous manner. In the former situation, the node is either congested or not congested; and in the latter, the node state can be represented by some performance measures such as flow-capacity ratio or vehicle density at this highway segment. With different cascading failure outcomes observed, one is likely to obtain different insights into the failure propagation process. Among those different types of cascading failure outcomes, the case of binary node states is the most universal yet most challenging one [123-125]. From the multi-scale complex system perspective, each node can be viewed as a small sub-system that demonstrates non-linear phase transitions [25]. Therefore, even when a node's state is a continuous quantity, it is always possible to identify a threshold that divides its dynamics into two phases (i.e. the subcritical and supercritical phases) which correspond to the two binary states of the node [70, 126]. This property from each node itself being a complex system grants the binary states universality. The case of binary states is also challenging because it provides the minimum amount of information on node-level dynamics, which makes it difficult to reveal the pattern of node failures and thus to infer how failures propagate [127]. Considering the above two factors, this dissertation focuses on the case of binary node states, which are termed the functional state and failed state respectively. A "failure" is thus defined as an event in which a node changes from the functional state to the failed state, and the reverse change is defined as "recovery". Assuming every node is in the functional state initially at the beginning of a cascading failure event, the cascading failure outcome thus refers to the time when each node transits to the failed state.

The term "failure propagation process" can be understood at two scales. At the node/link scale, a failure propagation process describes how the failure of one node, through its linkages to another

node, leads to the failure of the latter. This process can be viewed as either deterministic or probabilistic at the node/link scale: in the deterministic case, a source of failure can be uniquely identified for each node, e.g. as in [128] which claim the first node that propagates the failure to a node as its failure source; and in the probabilistic case, every node with a linkage to a given node has a probability to propagate failures to this node, and thus which node is the failure source remains uncertain [129]. At the network scale, the failure propagation process refers to a propagation path that traverses all failed nodes. It indicates how the failure "travel" from the firstly failed nodes (a.k.a. the seed nodes) to other parts of the network [130]. As shown later in this section, a failure propagation process at network scale is always probabilistic.

The above questions present a reverse problem with respect to the forward approach to modeling cascading failures. In the forward approach, with a predefined network structure and failure propagation mechanism (e.g. flow redistribution and node overloading), the failure propagation process is formulated, and then the outcomes of cascading failures such as failure sizes and failure durations are obtained. In this dissertation, the failure propagation process will not be formulated from a given network structure and failure propagation mechanism, but instead from the observed cascading failure outcomes. Therefore, the fundamental challenges in this dissertation are:

a) that the network structures (i.e. patterns of links between nodes and interdependencies between networks) as well as the failure propagation mechanisms (i.e. why the failure propagates) are unknown and unobserved. The only available information is the temporal changes in the states of individual nodes and potential external factors such as the intensity of damaging forces from a natural disaster; and

b) that with only node-level information, uncertainties exist in the failure propagation

process, as multiple failure propagation processes can give rise to the same observed node state changes. In figure 1, all three failure propagation processes generate the same cascading outcome. There is no definite answer to the question which failure propagation process is the true one.

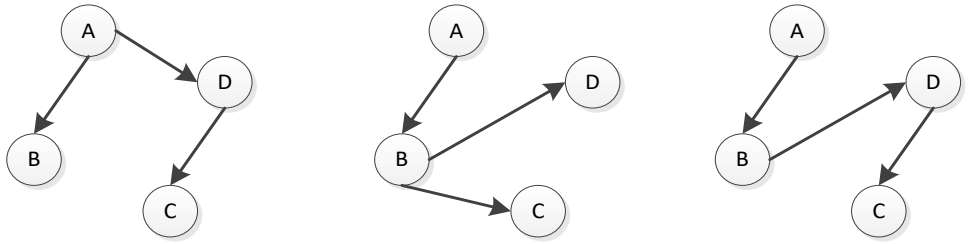

Figure 1: Example failure propagation processes that are consistent with the cascading outcome, in which node A, B, C and D fail at time 1, 2, 3 and 4 respectively.

To address these challenges, a methodology that combines advanced statistical models and network science models is devised, as is called the **backward approach** which indicates its reverse nature compared to the forward approach. The node-to-node failure propagation process that gives rise to cascading failures is modeled given only the observed outcomes of cascading failures, and minimum amount of knowledge in the network structure. More specifically, the time of failure for each node is taken as input, and a survival-analysis-based model is formulated to capture the sequential events of node failures and how the failures interact with each other. The model is estimated with a maximum likelihood estimation (MLE) approach, which returns the values of key parameters in the failure propagation process and thus enables reconstructing the process.

This methodology is tested and validated by applying it to four simulation studies and comparing the inference results obtained by the methodology to simulation results. These four simulation studies are: a) cascading failures in interdependent power and transportation networks in New York

City (NYC) during Hurricane Sandy; b) a hypothetical influenza epidemic in NYC; c) a congestion cascade scenario in the Sioux-Falls benchmark network [131]; and d) cascading power outages in the Wood-Wollenberg 6-bus benchmark system [132]. The Sioux-Falls benchmark network and the Wood-Wollenberg 6-bus benchmark system are widely-used cases for testing newly developed models in transportation network analysis and power system analysis, respectively. Results for (a) and (b) verify that the proposed methodology is mathematically sound: the backward approach is capable of precisely inferring the parameters associated with the failure mechanisms as well as recovering the simulated cascading failure process. The results for (c) and (d) cross-validate the robustness of the backward approach: the backward approach demonstrates solid performance when the failure data is independently generated using well-established domain-specific failure mechanisms, such as user rerouting in a roadway network and load re-balancing in a power grid. The simulation study (d) also validates the backward approach by comparing the inferred cascading failure process with data generated by a fully validated simulation procedure that has been tested in its ability to replicate a real-world process of cascading power outages [133-136]. All comparisons in the simulation studies between the inferred cascading failure process and simulation result return consistent patterns, suggesting the accuracy, robustness and generalizability of the proposed methodology.

This dissertation, however, is generalizable beyond the four simulation studies. The models developed in this dissertation will be readily transferrable to geographical areas other than NYC and to any case of type I or type II cascading failures. One advantage of the present methodology is that it is applicable to both type I and type II cascading failures (though it does distinguish between different failure mechanisms in type I and type II cascading failures), thus demonstrating

broad applicability and the potential toward a unified modeling framework for cascading failures of both types. In addition, the systems of interest are also not limited to power systems, transportation systems or disease transmission networks, and can be any system that is representable using a (spatially embedded) network or interdependent networks. The failure propagation process modeled in this dissertation is general, and not dependent on characterizing specific failure mechanisms. Therefore, any phenomenon involving failure propagations, including epidemics in which "failure" represents infection by a disease [137], news spreading in which "failure" represents a piece of information [138], financial crisis in which "failure" represents bankruptcy of an organization [139], and metabolism stability in which "failure" represents biochemical reactions [140], sees potential application of the present methodology with little to no modifications. It is worth noting however, that domain knowledge related to specific failure mechanisms can be easily integrated into the present methodology, as will be shown in the simulation study of influenza epidemics (b). The datasets required as inputs to the models are mostly publically available. For example, data of power outage complaints is available in most states, regulated by utility commissions. This data enables approximating the time when outages take place. Nearly all (if not all) states have transportation agencies that possess various forms of data on transportation system performances. Storm surge, wind speed and precipitation data, which is used to quantify the external factors underlying a cascading failure event during a hurricane, is available through National Hurricane Center at NOAA and NASA. And the damage-related data is available through FEMA. For other types of infrastructures beyond power and transportation systems and more broad domains of research that involves networks, the outcomes of cascading failures are also typically measurable, and can be obtained as input datasets to the present model in this dissertation.

Section 2
Research Setup and Contributions

In this section, important concepts involved in the dissertation are first defined. This section only discusses these concepts in a general way without reference to a specific cascading failure context. Specifications of the concepts in the four simulation studies will be presented in section 5. Following the definitions of concepts, the basic problem setup is described, and technical challenges and proposed solutions are discussed.

2.1. Research question

In a cascading failure event that materializes upon a networked system of unknown network structures (i.e. unknown physical layouts of the network(s) as well as their interdependencies), if what can be observed is at most the state of disruptions to the network(s) as failure spreads, and external factors (such as damaging forces of a natural disaster), this dissertation attempts to address the following questions in sequence.

a) given the outcomes of cascading failures, can we infer the underlying failure propagation process?

b) if the inference is possible, what level of certainty/confidence it can achieve?

c) what is the computational complexity of the inference algorithm?

Key terms involved in the research questions will be explained in the remaining of this section. An overview of the term definitions is presented in table 1.

Table 1: Glossary

Term	Definition
Network	A diagram of a system with its components represented by nodes and links.
Interdependency	The relationships or influences that a component in one system imparts upon another system [141].
Structure	The topology (i.e. how the links are arranged among nodes) of a network and where the interdependencies exist.
Physical layout	The network structure with consideration of the spatial distribution of nodes.
Community	The ensemble of infrastructure systems, environments and humans within a defined geographical area.
External factor	Any other system or system component (e.g. damaging forces in the environment) beyond the scope of a defined system.
Performance	The effectiveness of a system in providing products/service to humans and the society continuously. Performance can be evaluated at component level or at system level.
Disruption	Inhibited product-/service-providing function of a system due to external (e.g. natural or man-made disasters) or internal (e.g. performance fluctuations) reasons [142]. Disruptions to a system's performance can be evaluated at component level or at system level.
Failure	A disruption level above which the provision of products/service by a system (or its components) to a community is considered interrupted [143].
Failure propagation	The process in which the failure of one node or a set of nodes triggers the failure of other nodes.
Cascading failures	A sequence of node failures due to the combined effects of failure propagations and external factors, and the resulted shifting in system-level performances. An instance of cascading failures is also called a *cascade*.

Seed	Component(s) in a system where failures start due to external factors.
Failure source	The component(s) from which failure has propagated to a given component.
Process	A series of events that lead to the disruptions at a given node or in a network.
Outcome	The (observed) state of disruptions at a given node or in a network.
Mechanism	(Potential) reasons for the emergence of a phenomenon; or the driving forces for the progressing of a process.

2.2. Networks and interdependencies

A network, in general sense, consists of nodes connected by links [76]. Definitions of nodes and links vary by different systems, but can be categorized into two types. In the first type of networks, both nodes and links represent physical components of the system. An example of this type is a highway network where nodes are highway intersections and links are highway segments. In the second type of networks, only nodes represent the physical components of the system while links encode the interactions between the system's (physical) components [86]. An example of this type is a social network where nodes are individual people and links are friendship connections. Distinguishing between these two types of networks is critical for defining what are the functional units of the network. In a network that provide products/services to humans such as infrastructure networks, nodes are typically where the products/services are delivered and thus viewed as the functional units in the network [144, 145]. This is intuitive for nodes like transit centers and power stations that provide transportation service and power service in a transportation network and power network, respectively [146]. From this perspective, links that represent interactions between nodes are not functional units in a network. This dissertation adopts a modified version of this perspective, by extending "nodes" to all physical components that contribute to the functionality of the system. That is, any physical system component that contributes to the system functionality

(e.g. a highway segment that contributes to a highway network's functionality of facilitating human mobility) is viewed as a "node" in general which could fail and propagate failures during a cascading failure event. In other words, the concept of "node" in this dissertation is a vessel for functional unit, regardless of whether the functional units in a systems are (physical) nodes or (physical) links. This use of "node" stays consistent throughout the remaining of this dissertation, except in the simulation studies of congestion cascade (c) and cascading power outages (d), where the functional units refer exclusively to the (physical) links in a roadway network and power network, respectively. As for the concept of links, this dissertation takes it to be the interactions between two nodes (functional units). In existing literature, these interactions have referred to the dependence of one node's function on another node's function (which may or may not cohere to the presence of physical links) [147-149], and the geographical relation such as the distance or proximity between two nodes [150-152]. The above definition of node and link adopted in this dissertation is to reconcile the diverging definitions appearing in different disciplines, in order to maintain the general applicability of the proposed methodology.

Networked systems in the modern society usually do not stand alone, but rather are mutually dependent. The bidirectional relationships between different types of systems are termed interdependencies, through which the performances of the two interdependent systems are mutually influenced by each other [153]. The interdependencies between power systems and transportation systems which simulation study (a) in this dissertation accounts for represent one ubiquitous example of infrastructure interdependencies [89, 154]. Transportation systems demand electric energy from power systems as a fuel to facilities like subway trains and traffic signals, and operation of power systems requires transportation of maintenance personnel as well as bulk matter

like coal and oil as energy sources [155]. Disruption or failure in either the power system or transportation system could affect the other, and potentially lead to type II cascading failures.

It is also worth noting that interdependencies have spatial and temporal scales [75]. In terms of spatial scales, the interdependencies between two networks could exist either at the network level or at the node level [87, 156]. Interdependencies at the network level emphasize the correlation in network functionality between two networks, and failures of individual nodes/links in one network will not necessarily affect the other network, as long as the failures do not lead to a network-level collapse. This is the case when one network maintains high levels of redundancy [157], so the functionality of failed components in supporting other networks could be immediately substituted by other components that remain functional in the same network. However, systems in real world are usually designed without such redundancies in order to achieve efficiencies in their daily operations [158]. As a result, the node-level interdependencies are more common in real world. Through this kind of interdependency, failure of one node in a network could directly cause one or more nodes to fail in another network, contributing to a type II cascading failure event. The presence of node-level interdependencies in infrastructure systems has been proven in past disasters such as 2003 Italy blackout [24], Hurricane Katrina [159] and Hurricane Sandy [160], and is one of the primary interests of ongoing modeling efforts for cascading failures. This dissertation accounts for only the node-level interdependencies considering their ubiquity.

In addition to the spatial scales, temporal scales of interdependencies also influence which types of interdependencies should be considered in an analysis. The time scale within which an interdependency is relevant to an analysis varies across a wide range [75, 161]. For example, the

aforementioned interdependencies between power systems and transportation systems, through which transportation systems receive electricity as fuel from power systems, and power systems collect energy sources from transportation systems, are effective at different time scales. When power supply is cut off, transportation facilities like subway will almost immediately stop running, therefore this direction of the interdependencies is a fast process [162]. The other direction, in which the operation of power systems relies on transportation systems, is a comparatively slow process, as power plants usually hold stockpiles of coal or oil, and disruptions in transportation systems will likely impact power systems only days later. When considering node-level interdependencies, this means a node (e.g. a power generating station) could be involved in both fast processes such as cascading power outages and consequent transportation service shutdown, and slow processes such as refueling its oil tanks, which was the case during Hurricane Sandy [49]. It is thus important that a cascading failure model for interdependent networks captures failure propagation processes occurring at different temporal scales [75, 153], which poses a key challenge to the prevailing analytical approaches using differential equations [163].

2.3. The service perspective for infrastructure disruptions

There have been two perspectives in infrastructure research since its beginning [164]. The physical perspective focuses on the physical forms of the infrastructure systems, and therefore is concerned with damages to the constructed facilities such as subway stations and tunnels, roads, bridges, power lines and generators, and all kinds of buildings [87, 165]. Studies from the physical perspective typically adopt one or more performance measures indicating functionality of the facilities [166], and use them to analyze, assess and optimize the resilience or efficiency of infrastructure systems in their design and operations [167]. Consideration of human factors in these

studies is implicit and limited to regarding them as one of the inputs that affect infrastructure performance. The service perspective, on the other hand, is less concerned with the (physical) facilities of infrastructure systems, and focuses more on human utilization of infrastructure services [168], compared to the physical perspective. Therefore, performance measures from the service perspective typically evaluate how well a community is served by a defined infrastructure system [169, 170], instead of the damages to infrastructure facilities. The distinctions in treating infrastructure performance between these two perspectives also result in different definitions of infrastructure failure. From the physical perspective, an infrastructure facility fails if it is damaged to a level where its operation has to stop; and from the service perspective, failure means a community no longer receives products/service from the defined infrastructure system [171, 172]. In most cases, definitions from these two perspectives stay consistent. However in a highly distributed/redundant infrastructure system, the two may not match, as a community could have alternatives in obtaining the needed products/service other than from the (physically) failed infrastructure facilities.

The simulation study of interdependent infrastructure cascading failures embraces the service perspective, upon the following two considerations. Firstly, infrastructures exist to provide products/service to people, and therefore their abilities to provide the designated products/service, rather than the operation of the facilities themselves, should be the key factor in assessing their functionalities [173, 174]. More broadly speaking, infrastructure systems are integrated parts of a community and thus their performances are certain aspects of the community performance [164, 175, 176]. Adopting the service perspective grants the opportunity to achieve consistency between research concerning infrastructure performance and research concerning the wellbeing of

communities and humans. Secondly, there are various types of infrastructures in real world. Even though this simulation study considers only two of them – the power system and transportation system, these two infrastructure systems are of distinct natures in terms of what their nodes and links typically represent (see section 2.2). The physical perspective thus requires a network representation for each individual infrastructure system, which not only unnecessarily increases the model complexity, but also limits the generalizability of the model if a new type of infrastructure (e.g. water supply facilities) is included in the model setup. In addition to simplifying the problem of learning cascading failure dynamics involving the power and transportation infrastructures, adopting the service perspective and exploring a unified representation of the two systems also presents greater intellectual merits by enabling easy extension of the methodology developed in this dissertation to other infrastructure systems.

However, it is worth noting that the present methodology is transferrable between the physical perspective and the service perspective, with two minor modifications. Firstly, networks consisting of infrastructure facilities (e.g. highway intersections) and the physical links (e.g. highway segments) between them, instead of networks of infrastructure service at communities, need to be set up. And secondly, different performance measures and criteria of failure need to be employed. While "failure" in the simulation study of interdependent infrastructure cascading failures (a) means a community no longer receives a given infrastructure product/service (Table 1), transferring to the physical perspective will shift the failure definition to a more damage-centric way concerning the infrastructure facilities. From either the physical perspective or service perspective, the model formulation as specified in section 4 is applicable. The simulation studies of congestion cascade (c) and cascading power outages (d) present two examples of applying the

proposed methodology to cascading failures described from the physical perspective.

2.4. Problem setup

The core of answering the questions in section 2.1 is to devise an approach to inferring the failure propagation process from cascading failure outcomes. The specific problem to be solved at this stage is, what leads to the observed failures of every node that is affected in a cascading failure event. It is assumed that node-level failures can be attributed to either internal factors or external factors, or both: internally, disruptions at other nodes that are connected to a given node could increase the susceptibility of the given node and thus its probability of being disrupted and failure [11]; and externally, damaging forces from either natural or man-made disasters could also disrupt the given node [172]. The following setup of the problem accounts for the combination of internal and external factors.

2.4.1. Network setup

As failures in networks can be understood from either service perspective or physical perspective, there exist correspondingly two ways of setting up the network(s) for modeling cascading failures. The service perspective applies to most infrastructure networks. Imagine an area with N/K (where K is the number of networks in a multi-network system) zones, each representing a community. The size of a zone can be determined by the purpose of a study. In the simulation study of interdependent infrastructure cascading failures, administrative census tracts are used as communities. There are infrastructures serving each zone, for example, transportation and power. Following the service perspective, each type of infrastructure service in a zone is viewed as a node in the corresponding infrastructure network. For example, the transportation service that people

living in a zone receive corresponds to a node in the transportation network. The transportation service in a zone could represent accessibility to/from other zones, or ease of travel within the zone. This network setting has two advantages over a setting from the physical perspective. Firstly, it avoids the unnecessary complexity involved by representing and modeling the physical layouts of the infrastructures, which are typically complicated and unknown. Such complexity is unnecessary for analyzing cascading failure dynamics because certain cluster of infrastructure facilities share their fates in a cascading failure event, and therefore can be modeled as a single node [177]. And secondly, it makes no assumption on the usage pattern of infrastructure facilities. In order to quantify infrastructure performance from the physical perspective, certain assumptions on the facility usage patterns, such as that people always use the nearest facility to them [178, 179], need to be made. In the present network setting, no such assumptions are made. The infrastructure service in a zone could come from the infrastructure facilities within the zone, from another zone, or from multiple zones. From the physical perspective, network setup is relatively straightforward. The basic functional units (see section 2.2) in the network are viewed as nodes. Examples of this setup include highway segments as nodes in a highway network, power lines as nodes in a power transmission network, and individual people as nodes in a social network.

Therefore, the networks are constructed as following. From the service perspective for infrastructure networks, a number of K nodes are placed in each zone, with each of the K nodes representing a particular type of infrastructure service to the corresponding zone. In the case of interdependent transportation and power networks for example, K=2. The total number of nodes in the interdependent networks is N, and $N=K\times J$, where J is the number of infrastructure services considered. What concerns this dissertation is how infrastructural services provided in one zone

may be affected by each other and by service disruptions in other zones as well as by external factors. From the physical perspective on the other hand, nodes that represent (physical) components of a system are placed at their exact locations. This means the spatial distribution of nodes in a network constructed from the physical perspective has the same spatial layout as the real system. This also means these nodes may have (spatial) dimensions. For example, a node in a power transmission network is placed where a power line is, and a node in a social network is placed where a person's home location is. From either the service perspective or physical perspective, link information is regarded unavailable. Whether given two nodes are linked, and what is the type of the link if they are, belong to the unknowns and are subjects of inference in the model.

2.4.2. Problem statement

Considering the network setup, the research questions in section 2.1 can be reiterated as: how the cascading failure process can be inferred, given the state of disruptions to every node as the known information. Such information can be available at different levels of details, which corresponds to unique temporal and spatial scales. The observed cascading failure outcome could simply be the time when each node fails, such as when the majority of households in a zone lose power, which corresponds to the failure time of the power node in the zone from the service perspective, or when a power line is tripped, which corresponds to its failure time from the physical perspective. More complicated cascading failure outcomes could refer to temporal trajectories of the nodes' performances that are observed at multiple time points. As discussed in section 1.3, only the former case will be studied in this dissertation, considering its ubiquity and being the most challenging case. Spatially, not all information comes in the designated node level. In an influenza epidemic

for example, infection case reports could appear at individual level (typically at early stages of the epidemic), hospital level or regional level.

This dissertation starts with the simplest case of knowing the exact failure time of each of the N nodes. The level of details in the failure time is consistent with the time unit of the study. For example, if the analysis is on a daily basis, the failure time of a node will be as specific as the day when this node fails. The first problem this dissertation will address is thus:

Problem 1. Given $\vec{t}$, find PT.

Here PT refers to the underlying cascading failure process, and $\vec{t}$ is a vector denoting the observed failure time for each node. The number of entries in $\vec{t}$ is thus equal to the number of nodes N. If a node n reports no failure throughout the study period, t_n equals to ∞, suggesting that node n is right-censored. Depending on the assumptions regarding PT, there exist three cases:

Case 1.1. PT is a tree. In this case the failure of a node is caused by the failure of another node. In other words, if a node fails in a cascading failure event, it is always possible to identify a single node that is responsible for its failure (which will be termed the parent node or failure source in the remaining of this dissertation, and the failed node will be termed the child node).

Case 1.2. PT is an acyclic graph. This is a more general case than case 1.1, in which multiple parent nodes for a failed node could exist.

Case 1.3. PT is an arbitrary graph where cycles are allowed.

Case 1.1 is ubiquitous in propagation of disease or information [180, 181], in which a single source that leads to individual's infection or information reception can always be identified. Case 1.2 has been studied in technology adoptions by individuals who may be under the influence of multiple others to make the decision of adopting the new technology [182]. Infrastructure failure propagations also belong mostly to case 1.2, since a single failure source for every node is not guaranteed. For example, a transportation node could be supported by multiple power nodes each serving as a backup once the others have failed. In this scenario without considering the rest of the network, the transportation node would fail if and only if all the supporting power nodes fail, or in other words, the power nodes' failures together contribute to the failure of the transportation node. However, it is also worth noting that case 1.2 is inclusive of case 1.1 with case 1.1 permiting only one parent node and case 1.2 permiting an arbitrary positive integer number of parent nodes for every failed node, and therefore this dissertation will account for case 1.1 as a special and simpler instance of case 1.2.

While case 1.3 is the most general case, it reduces to case 1.2 with the assumption that there exist no cycles in the failure propagation process. This assumption is viable in the well-established susceptible/infective/recovered (SIR) model in epidemiology [183]. A failure propagation process can be viewed as an SIR process as long as failure of a node is not recurring. It is worth noting that this does not mean a failed node can not be restored to function. Given that cascading failures typically proceed rapidly and recovery is much slower, e.g. infrastructure cascading failures happen within hours while restoration of failed infrastructures may takes days [184] and diseases like influenza spread much faster than recovery of infected individuals [185], this assumption is viable because the time frame of a cascading failure process likely will not permit the restoration

of any failed node. Therefore, case 1.3 is considered as beyond the scope of this dissertation.

For case 1.1 and 1.2, it is worth noting that multiple cascading failure processes can give rise to the same $\vec{t}$, as demonstrated in figure 1. In figure 1, three example failure propagation processes give rise to the same set of failure time. Therefore, each of case 1.1 and 1.2 presents the following two sub-problems.

Sub-problem 1.1(2).1. Given $\vec{t}$, find *PT* that is the most likely.

Sub-problem 1.1(2).2. Given $\vec{t}$, find the likelihood for an arbitrary *PT*.

A widely adopted assumption in existing studies that investigate failure propagation process is the independent cascade assumption [186, 187], under which the probability of failure propagation from one node to another node depends only on these two nodes and is not affected by other nodes or their probabilities of transmitting failures. This property evokes an easy solution to sub-problem 1.1(2).1 once the failure propagation probability between any two nodes is known. More interestingly, it has been proven that under the independent cascade assumption, any function that maps a subset of nodes/links to a real number is submodular [182]. When considering the probability of a progressing failure propagation process as such a function, submodularity means that the marginal gain in the probability of a failure propagation process always decreases as the set of failed nodes expands. Therefore, selecting the failure propagation process that maximizes such marginal gains every time failure propagates will ensure that the selected failure propagation process has the highest probability over other failure propagation processes. It suggests that under the independent cascade assumption, a computationally tractable solution can be guaranteed for

sub-problem 1.1(2).1. Given these properties of the independent cascade assumption, this dissertation sets up the special case of failure propagation under this assumption as a baseline problem.

Baseline problem 1. Given $\vec{t}$, find the pairwise failure propagation probability from every node to every other node.

Under the independent cascade assumption, sub-problem 1.1(2).1 and 1.1(2).2 can be solved by solving baseline problem 1, which will be shown in the methodology section (section 4). A two-step approach is proposed for solving baseline problem 1: first, the methodology seeks to understand the (general) failure mechanisms underlying a cascading failure process; and second, pairwise failure propagation probabilities are evaluated from the quantified failure mechanisms. Thereby, solving baseline problem 1 involves solving the following two sub-problems sequentially, which are named the inference problem and the reconstruction problem, respectively.

Baseline sub-problem 1.1 (inference problem). Given $\vec{t}$, quantify the failure mechanisms by estimating the parameters θ associated with the failure mechanisms.

Baseline sub-problem 1.2 (reconstruction problem). Given quantified failure mechanisms in terms of parameter estimates $\hat{\theta}$, evaluating pairwise failure propagation probabilities from every node to every other node.

Methods of solving these two baseline sub-problems are presented in section 4.2.1 and 4.2.2, respectively. With pairwise failure propagation probabilities evaluated, sub-problem 1.1(2).1 and

sub-problem 1.1(2).2 can be solved by utilizing the submodularity of the likelihood function for failure propagations [188].

Problem 1, and its sub-problems and special cases assume availability of node-level information on the cascading failure outcomes, i.e. the time of node failures. In real-world cases however, cascading failure processes could generate outcomes at different spatial scales, and node-level information that reveals the failure of infrastructure services in a community or an individual person's infection by influenza is not always available. In the case of Hurricane Sandy for example, loss of power service was recorded for individual customers, which typically correspond to households or buildings [189]. Disruptions to transportation service on the other hand, are manifested at facility level, with examples such as flooded and shutdown subway stations and congested bridges on the East River [48, 190]. Therefore, when put in a practical setting, the methodology first needs to address the following problem.

Problem 2. Given $\vec{D}$, find $\vec{t}$.

Here $\vec{D}$ represents disruptions to a network's functionality. The spatial scale at which $\vec{D}$ is measured is not necessarily the same as the spatial scale of $\vec{t}$. And for different networks in a system composed by interdependent networks, the spatial scales of $\vec{D}$'s measurements may be inconsistent. The goal of solving problem 2 is thus to convert the cascading failure outcomes observed at multiple spatial scales into a single scale as the node failure time. This dissertation assumes that problem 2 is already solved and its output, i.e. the node failure time, is viewed as known. The focus of this dissertation is to use the output of problem 2 to solve problem 1.

2.4.3. Examples of problem settings

Two examples using infrastructure network failures, one for problem 1 and problem 2 each, are provided to illustrate the general problem settings described in section 2.4.2. A case in which the node failure time can be recorded happens when a community is served by a single power facility, and none of the customers in this community has backup power sources. As a result, power service in this community has only two status: one being that this community is served with power when the facility is functional, and the other being that this community has no power when the facility fails. Therefore, the failure time of power service in this community is simply the failure time of the power facility that serves this community, which is typically monitored closely by utility providers [191]. The same case could happen to the transportation network as well. If traveling by the residents in a community is heavily dependent on a subway station or bus stop, its closure may limit people's ability to travel and deprive the transportation service to this community [192, 193]. In this case, the failure time of transportation service in this community is equal to the time when the subway station/bus stop is closed.

In real-world infrastructure systems however, such a homogeneous service condition within a community is rarely the case, and consequently, problem 2 frequently emerges. An example is that customers in a community could experience and report power outages at different timestamps, and some may experience outages without reporting them. When this customer-level information is available but potentially incomplete, problem 2 needs to be solved in order to convert customer-level outage information into power service failure at community level. Quantifying transportation network failures faces the same challenge: facility-level damages or function losses are not

necessarily associated to community-level transportation service failures [194-196], due to two primary reasons. Firstly, people could have different travel behaviors in a community. It means they are likely to utilize different transportation facilities in their daily life, and therefore, damages to a given facility would impact their abilities to travel differently. And secondly, people's vulnerabilities to transportation service disruptions also vary. For example, a household with automobile is less likely to experience transportation service disruptions caused by transit facility damages compared to those without private vehicles [197, 198]. Transportation service failure at community level in these cases, is not naturally defined due to the fact that facility failures would produce non-uniform effects across a community, and thus requires solving problem 2 that synthesizes facility failures and individual/household-level information into community-level transportation service dynamics.

2.5. Research contributions and challenges

This dissertation attempts to develop a general methodology to infer cascading failure dynamics in networked systems, with a focus on cascading failures in infrastructure networks. Infrastructure systems frequently set the backdrop for real-world cascading failures of both type I and type II (see section 1.1), and therefore developing an approach to understanding the failure propagation process in infrastructure systems has its practical needs. By modeling and understanding a simulated or real-world cascading failure event in infrastructure networks or more broadly any type of networked systems, two kinds of nodes (e.g. infrastructure facilities) can be identified: those that are the most vulnerable to failures, and those that are the key to propagating failures and causing system collapse. Through strengthening these two kinds of nodes, engineers can secure the critical functions of infrastructures during extreme events, as well as the wellbeing of our

society. For other disciplines such as epidemiology and information science, identifying these two kinds of nodes provides an avenue to controlling the dynamics of phenomenon such as the spreading of infectious diseases and rumors. A methodology of inferring failure propagation patterns like the one presented in this dissertation also has the power of predicting possible failure propagation paths in recurring cascading failures, which are common in many natural and man-made systems. The capacity of forecasting how the failures will propagate across the networks grants the opportunity to stop a cascading failure event before a system-level collapse (e.g. a traffic gridlock) is triggered.

More broadly speaking, this dissertation contributes to a methodology that is generally applicable to a variety of systems and types of cascading failures, whether existing ones with well-understood failure mechanisms or future ones with unknown mechanisms. The state of the art, which mostly falls into the forward approach, is inefficient for the communication between cascading failure research in different disciplines and identifying universal patterns in cascading failures (see section 1.2). This dissertation advances the state of the art in interdisciplinary cascading failure research by proposing and testing a methodology with general applicability. The proposed methodology addresses multiple critical limitations of the state of the art (see section 1.2) by removing the requirement for network topologies as input, formulating the node-to-node failure propagation process probabilistically, and adopting the four general failure mechanisms (see section 4.2.1). These three measures grant the proposed methodology generalizability. This dissertation thus facilitates a unified understanding of cascading failures and more general system dynamics across different disciplines.

As to its relationship with the propagation learning techniques devised in other disciplines (see section 3.2), this dissertation is NOT a simple application of those techniques to the field of infrastructure research and cascading failure research. It attempts to address the following challenges that propagation learning studies in epidemiology, information science and social science have not considered, or have encountered but not addressed. Through addressing the following five challenges, this dissertation advances the state of the art in infrastructure studies, as well as studies of cascading failures in other disciplines by raising general settings of cascading failure problems, and developing a universal methodology for learning cascading failure dynamics that is applicable to a broad range of disciplines.

Firstly, the propagation inference problem in the context of interdependent networks is for the first time investigated and modeled in this dissertation. Previous studies that attempt to infer the propagation of either a disease, a piece of information or a technology focus only on single networks, and existing models are not extendable to the case of propagation in interdependent networks. The major challenge in devising a model for this purpose comes from different interpretations between links within a single network (which will be termed connective links) and links connecting two networks of different types (which will be termed interdependent links) [199, 200]. From modeling point of view, connective links are necessary for nodes' functions and failure propagation to a node would occur when all links connected to the node are cut off [24]. Interdependent links, on the other hand, represent the relationships between nodes' functions in two different networks, and thus failure of even a single node could cause the failure of another node through the interdependent relation between these two nodes [87]. Failure propagation in existing literature is treated the same way as an interdependent link, where failure of the parent

node is sufficient to cause the failure of the child node. The possibility of failure propagations in the manner of connective links have largely been overlooked.

Secondly, all constraints on network structures are removed and the modeling approach in this dissertation applies to arbitrary structures of two interdependent networks, in terms of both the connective link layouts and the interdependent link layout. Previous studies always assume certain types of networks such as random graphs or scale-free networks [85, 157], as well as the configuration of interdependencies such as the one-to-one interdependence between two nodes in [24] and [199]. In contrast, the present methodology requires no prior knowledge of the network structures (but can utilize it if available), and therefore grants (at least) the following modeling freedom: a) no predefined types of networks need to be claimed; b) there is no restriction on the directions or strengths of interdependent links; and c) the number of interdependent links a node can be connected to is an arbitrary positive integer. By allowing arbitrary network structures in the modelling procedure, this dissertation also addresses the challenge of changing network topologies during cascading failures [147]. In a cascading failure event, as the failure process progresses, nodes (and their incident links) are removed from networks and hence the topology of networks will likely change. Its effects on the cascading failure dynamics have been overlooked by previous studies, which use the initial network topologies in models from the beginning to the end of a cascading failure process [200].

Thirdly, external factors that could contribute to failures are incorporated for ALL nodes. Existing failure propagation inference methods typically try to describe a process in which cascading failures are initialized by one or multiple seed nodes and spread along network links to the rest of

a network. In these scenarios, external factors are only considered for the seed nodes [11, 20, 128]. The present approach has the following two advantages compared to the existing ones. First of all, it is a more holistic reflection of the factors that could potentially cause node failures than previous approaches that consider no external factors in the failure propagation process. Controlling the external factors is critical of avoiding the overestimation of propagation effect, that is, in cases where a node indeed fails due to external factors but an inference method, if overlooking the external factors, accredits the failure to the propagation from another node. In addition, incorporating external factors for all nodes enables the emergence of new seed nodes during a cascading event. In real-world cascading failure cases, seed nodes seldom emerge altogether at the beginning of a cascade, but could see their occurrence throughout the cascading failure process due to the effects of external factors over time [201]. Therefore, the present approach is a closer and more general imitation of a real-world cascading event than existing approaches.

Fourthly, uncertainties in the inferred failure propagation process are addressed in this dissertation. Existing studies that infer failure propagation processes from cascading failure outcomes all require multiple cascading failure instances in order to achieve a given confidence level in the inferred failure propagation process [127]. This is because uncertainties underlie the failure propagation process inferred from a single cascading failure event, as is shown in figure 1. This dissertation attempts to address the uncertainties directly instead of reducing them through multiple cascading failure observations as previous studies did. By solving the sub-problems in section 2.4.2, the existence of alternative failure propagation scenarios are accounted for and their probabilities are evaluated. It is worth noting that this is a more general approach to addressing the uncertainties in propagation process inference, as in the case when multiple cascading failure

instances are available, it still applies, with an altered (and potentially skewed) probability distribution over the alternative propagation scenarios.

Fifthly, this dissertation attempts to reconcile different temporal scales in the cascading failure dynamics. An interdependent infrastructure system involves at least two networks, and the temporal scales of their dynamics probably do not match. Cascading failures in power networks are known to be fast processes with entire network collapse happening within minutes [184]. Failures in transportation networks, on the other hand, progress much slower with a time scale from hours to days [202]. The resulting cascading failure outcomes will also likely be observed at different temporal scales, with failures of power nodes coming up within a short amount of time and transportation nodes becoming dysfunctional more gradually. Such inconsistence in temporal scales poses modelling challenges when accounting for the interdependencies between the two infrastructures, particularly in the case where only information on node failure time is available. These challenges are addressed by rendering heterogeneities among pairwise propagation probability distributions, so that the distributions could scale with the temporal scales at which the propagations take place.

Above all, the biggest intellectual merit of this dissertation is the creation of a universal approach to learning the cascading failure dynamics that requires no specific failure mechanisms or network structures. This approach is tested and validated through four simulation studies. Although the author illustrates this approach only in the context of infrastructure cascading failures and epidemics, the model formulations do not rely on any specific failure mechanism, which grants generalizability of this approach to any single network or interdependent networks, either among

infrastructure systems or involving other systems like information systems, social networks or biological networks. Despite of being a general methodology, the proposed approach demonstrates the versatility of easily integrating domain knowledge in various disciplines when modeling cascading failures in specific networks, as will be discussed in section 5.

Section 3
Literature Review

3.1. Modeling the dynamics of cascading failures

A detailed review of the state-of-the-art modeling techniques (the forward approach) for cascading failures is provided in this section. Existing analytical models for network dynamics can be categorized into four types [89, 203]: 1) dynamical system models that focus on the changes in individual nodes' states and their interactions; 2) percolation models that statistically characterize existence/non-existence of nodes and links; 3) sandpile models that simulate the redistribution of network flows and loadings; and 4) game theoretic models that quantify interactions between a pair of nodes or a group of nodes. All these four types of models have witnessed applications in cascading failure modeling, and are thereby reviewed below. It is noted that this review is NOT intended for an exhaustive overhaul of all modeling work on cascading failures, but attempts to present an overview of these four types of models by traversing their fundamentals and the milestone research that introduces them to the domain of cascading failure modeling. Empirical studies and non-model based simulation studies are excluded in this review.

3.1.1. Dynamical system models

Modeling of cascading failures originates in the study of power system dynamics. The first published model for cascading failures is devised by Parrilo et al. [68], in the context of a simple 10×10 square power grid composed of 4 power generators and 96 synchronic motors as nodes. Failures are initialized either by tripping of transmission lines or by power generator failures, and the failures propagate through the interactions between pairwise node dynamics and network topology changes. The initial failures break the existing equilibrium of power flow, i.e. the

consumed power equals the available supply for every part of the network, and drives the network to a new equilibrium. In the process, transmission lines may be overloaded, which leads to further failures. The key in the model is the formulation of node-to-node interactions. The authors use hybrid differential-algebraic equations (DAE) that enable both continuous and discrete cases to model the power flow dynamics between two nodes. The network is thus described by a system of DAE's which involve more than 200 state variables. Principle component analysis is employed to reduce the dimension of the state space.

To overcome the complexity involved in solving the equations describing system dynamics, Sachtjen et al. [204] reinvented the model of power flow redistribution and adopt a network-centric approach which discretizes the flow redistribution dynamics. In their work, the distribution of cascade sizes is investigated as functions of multiple network attributes, including node degrees (assumed to be homogeneous), redistributed flow amount, distance to the critical flow level that leads to entire network failure, and network topologies specified by average path length and clustering coefficients. The process their model describes is based on simple flow redistribution and conservation mechanisms: every day there is a (fixed) probability that one unit of power flow will be transferred between two nodes; and at every minute, if the flow at one node exceeds its capacity, a given amount (the second network attribute mentioned above) of flow will be redistributed to its connected neighbors. From this simple model setting, the authors discover a law of scaling for the cascade size in power networks which potentially extends beyond simulated network topologies like random graph or small-world networks. These two pioneer studies in cascading failure models, however are restricted to modeling dynamics unique to power networks, or at least networks with flows, and thus lacks universal applicability to cascading failures in other

systems.

3.1.2. Percolation models

A percolation model quantifies the probabilistic existence of an arbitrary node (site percolation) or link (bond percolation), and furthermore evaluates the probability that a path connects two randomly selected nodes [126]. It bridges local connection patterns such as pairwise connection probabilities and node degrees with higher-order network topologies such as shortest paths and clustering, and has been used by network scientists to characterize the topological properties of various (theoretical) network models since late 1990s [86, 98].

The first cascading failure model that takes advantage of percolation models is devised by Watts [69]. The author abstracts failure propagation process into a threshold rule, by which a node will fail if a larger-than-threshold proportion of its connected neighbors have failed, and investigates 1) whether cascading failures will spread to the entire network (termed as global cascades when they do) and 2) the size (number of failed nodes) of global cascades. The failure propagation dynamics under threshold rule is found to mimic a percolation process, and demonstrate phase transitions with varying (average) node degrees and node failure thresholds, i.e. the fraction of failed neighbors to trigger the failure of a given node. The condition for global cascades is thus derived from a percolation model, and is expressed in the form of a relationship between node degrees and node failure thresholds. To address the second question – what is the size of a global cascade once it happens, the author looks into the two phases (with global cascades) formed in the percolation process, which are distinguished by node degrees. It is discovered that when the average node degree is low (a.k.a. sparse network), the global cascade size follows a power-law distribution; and

when the average node degree is high, the distribution is bimodal. The divergence in global cascade size between low-connectivity and high-connectivity phases is attributed to different factors driving the failure propagations: in the low-connectivity phase, whether failure propagates to a node is determined by the degree of the node, while in the high-connectivity phase, the node failure threshold plays a critical role. Watts' study reveals the relation between two vulnerabilities to cascading failures in a network – the vulnerability of individual nodes and the vulnerability due to connectivity. Its considerations of local dependence for failure propagations between different pairs of nodes and heterogeneity in both node degrees and node failure thresholds are also remarkable among early work in cascading failure modeling.

A notable extension of percolation models is their recent adaptation to analyzing cascading failures in interdependent networks. Buldyrev et al. [24] studied cascading failures between two interdependent networks by formulating a percolation model for each of them as in [69]. These two percolation models, however, are constrained by the fact that functional nodes in one network must have their dependent nodes in the other network as functional as well. This constraint results in two interacting percolation process, where at each iteration, the probabilistic failure of nodes/links in one network is affected by the percolation outcome at the last iteration in the other network. This process gives rise to the co-evolution of the two networks, which end up with disconnected clusters of nodes in each of them, while corresponding clusters in the two networks are mutually connected. The authors' findings generally point to contrary behaviors of interdependent networks compared to single-network behaviors.

3.1.3. Sandpile models

The threshold rule is also mathematically formulated as a sandpile model by Goh et al [74]. Their model describes cascading failure process as grain toppling. To initialize the process, one grain, representing one unit of flow, is added to a randomly selected node. Every node has a capacity, prescribed by the authors to be a node's degree. If the number of grains (termed "height") at a node exceeds its capacity, one grain will topple from this node to each of its neighbors. The toppled grains may trigger further toppling at other nodes, creating a cascade. To obtain the analytical solution for the distribution of cascade size and cascade duration, the authors simplify a cascade to a tree structure, and employ the generating function formalism to articulate the process of tree branching. Since a cascade is typically short-living, its duration can not be measured directly in cascading failures. The authors instead assume a relation between cascade size s and cascade duration t as $s \sim t^z$, and explore the distribution of cascade duration by evaluating the exponent z. Explicit functional forms are discovered for the relations between node degree distribution and both the distributions of cascade size and the cascade durations.

Goh et al.'s sandpile model [74] addresses how network topologies affect the toppling dynamics, but not the other way round. Fronczak et al. [205] extend the sandpile model by introducing a rewiring process to capture the a network's self-organization during cascading failures. In addition to the sandpile toplling rule specified in Goh et al.'s sandpile model [74], the authors also define a rewiring rule as follows. Every link end in the network is marked with a timestamp denoting when this end of link is last rewired. Each time a cascade forms, the least recently rewired link end (i.e. the link end with the smallest timestamp) is disconnected from its current node, and reconnected to the node that triggers the cascade. This rewiring process simulates the spontaneous reaction of a network to cascading failures by enhancing the failure source, through compromising the

capacity (assumed to be equal to a node's degree) of other parts of the network that shows a history of being stable. The sandpile model incorporating rewiring process thus reconstructs the co-evolution of cascade dynamics and network topologies. The authors discover that at equilibrium, the node degree distribution and cascade size distribution always converge to the same distribution, revealing the robustness of sandpile model against changing network topologies and cascading dynamics.

3.1.4. Game theory

Game theory was originally employed by network scientists to model the evolutionary dynamics of social and economic networks [206]. Only recently has it been applied to analyzing cascading failures. The pioneer work was implemented by Wang et al. [139], who first introduce a failure mechanism absent in previous versions of game theoretic models. In their model devised for cascading failures in social and economic networks, three types of games – prisoner's dilemma games (PDG), snowdrift games (SG) and public goods games (PGG) – are played respectively, each representing a unique mechanism that facilitates failure propagations. Every node (representing individuals or businesses) in the network can adopt either a cooperative strategy or a defective strategy at any given time step, and receives a payoff based on the strategy it currently adopts and the game played. Under PDG, the payoff a node receives from interacting with another node is as follows in decreasing order: 1) this node is defective and other node is cooperative; 2) both nodes are cooperative; 3) both nodes are defective; and 4) this node is cooperative and other node is defective. SG has similar payoff setting but the orders of 3) and 4) are reversed. PGG is a group game played by a node and all its connected neighbors, in which there exists only a group payoff shared equally by all players, while cooperative nodes suffer a cost but defective nodes do

not. Every node needs a minimum level of payoff to stay functional, and otherwise would fail. At every time step, one round of game is played and the total payoff at a node is calculated, and the state of this node is determined by comparing its total payoff with its minimum payoff. At the end of the time step, a node will switch its strategy to that of a randomly selected neighbor, with a probability evaluated as a function of their payoff difference. By investigating the fraction of functional nodes at equilibrium (i.e. when no more failure could potentially happen), the authors identify two phases with nonlinear transitions: a survival phase where the majority of the nodes remain functional, and an extinction phase where all nodes fail. However, unlike the two phases resulting from percolation [69] where the survival of a node is completely random, only cooperative nodes that form cooperative clusters survive. The authors further reveal that the process of failure propagations is in fact dominated by the underlying spreading pattern of the defective strategy. These findings have been shown to be robust against different games played and varying network topologies.

3.1.5. Concluding remarks

The forward approach to modeling cascading failure dynamics, as reviewed above, has greatly deepened human understanding of cascading failures from the following two aspects. Firstly, methods of quantitatively describing cascading failure dynamics are developed. For example, almost all studies along this line monitored the key indictors of the progress in cascading failures, such as failure sizes and failure durations in their models. In terms of the failure propagation process, the percolation models and sandpile models particularly describe it as a branching process, in which failures propagate randomly from parent nodes to their child nodes through a tree structure. The characterization of cascading failure dynamics lays the foundation of formulating a

cascading failure process mathematically, and enables researchers to look into the failure propagation mechanisms that drive the cascading failure processes. And secondly, the linkage between characteristics of cascading failures and network properties such as its topologies has been established. What concerns the forward approach most is how the outcomes of cascading failures would change with network topologies and initial failure conditions. Through the above four types of models, researchers have uncovered a universal existence of non-linearity and phase transitions between network properties and cascading failure characteristics such as its sizes, extents and durations [70, 76, 89, 207, 208]. It is worth noting that the present dissertation diverges from the forward approach in the second aspect.

The line of forward approach, however, faces three critical challenges. Firstly, it focuses on the outcomes of cascading failures, and learning the process that leads to the outcomes is still difficult if not impossible. This is because in the current state of the art, solutions to the network dynamic models exist only at equilibrium conditions, when the cascading failure process stops and the networks are stable. The transient states of the networks, while the cascading process is proceeding, can not be obtained or only obtainable at a high computational cost. A direct consequence of this limitation is that how the network properties will affect the cascading failure processes (instead of outcome quantities such as failure sizes/durations), e.g. whether failure will propagate along a different path (but potentially lead to the same cascading outcomes) with varying network topologies, has never been studied. Insights from revealing such a relationship, however, are of great practical importance, as predicting the propagation path of failures is critical of preventing the progression of cascading failures. Secondly, the forward approach relies on knowledge of network properties, which may not be available. For example, the detailed physical layouts of

power networks in some regions are kept secret for commercial or security reasons, or are accessible only at a coarse scale [104]. Moreover, network properties (e.g. their topologies) evolve with the cascading failure process. While the forward approach typically assumes constant network topologies that remain unchanged through the cascading failure process, a more rigorous modeling approach that requires retrieving the time-varying network topologies at a fine temporal scale can be computationally challenging [113]. And thirdly, the forward approach requires specifying a prescribed failure mechanism such as flow redistribution, a threshold rule or interactive games in the models, which drives the cascading process. However, in the interdependent network context, networks could be subject to various failure mechanisms and thus fit different models. Selecting one model or integrating multiple models to account for the varying failure mechanisms may prove to be a complex and challenging task.

3.2. Network inference from cascading outcomes

With the challenges and limitations posed by the forward approach, learning cascading failure dynamics from cascading failure outcomes, which is named the “backward approach” in this dissertation, presents the potential to address those challenges and limitations and further advance the state of the art and knowledge in studying cascading failures. The core of the backward approach includes inferring failure propagation patterns and the underlying network structures, given only the observed failure outcomes, which is also known as the network inference problem in literature [209]. The emergence of the backward approach is only a recent phenomenon [210]. It has its origin in the research of epidemics, which seeks to understand the dynamics of disease spreading. Parametric models at population level such as the susceptible-infectious-recovered/removed (SIR) model have a long history of adoption by epidemic researchers to

evaluate whether a disease would develop into epidemics and the size of epidemics, through estimating a system of differential equations [211]. These models however, adopt impractical assumptions about the lifecycle of diseases, such as a fully-mixed population, constant transition rates between different stages of a disease over time and homogeneity in the transmission potential for all infected agents [212-214].

Since early 2000s, there have been numerous studies that investigated the dynamics of disease spreading in networks in attempts to address the limitations of the parametric models. As this is a vast study field, the following literature to be reviewed is selected based on the criteria that these studies have similar problem settings as ours: the inputs of their methodology are or at least contain the timestamps of node/agent failures, and these studies seek to solve a problem that would output pairwise transmission probabilities at the local level and failure propagation patterns at the global level.

The first non-parametric approach to modeling the disease spreading patterns was devised by Haydon et al. [130] in early 2000s inspired by epidemics such as the foot-and-mouth disease and SARS. Their study raised the research task of reconstructing an epidemic tree from the time when each agent (i.e. a farming property) was infected and known infection source for some agents, in order to calculate the case-reproduction ratio and its temporal-spatial variations which are of particular interest to epidemic researchers and assess the effectiveness of control measures. The authors tested three algorithms of identifying disease sources for individual agents after determining a “candidate” source list for each agent based on constraints to infection times and geographical distances between agents: (i) the geographically closest agent in the candidate list is

the infection source; (ii) every agent in the candidate list is the infection source with equal probability; and (iii) every agent in the candidate list is the infection source with a probability function of distance, estimated from the agents with known infection sources. Results shows that these three algorithms produce similar propagation patterns. One interesting notion by Haydon et al. is the multi-scale spreading scenario [215]: long-distance transmission renders the disease to spread nationwide and gives rises to multiple "sub-epidemics" where the disease spreads locally with transmission distance less than 20 km. This leads to a deeper understanding of the roles of different spreading mechanisms (e.g. long-distance transporting of cattle versus animal-to-animal close-contact) in creating the epidemic, and paves the way to future study of how local transmission characteristics such as reproductive numbers and generation times give rise to global epidemic dynamics like the growth of infected population [137, 216]. Although the authors realized the existence of uncertainties in the disease spreading patterns, the uncertainties are not addressed as the authors attempted to infer the spreading pattern deterministically.

The first probabilistic model for inferring disease spreading patterns was proposed and tested in the context of SARS by Wallinga and Teunis [217]. They are the first to introduce the independent cascade model [187] (see also section 2.4) to the line of research in network inference, whose assumptions would be widely adopted later on. This study also overcomes the reliance on spatial relations between agents to infer who infects whom in previous studies [130, 218], and uses only times of infections for the agents (which, however, is also a drawback of their methodology, as discussed later). It is assumed that the generation intervals τ (i.e. the time interval between two infections) follow a known Weibull distribution $\tau \sim w(\tau|\alpha,\beta)$, where the parameters α and β correspond to the mean and standard deviation of generation intervals and are calculated from a

portion of cases whose infection sources are observed. The authors then specified the pairwise transmission probability between two agents as the relative likelihood of observing the generation interval if transmission takes place between these two agents, which turns out to be

$$P_{i-j} = \frac{w(\tau_{i-j}|\alpha,\beta)}{\sum_{m\neq j} w(\tau_{m-j}|\alpha,\beta)}$$

where P_{i-j} is the probability of pairwise transmission from agent i to agent j, and τ_{i-j} is the generation interval between agent i and agent j. Evaluating the pairwise transmission probabilities enables calculating the mean reproduction number (i.e. the number of infections caused by an infected agent) that are of the key interest to Wallinga and Teunis. However, considering only the temporal correlation of two case occurrences can be misleading, as two spatially distant but close-in-time case occurrences are unlikely to be linked in a given epidemic. It is however worth noting that such a scenario of long-distance but short-in-time transmissions is still possible in Wallinga and Teunis' study because of long-distance transport of potentially infected cattle. Hampson et al. [219] extended Wallinga and Teunis' framework and took into account both the temporal correlation and spatial correlation between two cases when applying the epidemic tree reconstruction technique to Rabies transmissions among dogs in Africa. They specify the pairwise transmission probability as

$$P_{i-j} = \frac{G(t_{ij})K(d_{ij})}{\sum_{m\neq j} G(t_{mj})K(d_{mj})}$$

where $G(t_{ij})$ is the probability distribution of the transmission time interval between case i and j, and $K(d_{ij})$ is the spatial infection kernel. $G(t_{ij})$ and $K(d_{ij})$ are estimated separately: t_{ij} is calculated as the sum of incubation period and "time-to-bite", fitted to a gamma distribution and uniform distribution respectively; and $K(d_{ij})$ is a gamma distribution over the distance between case i and j, with its parameters estimated from cases with known infection sources.

Wallinga and Teunis' study marks a milestone in the network inference methodology with the introduction of probabilistic transmission formulation and the independent cascade model. Their framework is widely adopted, and witnesses multiple variations and extensions from later development. The recent revisit to this framework by social scientists and information scientists is probably the most significant advancement along this line of research.

Rodriguez et al. [188] proposed the NetInf algorithm for inferring the network underlying an information diffusion process. Their work extended the independent cascade model to the case of continuous time, and is the first to tackle the computational complexity in network inference methods. Similar to Wallinga and Teunis [217], the authors predefined a relation between the pairwise transmission probability and the time interval between the failures of the two nodes, by specifying a probability distribution (either exponential or power-law) for the time intervals. The NetInf algorithm, however, does not depend on the choice of a particular time interval distribution, as it is the comparison between the pairwise transmission probabilities along different links that would determine who affects whom. By the independent cascade model and given multiple instances of cascades, the probability of observing these cascades is formulated as

$$P(C|G) = \prod_{c \in C} \left\{ \sum_{T \in T(G)} \left[\prod_{(i,j) \in T} P_c(i,j)\, P(T|G) \right] \right\}$$

where $P_c(i,j)$ is the pairwise transmission probability from node i to node j in cascade c, C represent all the cascade instances, $T(G)$ is the set of all spanning trees in network G, and $P(T|G)$ is the probability distribution for a particular spanning tree T in network G. The challenge in this formulation is the large number of trees to be considered (i.e. the size of $T(G)$) even for a small graph. The authors thus considered only the most likely tree. Under the most likely propagation

tree, the formulation of $P(C|G)$ can be rewritten as $P(C|G) = \prod_{c\in C}\left\{\max_{T\in T(G)}\left[\prod_{(i,j)\in T} P_c(i,j)\, P(T|G)\right]\right\}$. By introducing a null network $\overline{K}$ which serves the baseline, the log-likelihood functions for a single cascade c and for the set of cascades C are respectively

$$F_c(G) = \max_{T\in T(G)} \log\left[\prod_{(i,j)\in T} P_c(i,j)\right] - \max_{T\in T(\overline{K})} \log\left[\prod_{(i,j)\in T} P_c(i,j)\right]$$

$$F_C(G) = \sum_{c\in C} F_c(G)$$

The network inference problem is thus mathematically formulated as a maximizing the likelihood function $F_C(G)$:

$$\hat{G} = \operatorname*{argmax}_G F_C(G)$$

The authors proved that both $F_c(G)$ and $F_C(G)$ are submodular functions, which enables maximizing them using the greedy algorithm. The network can therefore be reconstructed in an iterative process, which starts with an empty network and iterates by adding a link that maximizes the marginal gain in $F_C(G)$ at each step.

While Rodriguez et al. [188] still assumes that pairwise transmission probability is available in the inference algorithm, Myers and Leskovec's study [220] is the first to assume no prior knowledge on the pairwise transmission probability and estimate the probability (more precisely, parameters in this probability). The authors introduced the pairwise transmission probability matrix A, whose entry A_{ij} is the transmission probability from node i to node j. Considering the constraint on transmission time, the pairwise transmission probability from node i to node j with time interval τ_{i-j} is

$$P_{i-j} = w(\tau_{i-j})A_{ij}$$

where $w(\tau_{i\text{-}j})$ is the probability distribution of the transmission time interval (i.e. difference in time between the failure of node i and failure of node j) from node i to node j and the distribution is assumed known. Compared to the formulation in Wallinga and Teunis' study [217] discussed above, introducing A_{ij} enables a more detailed decomposition of the pairwise transmission process: A_{ij} determines whether the transmission will happen or not, and $w(\tau_{i\text{-}j})$ imposes the constraint on transmission time (given that the transmission happens). Therefore, the likelihood of observing a cascading failure event c during which the failure time τ_i of each node i is observed is formulated as:

$$L(c|A) = \left\{ \prod_{i:\tau_i<\infty} \left[1 - \prod_{j:\tau_j \le \tau_i} \left(1 - w(\tau_i - \tau_j) A_{ji}\right) \right] \right\} \left[\prod_{i:\tau_i=\infty} \prod_{j:\tau_j<\infty} \left(1 - A_{ji}\right) \right]$$

The first term of multiplication (in braces) represents the likelihood for the failed nodes and the second term (in brackets) quantifies the effect of right censoring, i.e. some nodes do not fail at the end of observation and the failure times of these nodes will be ∞. The authors deal with the computational complexity of estimating A in the following ways: 1) they prove that maximizing $L(c|A)$ can be transformed into a convex optimization problem; 2) they assume that failure transmissions to two different nodes take place independently, so every column of A can be estimated separately; and 3) the number of parameters to be estimated can be reduced, because the diagonal of A is zero, and if node i and j are not both failed, A_{ij} is also zero. To utilize the third property, the authors further transform the maximum likelihood estimation problem, whose final form would encourage a sparse solution.

Rodriguez et al. [128] is the first to rigorously model the continuous temporal dynamics of failure propagations, which introduced pairwise transmission rate A_{ij} from node i to node j as the

dynamical parameter in pairwise transmission likelihood formulation. It denotes how frequently failure will propagate from node *i* to node *j*. The set of A_{ij}'s are heterogeneous among different pairs of nodes, and vary with time. It is worth noting that in the case of continuous time, the pairwise transmission likelihood is not equal to the pairwise transmission probability. The formulation of pairwise transmission probability takes into account this difference by employing the survival model formalism. The pairwise transmission *likelihood* from node *j* (which fails at time t_j) to node *i* (which fails at time t_i) is denoted as $f(t_i|t_j;\ A_{ji})$, while the survival function $S(t_i|t_j;\ A_{ji})$ indicates the *probability* that the transmission does not happen by the time t_i. The likelihood of observing a cascading failure event *c* is thus formulated as:

$$L(c|A) = \prod_{i:t_i \le T} \left\{ \sum_{j:t_j<t_i} \left[f(t_i|t_j;\ A_{ji}) \cdot \prod_{k:t_k<t_i, k\neq j} S(t_i|t_k;\ A_{ki}) \right] \right\} \cdot \prod_{i:t_i \le T} \prod_{m:t_m>T} S(T|t_i;\ A_{im})$$

where *T* is the time when the observation ends. The term in the brackets is the likelihood that node *j* infected node *i*. It is assumed that every node *i* only have one other node responsible for its failure. The term in the braces represents the likelihood that node *i* failed by time t_i, as all possible cases for *j* are considered. The term following the braces accounts for the right-censoring effect, i.e. the contribution to the likelihood function by the nodes that have not failed at the end of observation. This formulation of cascading failure likelihood is similar to Rodriguez et al. [188], but accounted for the differences between likelihood and probability in continuous time domain, which is overlooked by Rodriguez et al. [188] and all previous studies. This flaw could generate serious problems in previous formulations. For example, $1 - w(\tau_i - \tau_j)A_{ji}$ can be negative and does not have a meaning in Rodriguez et al.'s formulation [188]. The pairwise transmission rates (A) can be estimated through maximizing $L(c|A)$. The pairwise transmission likelihood during a cascade *c* can be calculated from the estimated A and failure times of the two nodes. The authors assume that

a directed link exists from node *i* to node *j* if the estimated A_{ij} (i^{th} row and j^{th} column of A) is greater than zero.

One limitation of Rodriguez et al.'s study [128] is that the pairwise transmission likelihood $f(t_i|t_j;\ A_{ji})$ in the entire network is characterized by a pre-defined fixed distribution (either exponential, power-law or Rayleigh). Du et al. [221] find that the formulation of a single distribution family for all links is far from reality, and proposed a kernel-based method to capture the heterogeneity in pairwise transmission likelihood. They employed the survival model and formulated the likelihood of observing a cascading failure event in a similar manner as in Rodriguez et al. [128]. Instead of assuming a distribution for the pairwise transmission likelihood, Du et al. specifies the hazard function (and thus the pairwise transmission likelihood and survival functions) as the sum of a number of weighted kernel functions.

$$h_{ji}(\tau_{j-i}) = \sum_{l=1}^{m} \alpha_{ji}^{l} k(\tau_l, \tau_{j-i})$$

where $h_{ji}(\tau_{j-i})$ is the hazard function of failure transmission from node *j* to node *i*, $k(\cdot)$ is the kernel function (particularly in this study the Gaussian kernel), and α_{ji}^{l} is the weight parameters to be estimated. The observation period is divided uniformly into *m* intervals and τ_l is the starting time of each interval. If the estimated $\alpha_{ji}^{l} = 0, \forall\ l$, it is considered that there is no link from node *j* to node *i*. To encourage a sparse solution (otherwise it would be difficult to obtain an estimation of $\alpha_{ji}^{l} = 0$) [220], the authors imposed the grouped lasso type of regularization by adding the term $\left(\sum_j \|\vec{\alpha}_{ji}\|\right)^2$ to the negative log-likelihood of observing the failure of node *i*, where $\vec{\alpha}_{ji} = \left(\alpha_{ji}^{1}, \cdots, \alpha_{ji}^{m}\right)^{\mathrm{T}}$.

Recent studies start to develop inference methods that are not solely based on node failure timestamps. The most recent study along the line of network inference research has taken into account the effect of information properties on information propagation patterns. Du et al. [222] proposed a survival-model-based approach to infer the transmission rates of information of different topics in order to predict the spreading speed of certain pieces of information. In addition to the timestamps of node failure (i.e. when a node receives a piece of information), the content of the information also serves as the inputs. The formulation of the likelihood function for the information propagation process in this study follows Rodriguez et al. [128]. The innovation of this study is that it introduced a topic model into this formulation. Similar to Rodriguez et al., the authors assume Rayleigh distributions for the pairwise transmission likelihood with parameter a_{ij} denoting the transmission rate from node i to node j. Instead of estimating $a_{ij}\ \forall i,j$ directly, the authors assume that the transmission rates between nodes are related to the topics conveyed by a piece of information, and formulated a_{ij} as below:

$$a_{ij} = \sum_{l=1}^{K} a_{ij}^{l} m_l$$

where $m_l \in [0,1]$ is the weight of a topic l in this piece of information, and a_{ij}^{l} is a parameter indicating the topic preference for the information transmission from node i to node j. The parameters $a_{ij}^{l}\ \forall i,j,l$ are estimated through MLE in a similar manner as [128].

Another study that incorporated extra information in addition to node failure timestamps was performed by Wang et al. [223], who devised a model to reconstruct the information propagation network on Twitter. The authors formulated the likelihood of observing a cascade by employing the survival-model formalism similar to Rodriguez et al. [128]. The uniqueness of this study is that

1) it accounts for the node-level (i.e. twitter users) features and 2) it expanded Rodriguez et al.'s framework to the scenario in which a node could fail multiple times during a cascade (i.e. a twitter user could post multiple tweets discussing the same piece of information). Node-level features in this study refer to the language and set of words a twitter user use when posting tweets. Based on these two features, the authors define the node distance which characterizes the difference in the features of two nodes *i* and *j* as:

$$d_{L+J}(f_i, f_j) = w_L d_L(f_i, f_j) + w_J d_J(f_i, f_j)$$

which is the weighted (with w_L and w_J as weights) sum of language difference $d_L(f_i, f_j) = \begin{cases} 0, & \text{if user I and j use the same language} \\ 1, & \text{otherwise} \end{cases}$ and word set difference $d_J(f_i, f_j) = 1 - \frac{|f_i \cap f_j|}{|f_i \cup f_j|}$. The node distance function is fed into the formulation of pairwise transmission likelihood by including a term $e^{-d_{L+J}(f_i, f_j)}$:

$$f(t_j, f_j | t_j, f_j; a_{ij}) = e^{-d_{L+J}(f_i, f_j)} f(t_j | t_j; a_{ij})$$

where $f(t_j | t_j; a_{ij})$ is the pairwise transmission likelihood considering only the node failure timestamps as specified in [128]. To address the issue of multiple failures of a node during a cascade, the authors considered a splitting case and a non-splitting case which are distinguished by whether the process is memoryless or not. Only the non-splitting case is investigated in this study, which transformed the survival function for the failure transmission from node *i* to node *j* into:

$$S(t_j | t_i; a_{ij}) = \prod_{j: t_j^{(1)} \le T} \prod_{l: 1 \le l \le N_j} \prod_{i: i \ne j, t_i^{(1)} < t_j^{(l)}} S\left(t_j^{(l)} \middle| t_i; a_{ij}\right)$$

where *T* is the time when the observation ends, $t_j^{(l)}$ is the time of node *j*'s l^{th} failure, and N_j is the total number of failures of node *j*. The above equation conveys the meaning that for the l^{th} failure

of node j, the transmission could take place any time during the time interval $\left(t_i^{(1)}, t_j^{(l)}\right)$, and the probability that the transmission does not happen (i.e. survival of node j) needs to incorporate all N_j transmission (random) events. The formulation of the likelihood of observing a cascade in this study is similar to Rodriguez et al.'s, with modifications corresponding to the changes in characterizing the pairwise transmission process.

In summary, the existing literature has made the following achievements in network inference methodologies by the time this dissertation is written:

- Addressing the probabilistic nature of cascading failures: failure propagations are viewed as random events instead of being deterministic on several factors. The probabilistic understanding of cascading failures facilitates bridging between the local (node/link-level) dynamics and global (network-level) dynamics, and helps to explain phenomenon such as why a system as a whole can have multiple states. Methodologically, it also makes the maximum likelihood estimation a well-established method for solving network inference problems.
- Accounting for the heterogeneity within a network: it is not only recognized that links in a network could have different failure transmission probability and rates (which are typically the parameters for the transmission probability distribution), recent studies also started to address the scenario in which different links have different transmission probability distributions.
- Imposing sparsity in inference problem solutions: the drawback of MLE is that it tends not to generate estimation of zero for the parameters, which would make the inferred network approximate a complete network. Existing research has imposed the grouped lasso type of

regularization to fix this issue. Under this regulation, the output matrix of MLE will have more zero entries, which is closer to real-world network adjacency matrices.

- Reducing computational complexity: existing research has invested considerable efforts in making network inference algorithms computationally tractable. The common techniques include: localization of optimization problems by exploiting the assumed (conditional) independence between pairwise transmissions and between node failures, exploring the convexity and submodularity of likelihood functions, and reducing the number of parameters by utilizing causal properties (e.g. there will be no transmission from a node to another node that fails earlier in time).
- Incorporating node-level factors: the most recent studies start to take into account node characteristics in determining the pairwise transmission probability to or from a given node. It is particularly the case in the research of information diffusion networks, which addresses the effect of information properties and individual preferences to different types of information on the information propagation process.

However, as discussed in detail in section 2.5, this line of research in network inference also poses the following six challenges and limitations:

- Its state of the art can not be applied to interdependent networks, which serve more and more frequently as backdrops of cascading failures.
- It assumes fixed network structures throughout the cascading failure process, while in real-world cases network structures typically evolve with the cascading failure process.
- External factors that could potentially lead to failures are rarely considered, or only considered at the beginning of the cascading failure process.

- Uncertainties, which means multiple failure propagation processes could give rise to the same observed failure outcome, are not addressed.
- The heterogeneity of temporal scales at which cascading failures in different networks take place is overlooked, while it plays a critical role especially in the interdependent network context.
- Modeling assumptions such as the independent cascade assumption and tree pattern assumption (which means every node has only one other node as the failure source) limit the generalizability of its methodologies to modeling a broader range of cascading failures.

Section 4
Methodology

4.1. Methodology overview

Failure propagation is a process that takes place at multiple scales [128]: at local scale, this process is represented by failure transmission along the network links and the resulting failures of nodes; at the global scale, the process embodies itself as a propagation pattern (e.g. a tree structure). Figure 2 shows how the likelihoods associated to the processes at each scale are linked with each other conceptually.

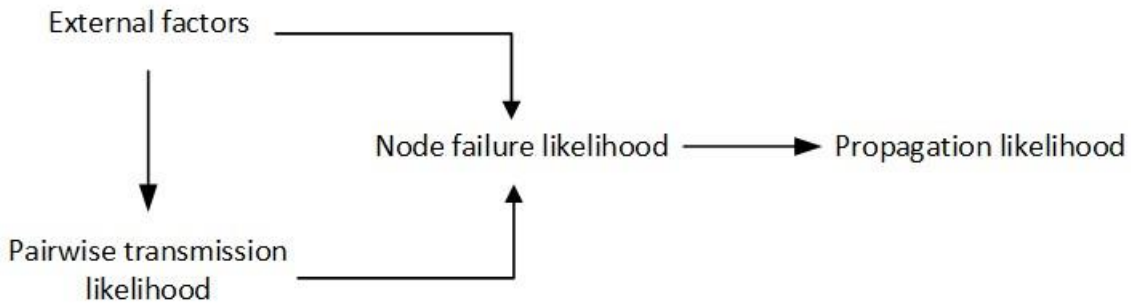

Figure 2: Formulation of likelihood function for a propagation pattern.

External factors such as the damaging forces from a natural disaster could either directly disrupt nodes and cause them to fail, or increase the probability that failures propagate from one node to another. An example of the latter is that during Hurricane Sandy, storm surges make the subway system dependent on the diesel fuel supply system whose failure halted the repairing operation of the inundated subway facilities, while regularly a fuel shortage would not pose an impact on the subway operation [46, 49]. The pairwise failure propagations, together with the external factors, contribute to the failure of a given node. A failure propagation pattern, thereafter, consists of a sequence of node failures. A key difference in this formulation from the existing network inference literature (section 3.2) is that a propagation pattern is viewed as node failure events

(which is called “node perspective”) here instead of as a series of failure transmission events (which is called “link perspective”) as in the network inference literature. Embracing the node perspective by this dissertation is based on the following three considerations. Firstly, it is a convention to view nodes as the functional units of a network. Therefore, modeling cascading failures as node-level dynamics complies with this convention compared to as link-level (i.e. failure transmission) dynamics. Secondly, as external factors are incorporated, the node perspective enables accounting for the direct effect of external factors on node failures. And thirdly, the node perspective relaxes the independent cascade assumption, as discussed in section 4.2.

4.2. Model formulation

The model seeks to infer the failure propagation process – how failures spread from a node to other nodes – from external factors that potentially cause the failures, the spatial relations between nodes (spatial dependence), node failure time (temporal dependence), and prior knowledge of network structures (functional dependence), by formulating a maximum likelihood estimation (MLE) problem. MLE has been applied to modeling the spreading dynamics of disease [127, 217, 219, 224, 225] and information [128, 222, 226, 227]. These two lines of research however, accounts for only the temporal dependence (i.e. the failure time interval) between nodes, and thus requires multiple recurrences of cascades for the estimation. By synthesizing external factors, spatial dependence and prior knowledge on network topologies in addition to the temporal dependence, the data requirement on cascading failure observations is

reduced, which enables estimation with only one observed cascade instance.

A general model formulation that has universal applicability to all types of cascading failures is first presented in section 4.2.1 and 4.2.2. From the general formulation, four specific model implementations for the cascading failures in interdependent power and transportation networks, influenza epidemics, congestion cascade and cascading power outages, respectively, are further developed. These four cascading failure instances are used later to validate the model on its accuracy in inferring the cascading failure process and its robustness against varying failure propagation mechanisms.

4.2.1. General formulation using survival model

In a discrete time setting, the observed failure time of every node is denoted as $\boldsymbol{t} = [t_1, \dots, t_N]$, where N is the total number of nodes in the targeted network(s), and t_i is the time step in which node i was observed to fail. A random vector $\boldsymbol{T} = [T_1, \dots, T_N]$ corresponding to $\boldsymbol{t}$ represents the survival time of each node. The general-form MLE problem is formulated by equation (1).

$$\langle \boldsymbol{\beta} \rangle = \underset{\boldsymbol{\beta}}{\operatorname{argmax}}\, P\left(\boldsymbol{T} = \boldsymbol{t} \middle| \boldsymbol{E}, P_{j\to i}\ \forall\, i \in \mathbb{N}, j \in \mathbb{N}, i \neq j\right), \tag{1}$$

where $\boldsymbol{\beta} = \{\boldsymbol{\beta^E}, \boldsymbol{\beta^S}, \boldsymbol{\beta^F}\}$ is a set of parameters associated with external factors ($\boldsymbol{\beta^E}$), spatial dependencies ($\boldsymbol{\beta^S}$) and functional dependencies ($\boldsymbol{\beta^F}$) respectively, $\boldsymbol{E}$ is a set of external factors, $P_{j\to i}$ denotes the probability of failure for node i due to failure propagation from node j to node I (which will be defined later), and $\mathbb{N}$ is the set of nodes in the network(s). Equation (1) suggests that failure of a node i at time t_i is attributed to a combination of effects from external factors and failure propagations. External factors could vary with the context of cascading failures. In infrastructure network failures for example, they could be disaster impacts that initialize the

cascade [153]; and in epidemics, they may refer to climate variability which could trigger disease outbreaks such as malaria [228]. Nodes that fail due to external factors become failure sources (seeds) that may further spread the failure to other nodes. The failure propagation term $P_{j\to i}$ accounts for three mechanisms of failure propagations: temporal, spatial and functional. The temporal/spatial mechanism specifies how the failures propagate in time/space: failures tend to propagate from one node to another node if these two nodes fail close in time/distance. And the functional mechanism specifies failure propagations rising from nodes' logical connections which correlate the functions of given two nodes. These three failure propagation mechanisms are abstract mechanisms that apply universally to a broad range of networks, instead of being specific ones existing in certain domains such as flow redistribution or load unbalancing in power networks.

It is assumed that given all the mechanisms leading to node failures, the survival time of nodes is conditionally independent of each other. This assumption is consistent with the rules of conditional independence derived from Bayesian networks, which state that two nodes in a Bayesian network are conditionally independent given their parent nodes [229]. Equation (1) can thus be rewritten in terms of node failure probabilities as in equation (2).

$$\langle \boldsymbol{\beta} \rangle = \underset{\boldsymbol{\beta}}{\operatorname{argmax}} \prod_{i\in\mathbb{N}} \prod \left[1 - P\left(T_i = t_i - 1 \middle| \boldsymbol{E}, P_{j-i}\ \forall\, j \in \mathbb{N}\backslash i\right)\right] \cdot P\left(T_i = t_i \middle| \boldsymbol{E}, P_{j\to i}\ \forall\, j \in \mathbb{N}\backslash i\right), \quad (2)$$

which decomposes the cascading failure event into a sequence of (conditionally) independent node failures. The term $\left[1 - P\left(T_i = t_i \middle| \boldsymbol{E}, P_{j\to i}\ \forall\, j \in \mathbb{N}\backslash i\right)\right]$ accounts for a necessary condition for node *i* to fail at time t_i: that this node has not yet failed at the previous time step $t_i - 1$. Since the network has unknown topology, it is assumed that every node other than *i* itself has a probability of spreading failures to node *i*. This assumption will be relaxed later. The node failure

probability $P\left(T_i = t_i \middle| \boldsymbol{E}, P_{j\to i}\ \forall\, j \in \mathbb{N}\backslash i\right)$ in equation (2) is also the conditional density of survival time T_i, which enables formulating it as in equation (3-5) using the hazard function $\lambda_i(t_i)$ and the survival function $S_i(t_i)$. For readability, the conditional terms in the equations will be left out in the rest of the dissertation text. However, all node failure probabilities (or survival densities), survival functions and hazard functions are conditioned on the external factors and failure propagations except those explicitly declared (as in equation (6)).

$$P(T_i = t_i) = S_i(t_i) \cdot \lambda_i(t_i) = \prod_{\tau=1}^{t_i-1}[1 - \lambda_i(\tau)]\, \lambda_i(t_i), \forall i\ t_{OS} < t_i \le t_{OE}; \tag{3}$$

$$P(T_i = t_i) = S_i(t_{OE}) \cdot [1 - \lambda_i(t_{OE})] = \prod_{\tau=1}^{t_{OE}}[1 - \lambda_i(\tau)]\,, \forall i\ t_i > t_{OE}; \tag{4}$$

$$P(T_i = t_i) = 1 - S_i(t_{OS}) = 1 - \prod_{\tau=1}^{t_{OS}}[1 - \lambda_i(\tau)]\,, \forall i\ t_i \le t_{OS}; \tag{5}$$

where t_{OS} and t_{OE} are the time when observation starts and ends, respectively. Equation (3), (4) and (5) concern the cases of completely observed node failures, right-censored nodes and left-censored nodes, respectively. Proof of equation (3) is provided below, and equation (4) and equation (5) can be derived similarly. Node failure probabilities in all three cases thus reduce to function forms in terms of hazard functions.

Proof of Equation (3). Supposing the probability density distribution of survival time T_i is denoted as $f_i(t_i)$. Based on the proven relation between survival function, hazard function and survival time density $f_i(t_i) = S_i(t_i) \cdot \lambda_i(t_i)$, the following relation stands.

$$1 - \lambda_i(t_i) = 1 - \frac{f_i(t_i)}{S_i(t_i)} = \frac{S_i(t_i) - f_i(t_i)}{S_i(t_i)} = \frac{P(T_i \ge t_i) - P(T_i = t_i)}{S_i(t_i)} = \frac{P(T_i \ge t_i) - P(T_i = t_i)}{S_i(t_i)}$$

$$= \frac{P(T_i \geq t_i + 1)}{S_i(t_i)} = \frac{S_i(t_i + 1)}{S_i(t_i)} \tag{P1}$$

Thereby, the following series of equations stand.

$$1 - \lambda_i(1) = \frac{S_i(2)}{S_i(1)}$$

$$1 - \lambda_i(2) = \frac{S_i(3)}{S_i(2)}$$

$$\vdots$$

$$1 - \lambda_i(t_i - 1) = \frac{S_i(t_i)}{S_i(t_i - 1)}$$

Multiplying them together produces the following relation as in equation (3).

$$S_i(t_i) = \prod_{\tau=1}^{t_i-1} [1 - \lambda_i(\tau)] \tag{P2}$$

The proof is thereby complete. It is worth noting that the derivation process does not involve the assumption that the failure hazards of a node at different time steps are independent (i.e. lack of auto-correlations), as seemingly implied by equation (P2). Therefore, equation (3) and similarly equations (4) and (5) are general and apply to any arbitrary failure process.

To formulate the hazard function, no interactive effect between external factors and failure propagations is assumed, and thus failure due to external factors and failure due to propagations are viewed as independent events, which leads to equation (6).

$$\lambda_i(t_i) = 1 - [1 - \lambda_i(t_i|\boldsymbol{E})] \prod_{j \in \mathbb{N} \setminus i} \left(1 - P_{j \to i}\right), \tag{6}$$

where $\lambda_i(t_i|\boldsymbol{E})$ is the failure hazard of node *i* at time t_i associated with external factors. The right-hand side of equation (6) specifies the probability that the external factors and propagations

combined lead to the failure of node *i* at time t_i. The quantity $P_{j\to i}$ is the probability that failure propagation from node *j* to node *i* leads to the failure of node *i* at the observed time step t_i. It suggests the **causality** between the failure of node *i* at time t_i and failure propagation from node *j* to node *i*.

For this causal relation to hold, the following two statements must be true at the same time.

Statement 1: If failure propagation from *j* to *i* happens, node *i* fails at time t_i; and

Statement 2: If failure propagation from *j* to *i* does not happen, node *i* does not fail at time t_i.

These two statements are illustrated in figure 3, with figure 3a showing the condition in statement 1 that failure propagation from *j* to *i* happens and figure 3b showing the condition in statement 2 that failure propagation from *j* to *i* does not happen. It is worth noting that failure propagations to *i* from nodes other than *j* are disabled, i.e. $P(\mathbb{N}\backslash j \to i) = 0$ where $\mathbb{N}$ is the set of nodes and "$\mathbb{N}\backslash j \to i$" denotes failure propagations from nodes other than *j* to node *i*. This setting removes the confounding factors for the failure of node *i*. The notation $j^- \nrightarrow i$ is introduced to denote this setting, which means the failure propagations from nodes other than *j* (symbolized as j^-) to node *i* are all impossible. Similarly, the notations $j \to i$ and $j \nrightarrow i$ are used to denote the conditions that the failure propagation from node *j* to node *i* could happen and could not happen, respectively. Therefore, $P_{j\to i}$, the probability that failure propagation from node *j* to node *i* causes the failure of node *i* at time step t_i and furthermore the probability that statement 1 and statement 2 are both true, can be rewritten in the following terms.

$$P_{j\to i} \coloneqq P(\text{Statement 1}) \cdot P(\text{Statement 2})$$
$$= P(T_i = t_i | j \to i, j^- \nrightarrow i) \cdot P(T_i \neq t_i | j \nrightarrow i, j^- \nrightarrow i).$$

In the above equation, $T_i = t_i | j \to i, j^- \nrightarrow i$ and $T_i \neq t_i | j \nrightarrow i, j^- \nrightarrow i$ are equivalent terms for

statement 1 and statement 2, respectively.

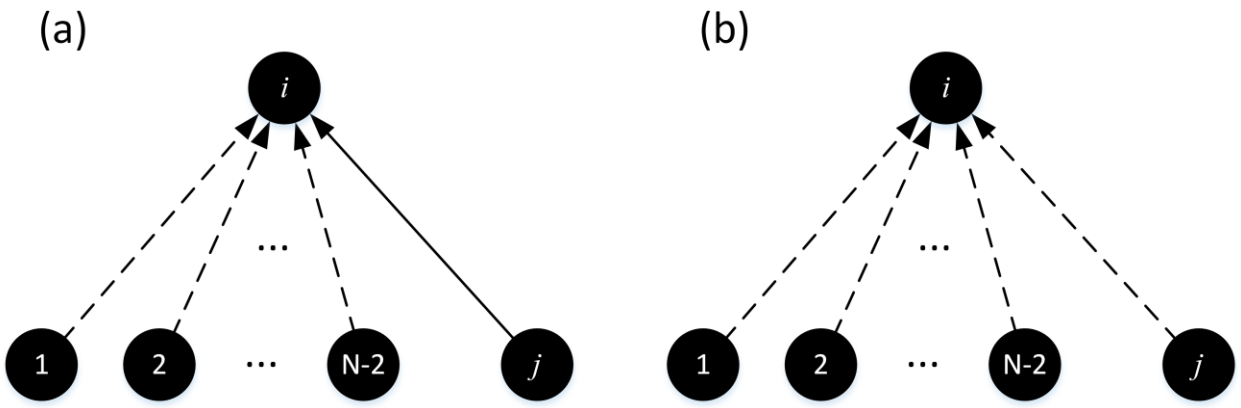

Figure 3: Defining P_{j-i} with causal statements. (a) and (b) illustrate the conditions in statement 1 and statement 2, respectively. Dash lines indicate impossible (direct) failure propagation paths; and a solid line indicates that failure propagation could happen (with a probability).

Further assuming a closed environment where no additional events besides failure propagations from nodes other than *i* to *i* could cause the failure of node *i*, it would then be impossible for node *i* to fail if none of the failure propagations takes place (e.g. $j \nrightarrow i, j^- \nrightarrow i$). Under this assumption, $P(T_i \neq t_i | j \nrightarrow i, j^- \nrightarrow i) = 1$, and consequently,

$$P_{j \to i} = P(T_i = t_i | j \to i, j^- \nrightarrow i). \tag{7}$$

Equation (7) suggests that the probability of node *i* failing at time t_i due to failure propagation from node *j* can be quantified by a single conditional probability $P(T_i = t_i | j \to i, j^- \nrightarrow i)$ which denotes the probability that node *i* fails at t_i when failure propagation from node *j* to node *i* happens (probabilistically). Conceptually, the event "failure propagation from node *j* to *i* causes node *i* to fail at time t_i" consists of three events happening in sequence: 1) node *j* fails at time t_j; 2) failure propagation from node *j* to node *i* happens after a time interval $t_i - t_j$; and 3) node *i* fails at time t_i. The probability $P_{j \to i}$ can thereby be formulated as the probability that these three

events all happen as in equation (8).

$$P_{j\to i} = \sum_{t_j : t_j < t_i} P\big(T_j = t_j\big) P\big(\tau_{j\to i} = t_i - t_j \big| j \to i, j^- \nrightarrow i\big), \tag{8}$$

where $\tau_{j\to i}$ denotes how much time it takes for failure to propagate from node *j* to node *i*. The summation over t_j accounts for the uncertainty in node *j*'s failure time, as it is not specified by $P_{j\to i}$. The probabilities $P\big(T_j = t_j\big)$ and $P\big(\tau_{j\to i} = t_i - t_j\big)$ are the probabilities for the events 1) failure of node *j* at time t_j and 2) failure propagation from node *j* to node *i* happening after $t_i - t_j$, respectively. It is assumed that the occurrence of these two events is sufficient to trigger the event 3) failure of node *i* at time t_i, i.e. $P\big(T_i = t_i \big| T_j = t_j, \tau_{j\to i} = t_i - t_j\big) = 1$, whose probability would thus be redundant to be included in equation (8). Proof of equation (8) is provided in the following subsection.

Proof of Equation (8). Introducing another variable T_j to the probability $P(T_i = t_i | j \to i, j^- \nrightarrow i)$ results in equation (P3).

$$P(T_i = t_i | j \to i, j^- \nrightarrow i) = \sum_{t_j} P\big(T_i = t_i, T_j = t_j \big| j \to i, j^- \nrightarrow i\big)$$

$$= \sum_{t_j} P\big(T_i = t_i \big| T_j = t_j, j \to i, j^- \nrightarrow i\big) \cdot P\big(T_j = t_j \big| j \to i, j^- \nrightarrow i\big). \tag{P3}$$

The failure time of node *i* can be written as the failure time of node *j* plus the time interval it takes for failure to propagate from node *j* to node *i*, i.e. $T_i = T_j + \tau_{j\to i}$. The first term in the summation in equation (P3) can thus be written as in equation (P4).

$$P\big(T_i = t_i \big| T_j = t_j, j \to i, j^- \nrightarrow i\big) = P\big(T_j + \tau_{j\to i} = t_j + t_i - t_j \big| T_j = t_j, j \to i, j^- \nrightarrow i\big)$$

$$= P\big(\tau_{j\to i} = t_i - t_j \big| T_j = t_j, j \to i, j^- \nrightarrow i\big), \tag{P4}$$

Equation (P4) connects failure of a node with the failure propagation to it. The probability $P\left(\tau_{j\to i} = t_i - t_j \middle| T_j = t_j, j \to i, j^- \nrightarrow i\right)$ essentially quantifies the probability distribution of propagation time interval $\tau_{j\to i}$ if node *j* fails at a given time and failure propagation from node *j* to node *i* takes place. Equation (P4) suggests that the distribution of propagation time interval $\tau_{j\to i}$ depends on the time of onset for the failure propagation, i.e. when the source node *j* fails and the failure propagation to node *i* (possibly) starts. We call this type of failure propagations **time-variant propagations**, where the dynamics of failure propagation between two given nodes change with time. In the case of real-world cascading failures however, typical failure propagations progress rapidly, and the evolution of failure propagation dynamics with time can be disregarded, leading to **time-invariant propagations**. In this case, the distribution of $\tau_{j\to i}$ can be approximated by a stationary distribution as shown in equation (P5). In the present study, only the time-invariant case is accounted for, considering that cascading failures in infrastructure systems such as traffic congestions and power outages are usually fast processes [162, 184, 230].

$$P\left(T_i = t_i \middle| T_j = t_j, j \to i, j^- \nrightarrow i\right) = P\left(\tau_{j\to i} = t_i - t_j \middle| T_j = t_j, j \to i, j^- \nrightarrow i\right)$$
$$= P\left(\tau_{j\to i} = t_i - t_j \middle| j \to i, j^- \nrightarrow i\right). \quad \text{(P5)}$$

For the second term in the summation in equation (P3), $P\left(T_j = t_j \middle| j \to i, j^- \nrightarrow i\right)$ denotes the probability that node *j* fails at time t_j if failure propagation from node *j* to node *i* (possibly) happens. The condition that failure propagation from node *j* to node *i* could happen imposes no constraints on the failure time of node *j* other than that node *j* has to fail before node *i* fails. Equation (P6) thus stands.

$$P\left(T_j = t_j \middle| j \to i, j^- \nrightarrow i\right) \equiv P\left(T_j = t_j \middle| t_j < t_i\right). \quad \text{(P6)}$$

Combining equation (7) and (P3)-(P6), the probability $P_{j\to i}$ can be written as in equation (P7).

$$P_{j\to i} = P(T_i = t_i | j \to i, j^- \nrightarrow i)$$

$$= \sum_{t_j} P\left(T_i = t_i \middle| T_j = t_j, j \to i, j^- \nrightarrow i\right) \cdot P\left(T_j = t_j \middle| j \to i, j^- \nrightarrow i\right)$$

$$= \sum_{t_j} P\left(\tau_{j\to i} = t_i - t_j \middle| j \to i, j^- \nrightarrow i\right) \cdot P\left(T_j = t_j \middle| t_j < t_i\right)$$

$$= \sum_{t_j : t_j < t_i} P\left(\tau_{j\to i} = t_i - t_j \middle| j \to i, j^- \nrightarrow i\right) \cdot P\left(T_j = t_j \middle| t_j < t_i\right)$$

$$+ \sum_{t_j : t_j \geq t_i} P\left(\tau_{j\to i} = t_i - t_j \middle| j \to i, j^- \nrightarrow i\right) \cdot P\left(T_j = t_j \middle| t_j < t_i\right). \quad \text{(P7)}$$

For the first summation in equation (P7), the condition $t_j < t_i$ for the conditional probability $P\left(T_j = t_j \middle| t_j < t_i\right)$ is redundant, as $P\left(t_j < t_i\right) \equiv 1$, i.e. the condition is always true. Therefore, $P\left(T_j = t_j \middle| t_j < t_i\right) \equiv P\left(T_j = t_j\right)$. For the second summation in equation (P7), $t_j \geq t_i$ would result in $\tau_{j\to i} \leq 0$. As a time interval, $\tau_{j\to i}$ is not defined in the negative domain. Consequently, $P\left(\tau_{j\to i} = t_i - t_j \middle| j \to i, j^- \nrightarrow i\right) \equiv 0$ for $\tau_{j\to i} \leq 0$, which means the second summation is constantly equal to zero. Equation (P7) is thus simplified to equation (P8).

$$P_{j\to i} = \sum_{t_j : t_j < t_i} P\left(\tau_{j\to i} = t_i - t_j \middle| j \to i, j^- \nrightarrow i\right) \cdot P\left(T_j = t_j\right). \quad \text{(P8)}$$

Proof of equation (8) is therefore complete.

Putting equation (3)/(4)/(5), (6) and (8) together, it becomes obvious that evaluating the likelihood function in equation (1) reduces to evaluating two probabilities, $\lambda_i(t_i|\boldsymbol{E})$ and $P\left(\tau_{j\to i} = t_i - t_j \middle| j \to i, j^- \nrightarrow i\right)$, respectively (note that the hazard function λ is also a probability in discrete-time setting). The general functional forms for $\lambda_i(t_i|\boldsymbol{E})$ and $P\left(\tau_{j\to i} = t_i - t_j \middle| j \to i, j^- \nrightarrow i\right)$ can be described by equation 5 and 6, respectively.

$$\lambda_i(t_i|\boldsymbol{E}) = f_e(t_i, \boldsymbol{E};\, \boldsymbol{\beta^E}, \boldsymbol{\beta^T}), \quad (9)$$

$$P\left(\tau_{j\to i} = t_i - t_j \middle| j \to i, j^- \nrightarrow i\right) = f_p\left(\tau_{ji};\, \boldsymbol{\beta^S}, \boldsymbol{\beta^T}, \boldsymbol{\beta^F}\right). \quad (10)$$

The functional forms f_e and f_p, for external factors and propagations are determined by the type of cascading failures modeled. In each of the simulation studies, fixed probability distributions for f_e and f_p are assumed. The detailed formulations for $\lambda_i(t_i|\boldsymbol{E})$ and $P\left(\tau_{j\to i} = t_i - t_j \middle| j \to i, j^- \nrightarrow i\right)$ in each simulation study are discussed in section 4.3.

4.2.2. Quantification of failure propagation patterns

Besides $\lambda_i(t_i|\boldsymbol{E})$ and $P\left(\tau_{j\to i} = t_i - t_j \middle| j \to i, j^- \nrightarrow i\right)$, another quantity of interest is the probability of failure propagation from node *j* to node *i* given the observed failure time t_j and t_i, which can be written as $P\left(j \to i \middle| T_j = t_j, T_i = t_i\right)$. Evaluating this probability helps to answer the question: how likely failure has propagated from a given node to another node in an observed cascading failure instance? This subsection shows how $P\left(j \to i \middle| T_j = t_j, T_i = t_i\right)$ can be evaluated.

Introducing the variables "$j \rightsquigarrow i$"$\in \{j \to i, j \nrightarrow i\}$ and "$j^- \rightsquigarrow i$"$\in \{j^- \to i, j^- \nrightarrow i\}$ to account for the uncertainties in whether failure propagations from *j* to *i*, and from nodes other than *j* to *i* happen or not, $P\left(j \to i \middle| T_j = t_j, T_i = t_i\right)$ can be written as in equation (11).

$$P\left(j \to i \middle| T_j = t_j, T_i = t_i\right) = \sum_{j^-\rightsquigarrow i} P\left(j \to i, j^- \rightsquigarrow i \middle| T_j = t_j, T_i = t_i\right)$$

$$= \frac{\sum_{j^-\rightsquigarrow i} P\left(T_j = t_j, T_i = t_i \middle| j \to i, j^- \rightsquigarrow i\right) \cdot P(j \to i, j^- \rightsquigarrow i)}{\sum_{(j\rightsquigarrow i, j^-\rightsquigarrow i)} P\left(T_j = t_j, T_i = t_i \middle| j \rightsquigarrow i, j^- \rightsquigarrow i\right) \cdot P(j \rightsquigarrow i, j^- \rightsquigarrow i)}. \quad (11)$$

The second line of equation (11) applies Bayesian Theorem to the posterior probability $P\left(j \to i, j^- \rightsquigarrow i \middle| T_j = t_j, T_i = t_i\right)$. It decomposes this probability into the likelihoods of observing $T_j = t_j, T_i = t_i$ under four conditions: $(j \nrightarrow i, j^- \nrightarrow i)$, $(j \to i, j^- \nrightarrow i)$, $(j \nrightarrow i, j^- \to i)$ and $(j \to$

$i, j^- \to i$). The four conditions are considered separately below.

1) The first condition ($j \nrightarrow i, j^- \nrightarrow i$) suggests that no propagation to *i* happens, and thus node *i* could not fail, i.e. $T_i = \infty$. For finite values of t_i and t_j, $P\left(T_j = t_j, T_i = t_i \middle| j \nrightarrow i, j^- \nrightarrow i\right) = 0$.

2) The second condition ($j \to i, j^- \nrightarrow i$) leads to the likelihood $P\left(T_j = t_j, T_i = t_i \middle| j \to i, j^- \nrightarrow i\right)$ which can be evaluated by equation (12).

$$P\left(T_j = t_j, T_i = t_i \middle| j \to i, j^- \nrightarrow i\right) = P\left(T_j = t_j \middle| T_i = t_i, j \to i, j^- \nrightarrow i\right) \cdot P(T_i = t_i | j \to i, j^- \nrightarrow i)$$
$$= P\left(\tau_{j \to i} = t_i - t_j \middle| j \to i, j^- \nrightarrow i\right) \cdot P_{j \to i}, \quad (12)$$

where $P\left(\tau_{j \to i} = t_i - t_j \middle| j \to i, j^- \nrightarrow i\right)$ and $P_{j \to i}$ are quantified by equation (10) and (8), respectively.

3) The third condition ($j \nrightarrow i, j^- \to i$) suggests that node *j* can not propagate failure to node *i* while other nodes can. The probability $P\left(T_j = t_j, T_i = t_i \middle| j \nrightarrow i, j^- \to i\right)$ can be decomposed into the probabilities of two individual node failures as in equation (13).

$$P\left(T_j = t_j, T_i = t_i \middle| j \nrightarrow i, j^- \to i\right)$$
$$= P\left(T_i = t_i \middle| T_j = t_j, j \nrightarrow i, j^- \to i\right) \cdot P\left(T_j = t_j \middle| j \nrightarrow i, j^- \to i\right). \quad (13)$$

Evaluating these two probabilities is equivalent to quantify a cascading failure process in the subnetwork G^S as shown in figure 4.

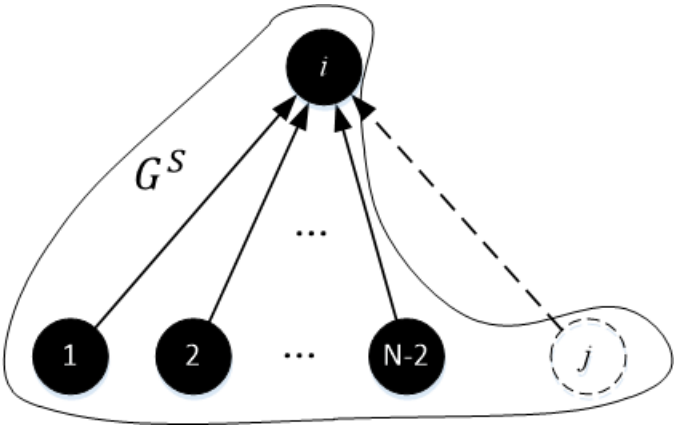

Figure 4: Subnetwork equivalence for the condition $(j \nrightarrow i, j^- \rightarrow i)$.

Therefore, $P(T_j = t_j | j \nrightarrow i, j^- \rightarrow i)$ is equivalent to the likelihood of node j failing in the subnetwork G^S, namely $P(T_j = t_j | G^S)$. Similarly, $P(T_i = t_i | T_j = t_j, j \nrightarrow i, j^- \rightarrow i) \equiv P(T_i = t_i | T_j = t_j, G^S)$. The probability $P(T_j = t_j | G^S)$ can be evaluated by transforming it into the form of hazard functions as in equation (3)-(5), and further quantifying the failure hazards of node j due to external factors and due to failure propagations in the subnetwork G^S, respectively. In general, $P(T_j = t_j | G^S) = P(T_j = t_j)$, as disabling the propagation path from node *j* to node *i* has no effect on either the failure of node j due to external factors or failure due to propagations, considering that the network is assumed to have no cycles which precludes the existence of any effect (direct or indirect) of $j \rightsquigarrow i$ on node *j*'s failure.

For the probability $P(T_i = t_i | T_j = t_j, G^S)$, it can also be transformed in terms of hazard functions, and furthermore in terms of the failure hazard due to external factors and due to failure propagations, as shown in equation (6-1), a modified version of equation (6).

$$\lambda_i(t_i | T_j = t_j, G^S) = 1 - [1 - \lambda_i(t_i | \boldsymbol{E})] \prod_{k \in \mathbb{N} \setminus \{i,j\}} (1 - P_{k \rightarrow i}), \tag{6-1}$$

where $P_{k \rightarrow i}$ is evaluated similarly as in equation (8).

$$P_{k\to i} = \sum_{t_k : t_k < t_i} P\left(T_k = t_k \middle| T_j = t_j, G^S\right) \cdot P(\tau_{k\to i} = t_i - t_k | k \to i, k^- \nrightarrow i), \qquad (8\text{-}1)$$

where, under homogeneity assumption, $P(\tau_{k\to i} = t_i - t_k | k \to i, k^- \nrightarrow i)$ is the same probability distribution as $P\left(\tau_{j\to i} = t_i - t_j | j \to i, j^- \nrightarrow i\right)$. As failure of node *j* has no direct effect on the failure of node *i* (due to failure propagation from node *j* to node *i* being disabled), equation (6-1) and (8-1) only consider the indirect effect of the condition $T_j = t_j$ through the failure of node *k*, which is quantified by the probability $P\left(T_k = t_k \middle| T_j = t_j, G^S\right)$. This probability again, can be written in the forms of hazard functions and furthermore in the forms of failure hazard due to external factors and failure hazard due to propagations. When quantifying the failure hazard of node *k* due to failure propagations, the condition $T_j = t_j$ needs to be accounted for, as in equation (6-2) that formulates the hazard function for node *k*.

$$\lambda_k\left(t_k \middle| T_j = t_j, G^S\right) = 1 - [1 - \lambda_k(t_k | \boldsymbol{E})]\left(1 - P_{j\to k}\right) \prod_{l \in \mathbb{N}\setminus\{k,j\}} (1 - P_{l\to k}), \qquad (6\text{-}2)$$

where $P_{j\to k}$ is the failure hazard of node *k* due to failure propagation from node *j*, which can be evaluated as $P_{j\to k} = P\left(\tau_{j\to k} = t_k - t_j | j \to k, j^- \nrightarrow k\right)$. This equation is an reduction from equation (8-1), without considering the uncertainties in the failure time of node *j*, since the failure time T_j of node *j* is given as t_j.

The above derivations imply that evaluating $P\left(T_i = t_i \middle| T_j = t_j, G^S\right)$, the probability of node *i* failing at the subnetwork G^S at t_i, requires a progressive algorithm. Starting at time step 1, the algorithm evaluates the hazard and probability of each node failing at this time step. Then it moves to the next time step and evaluates the hazard and probability of each node failing at the current time step. This process iterates until reaching time step t_i.

4) The fourth condition $(j \to i, j^- \to i)$ suggests that failure propagations from all nodes other than *i* to *i* are possible. The probability $P(T_j = t_j, T_i = t_i | j \to i, j^- \to i)$ can be evaluated in a similar way as for the probability $P(T_j = t_j, T_i = t_i | j \nrightarrow i, j^- \to i)$ under condition (3). However, as propagation from node *j* to node *i* is possible now, formulating the failure hazard of node *i* needs to account for the special case of failure propagation from *j* to *i*. Equation (6-1) for the failure hazard of node *i* thus needs to be reformulated as in equation (6-3), similarly as the failure hazard of node *k* in equation (6-2).

$$\lambda_i(t_i | T_j = t_j, G^S) = 1 - [1 - \lambda_i(t_i|\boldsymbol{E})](1 - P^C_{j\to i}) \prod_{l \in \mathbb{N}\setminus\{i,j\}} (1 - P_{l\to i}), \qquad (6\text{-}3)$$

where $P^C_{j\to i}$, the failure hazard of node *i* due to failure propagation from node *j* given $T_j = t_j$, is evaluated as $P^C_{j\to i} = P(\tau_{j\to i} = t_i - t_j | j \to i, j^- \nrightarrow i)$.

The above derivations enable formulating and evaluating the likelihood of observing $T_j = t_j, T_i = t_i$ under the four conditions (1), (2), (3) and (4), namely $P(T_j = t_j, T_i = t_i | j \nrightarrow i, j^- \nrightarrow i)$, $P(T_j = t_j, T_i = t_i | j \to i, j^- \nrightarrow i)$, $P(T_j = t_j, T_i = t_i | j \nrightarrow i, j^- \to i)$ and $P(T_j = t_j, T_i = t_i | j \to i, j^- \to i)$. For the prior probabilities of these four conditions, they are inferred by generating null models and calculating the proportion of each condition in the null model ensemble.

A null model is a network with some properties predefined while all other properties are randomized [177]. It enables utilizing existing knowledge in failure propagation patterns in certain networks. A null model ensemble is a set of null models that share the predefined properties, which

correspond to the existing knowledge in failure propagation patterns. For example, existing literature has shown that the propagation networks in power systems and transportation systems have degree distributions which follow exponential distribution and power-law distribution, respectively [231-235]. A null model for failure propagations in a power system will thus be a network with a given exponential degree distribution, whose other (topological) properties are randomized.

The null models are applied in the simulation studies of interdependent infrastructure cascading failures, congestion cascade and cascading power outages. These three simulation studies involve modeling failure propagations in a power system, in a transportation system, and between a power system and a transportation system through interdependencies. Therefore, null models need to be generated for each of these three types of failure propagations. For failure propagations in power systems, an ensemble of null models that share the following exponential degree distribution is constructed.

$$p(o > O) \sim exp(-\zeta O),$$

where o and O are the random variable and a realization corresponding to the node degree, respectively, and the coefficient $\zeta = 0.5$ for North American power systems [231, 236]. For failure propagations in transportation networks, the following power-law degree distribution is used instead.

$$p(o = O) \sim O^{-\gamma},$$

where the power-law coefficient γ has a value of 4 [235]. For failure propagations through interdependencies, it is assumed that nodes with a high degree, typically larger than 10, have a function of mutual supporting [147]. Therefore, two high degree nodes in a power system null

model and a transportation system null model respectively are viewed as being interdependent.

To generate power/transportation system null models that follow the above distributions as well as the interdependencies, the steps specified by Catanzaro et al.'s uncorrelated configuration model (UCM) [237] are followed. First, for every node in a network, a random number is drawn from the corresponding degree distribution and assigned to the node as its degree. The random number o_i drawn for every node i is subject to the condition $\sum_i o_i$ is even $2 < o_i < N^{1/2}$ where N is the number of nodes in the network. Then nodes are randomly connected using $\frac{\sum_i o_i}{2}$ edges, by randomly selecting two nodes that have not yet reached their target degrees and connecting them. These two steps are implemented for the power system and transportation system, respectively. Interdependent links will emerge between a power node and a transportation node once both nodes reach a degree ≥10 following Duenas-Osorio et al. [147]. The above three steps generate a pair of interdependent power and transportation networks. An ensemble of 100 such pairs are generated by repeating the above three steps 100 times.

The prior probabilities of the four conditions, namely $P(j \nrightarrow i, j^- \nrightarrow i)$, $P(j \rightarrow i, j^- \nrightarrow i)$, $P(j \nrightarrow i, j^- \rightarrow i)$ and $P(j \rightarrow i, j^- \rightarrow i)$, can be evaluated based on the null models. For example, $P(j \rightarrow i, j^- \nrightarrow i)$ is the proportion of null models in which a link exists from node j to node i and there is no link from nodes other than j to i in the null model ensemble.

With each of the four prior probabilities (i.e. $P(j \nrightarrow i, j^- \nrightarrow i)$, $P(j \rightarrow i, j^- \nrightarrow i)$, $P(j \nrightarrow i, j^- \rightarrow i)$ and $P(j \rightarrow i, j^- \rightarrow i)$) and the four likelihoods of observing $T_j = t_j, T_i = t_i$ under the four conditions (i.e. $P(T_j = t_j, T_i = t_i | j \nrightarrow i, j^- \nrightarrow i)$, $P(T_j = t_j, T_i = t_i | j \rightarrow i, j^- \nrightarrow i)$,

$P\left(T_j = t_j, T_i = t_i \middle| j \nrightarrow i, j^- \rightarrow i\right)$ and $P\left(T_j = t_j, T_i = t_i \middle| j \rightarrow i, j^- \rightarrow i\right)$) evaluated, the inferred probability of failure propagation from a given node *j* to another given node *i* can be evaluated by equation (11).

4.3. Specific model formulation for the simulation studies

All quantities in section 4.2, including the likelihood function, node failure probabilities, node failure hazards (due to external factors or failure propagations) and failure propagation probabilities, as well as the probability of failure propagation within a given time interval which will be formally defined in section 5.1, are shown to be functions of two quantities: failure hazards due to external factors $\lambda_i(t_i|\boldsymbol{E})$ and the probability distribution of the time interval for failure propagations $P\left(\tau_{j\rightarrow i} = t_i - t_j \middle| j \rightarrow i, j^- \nrightarrow i\right)$. Therefore, formulating and evaluating these two quantities is the key to infer other quantities of interest. The formulations of $\lambda_i(t_i|\boldsymbol{E})$ and $P\left(\tau_{j\rightarrow i} = t_i - t_j \middle| j \rightarrow i, j^- \nrightarrow i\right)$ are determined by the functional forms f_e and f_p as in equation (9) and (10), respectively.

Two specific functional forms for f_e and f_p are employed in the four simulation studies. In the study of interdependent infrastructure cascading failures, geometric functions are adopted for both f_e and f_p as in equation (14) and (15). In the cases of influenza epidemic, congestion cascade, and cascading power outages, f_p is characterized by Weibull functions as in equation (16). With no external factors considered, f_e is not used in the latter three simulation studies.

$$f_{e,1}(t_i;\, \boldsymbol{\beta^E}) = \left[1 - p_{i,1}(\boldsymbol{\beta^E})\right]^{t_i - 1} p_{i,1}(\boldsymbol{\beta^E}), \tag{14}$$

$$f_{p,1}\left(\tau_{ji};\, \boldsymbol{\beta^S}, \boldsymbol{\beta^F}\right) = \left[1 - p_{ji,1}(\boldsymbol{\beta^S}, \boldsymbol{\beta^F})\right]^{\tau_{ji} - 1} p_{ji,1}(\boldsymbol{\beta^S}, \boldsymbol{\beta^F}), \tag{15}$$

$$f_{p,2}(\tau_{ji};\ \boldsymbol{\beta^S}, \beta^T, \boldsymbol{\beta^F}) = \exp\left\{-\left[\gamma_{ji,2}(\boldsymbol{\beta^S}, \boldsymbol{\beta^F})\tau_{ji}\right]^{\beta^T}\right\} - \exp\left\{-\left[\gamma_{ji,2}(\boldsymbol{\beta^S}, \boldsymbol{\beta^F})(\tau_{ji}+1)\right]^{\beta^T}\right\}, (16)$$

Where $\tau_{ji} \coloneqq t_i - t_j$ is the (observed) failure propagation time interval, $p_{i,1}$ and $p_{ji,1}$ are the likelihoods of failure due to external factors for node *i* and failure propagation from node *j* to node *i* at a single time step, respectively, and $\gamma_{ji,2}$ is the rate of failure propagations from node *j* to node *i*. Equation (14) assumes that the failure hazard of a given node *i* due to external factors at time t_i monotonically decreases with t_i, and that failure due to external factors is a Bernoulli process in which the events of failure/survival associated with external factors at every time step are independent and identical (IID). The Bernoulli process is characterized by the geometric distribution parameter $p_{i,1}(\boldsymbol{\beta^E})$ which is the probability of failure due to external factors for each Bernoulli trial on failure or survival. Similarly for equation (15), it assumes a Bernoulli process with IID Bernoulli trials on whether failure propagation happens at every time interval. Equations (14) and (15), one for failure due to external factors and the other for failure propagations, take similar functional forms based on the consideration that failure due to external factors can be viewed as a special type of failure propagation from ε-node [138]. The ε-node is a dummy node that represents external factors, whose time of failure is set to $t_\varepsilon = 0$, meaning that the ε-node fails prior to the failure of any other node. Therefore, failure of a node due to external factors is equivalent to failure propagation from the ε-node to this node.

While equations (14) and (15) both assume constant failure rate/probability (or failure propagation rate/probability) over time, equation (16) enables (monotonically) varying failure propagation rate (characterized by the shape parameter $\gamma_{ji,2}(\boldsymbol{\beta^S}, \boldsymbol{\beta^F})$ of the Weibull distribution) with time, whose trend is determined by the parameter β^T. The two different functional forms, geometric distribution and Weibull distribution respectively, are adopted in the simulation studies to test how

the detailed formulation of the inference model affects the model's performance.

4.3.1. Parameterizing the model for interdependent infrastructure cascading failures

Parameterizing the inference model involves specifying the functional forms of $p_{i,1}(\boldsymbol{\beta^E})$, $p_{ji,1}(\boldsymbol{\beta^S}, \boldsymbol{\beta^F})$ and $\gamma_{ji,2}(\boldsymbol{\beta^S}, \boldsymbol{\beta^F})$. In the simulation study of infrastructure cascading failures, the single-time-step failure likelihood due to external factors $p_{i,1}(\boldsymbol{\beta^E})$ is formulated as a function of the strengths of high winds (measured by wind speed) and storm surges (measured by flood depth), the two major damaging forces for Hurricane Sandy [238].

$$p_{i,1}(\boldsymbol{\beta^E}) = 1 - \frac{1}{e^{(\beta_1^E E_i^{WS} + \beta_2^E E_i^{FD})}}, \tag{17}$$

where E_i^{WS} and E_i^{FD} are the average wind speed and average flood depth at node *i* respectively, and β_1^E and β_2^E are the parameters indicating the damaging impacts of high winds and storm surges on the infrastructure service node *i* (see section 5.1 for infrastructure network setup). The functional form of Equation (17) is determined based on three considerations: 1) $p_{i,1}(\boldsymbol{\beta^E})$ should monotonically increase with E_i^{WS} and E_i^{FD} respectively; 2) when $E_i^{WS} = 0$ and $E_i^{FD} = 0$, $p_{i,1}(\boldsymbol{\beta^E}) = 0$, meaning that if the hurricane has no impact on a node, this node would not fail due to external factors; and 3) when $E_i^{WS} \to \infty$ or $E_i^{FD} \to \infty$, $p_{i,1}(\boldsymbol{\beta^E}) \to 1$, meaning that under (indefinitely) strong hurricane impact, a node would certainly fail (due to external factors).

The single-time-step failure propagation likelihood $p_{ji,1}(\boldsymbol{\beta^S}, \boldsymbol{\beta^F})$ in the study of infrastructure cascading failures is formulated as in equation (18).

$$p_{ji,1}(\boldsymbol{\beta^S}, \boldsymbol{\beta^F}) = \beta_1^S e^{-\beta_2^S d_{ji}} + \beta^F A_{ji}^{null} - \beta_1^S \beta^F A_{ji}^{null} e^{-\beta_2^S d_{ji}}. \tag{18}$$

The right-hand side of equation (18) is a combination of the failure propagation likelihoods

attributed to spatial dependence and functional dependence. The term $\beta_1^S e^{-\beta_2^S d_{ji}}$ denotes the failure propagation likelihood due to spatial dependence between two nodes *j* and *i*, where d_{ji} is the distance between the two nodes. The parameter β_1^S is termed co-location dependence because it quantifies how likely failure will propagate from node *j* to node *i* if they are in the same zone, i.e. $d_{ji} = 0$. When two nodes are separated by a distance, the failure propagation likelihood between them decreases with their distance, characterized by the exponent parameter d_{ji}. Two infinitely distant nodes, i.e. $d_{ji} \to \infty$, are not spatially dependent on each other, i.e. $\beta_1^S e^{-\beta_2^S d_{ji}} \to 0$.

The term $\beta^F A_{ji}^{null}$ denotes the failure propagation likelihood due to functional dependence, where A_{ji}^{null} is the functional dependence structure generated by a null model. Functional dependence in general captures the (direct) connections between node-level processes [162]. In interdependent infrastructure cascading failures, for example, it can be the connection between a transportation node (e.g. subway service) and a power node (e.g. electricity service) in which operation of the former depends on the later; and in epidemics, it can be the (direct) connections between individual (node) activities, which in the case of a contact-transmission diseases, are characterized by individual mobility [239]. Functional dependence in most cases can not be directly observed (in the simulation study of influenza epidemic however, functional dependence is observed). This issue is addressed by applying null models (see section 4.2.2) that utilize prior knowledge in failure propagations in a system. It is assumed that node *i* is functionally dependent on node *j* in a null model if these exists a (directed) link from *j* to *i* in this null model, which corresponds to $A_{ji}^{null} = 1$. Otherwise, no functional dependence of node *i* on node *j* exists, i.e. $A_{ji}^{null} = 0$. The parameter

β^F quantifies the likelihood of failure propagation (in addition to the likelihood of failure propagation due to spatial dependence) if two nodes are functionally dependent. In a null model ensemble, every null model suggests a different functional dependence structure. In the MLE, the likelihood function (as in equation (1)) is evaluated for each functional dependence structure present in the null model ensemble. The one that returns the highest likelihood is chosen to be the estimated functional dependence structure and the corresponding parameter estimate $\langle \beta^F \rangle$ will be the estimation result of β^F for the inference model.

4.3.2. Parameterizing the model for influenza epidemics

The formulation of the inference model for influenza epidemics is unique among the four simulation studies. Instead of adopting the general failure spreading mechanisms employed by the other three simulation studies, the inference model for influenza epidemics integrates spreading mechanisms specific to influenza epidemics into its model formulation in order to test the adaptability of the inference model to domain-specific spreading processes when their underlying mechanisms are well understood [240]. *Close human contact* has been identified as a major channel for influenza transmission in existing literature [239-241], and is modeled in the influenza epidemic process.

The close-contact rate between two individuals is modeled to be proportional to the travel rate (number of trips per day) with a coefficient $\beta_1^F \in [0,1]$ if these two individuals are located in different zones; and proportional to the population density (population per square mile) with a coefficient $\beta_2^F \in [0,1]$ if the two individuals live in the same zone [239]. It is worth noting that close human contact is viewed as a type of functional dependence for failure (i.e. influenza

infection in the context of influenza epidemic) propagations. This is because close human contact belongs to a general category of connections between individual human activities (e.g. social interactions) [242], which falls into the definition of functional dependence.

Spatial dependence in the inference model for influenza epidemic depends on zone proximity: any two individuals living in neighboring zones (which means the two zones share some boundaries) have additional likelihood $\beta^S \in [0,1]$ of transmitting influenza between them in addition to the transmission likelihood attributed to close contact. This treatment for spatial dependence is intended to take into account other but less common influenza spreading mechanisms such as exposure to contaminated fomites [240].

The failure propagation rate (i.e. the number of susceptible individuals who an infected individual transmits influenza to per time step) $\gamma_{ji,2}(\boldsymbol{\beta^S}, \boldsymbol{\beta^F})$ is parameterized by assuming linear relation between travel rate or zone density and failure propagation rate, as in equation (19).

$$\gamma_{ji,2}(\boldsymbol{\beta^S}, \boldsymbol{\beta^F}) = \begin{cases} \beta_1^F v_{ji} + \beta^S \cdot \mathrm{Prox}(i,j), & \text{if } z_i \neq z_j \\ \beta_2^F \rho_i + \beta^S, & \text{if } z_i = z_j \end{cases}, \tag{19}$$

where z_i and z_j are the zones individual i and j are located in, v_{ji} is the travel rate from z_j and z_i, ρ_i is the population density in z_i, and $\mathrm{Prox}(i,j)$ is an indicator of whether z_i and z_j are neighboring zone. Detailed explanation of the above quantities in the context of the simulation study is given in section 5.2.

In summary, the formulation of the epidemic model has three major differences from the infrastructure cascading failure model. Firstly, domain-specific failure spreading mechanisms are

formulated into the epidemic model, instead of using the general failure spreading mechanisms as in the infrastructure cascading failure model. This is because compared to the complex and difficult-to-model (specific) spreading mechanisms behind cascading failures of interdependent infrastructures [89], existing research, e.g. [239-241], has casted more insights and a better understanding into the spreading mechanisms of infectious diseases. Secondly, external factors are no longer considered in the epidemic model. This setting results from the fact that disease spreading within a region is the main driving force for the progress of an epidemic once it begins [130]. And thirdly, the failure propagation time intervals are assumed to follow Weibull distribution instead of geometric distribution according to [217].

As Weibull distribution has a more complex functional form than geometric distribution, the following subsection proves the mathematical validity of the parameterization in the epidemic model.

Proof of parameterization of the inference model in influenza epidemic. Denoting the observed failure propagation time interval from node j to node i as $\tau_{ji} \coloneqq t_i - t_j$ and its corresponding random variable as $\tau_{j\to i} \coloneqq T_i - T_j$, the cumulative distribution function of Weibull distribution is described by equation (P9).

$$P\left(\tau_{j\to i} \le \tau_{ji}\right) = 1 - \exp\left[-\left(\frac{\tau_{ji}}{\lambda_{ji}}\right)^k\right], \tag{P9}$$

where λ_{ji} is the scale parameter of Weibull distribution. Replacing the transmission time interval with transmission rate $Q_{ji} \equiv \frac{1}{\tau_{j\to i}}$ (in terms of realizations, $q_{ji} \equiv \frac{1}{\tau_{ji}}$) results in Equation (P10).

$$P\left(Q_{ji} < q_{ji}\right) = \exp\left[-\left(\frac{1}{\lambda_{ji} q_{ji}}\right)^{k}\right]. \tag{P10}$$

Consider the following linear relation with an error multiplier:

$$q_{ji} = \left[\gamma_{ji,2}(\boldsymbol{\beta^S}, \boldsymbol{\beta^F})\right] {\epsilon_{ji}}^{-\frac{1}{k}}, \tag{P11}$$

where ϵ_{ji} is the random error associated with the failure propagation rate from node *j* to node *i*. It is assumed that the random errors for different node pairs are independently and identically distributed exponential variables, which means small errors are more likely to occur than large errors. Therefore, the Weibull scale parameter λ_{ji} can be formulated as in equation (P12),

$$\lambda_{ji} = \frac{1}{\gamma_{ji,2}(\boldsymbol{\beta^S}, \boldsymbol{\beta^F})}, \tag{P12}$$

so that

$$P\left(Q_{ji} < q_{ji}\right) = \exp\left(-\epsilon_{ji}\right) = 1 - F\left(\epsilon_{ji}\right). \tag{P13}$$

Equation (P13) suggests that parameterization of the Weibull distribution as in equation (P11) and (P12) can address the uncertainties in the failure propagation rates under I.I.D. exponential random errors by separating the systematic component of failure propagation rate characterized by $\gamma_{ji,2}(\boldsymbol{\beta^S}, \boldsymbol{\beta^F})$ and the random component characterized by ϵ_{ji}. Under the parameterization specified by equation (P11) and (P12), the Weibull distribution in equation (P9) is transformed to the Weibull function in equation (16), which enables writing the hazard of failure propagation in terms of temporal, spatial and functional dependences, characterized by the parameters β^T, $\boldsymbol{\beta^S}$ and $\boldsymbol{\beta^F}$, respectively.

4.3.3. Parameterizing the models for congestion cascade and cascading power outages

The inference models for congestion cascade and cascading power outages share the same

inference model formulation, which is similar to the inference model formulation for interdependent infrastructure cascading failures but different from it in two ways. Firstly, external factors are not considered in congestion cascade and cascading power outages. This means $\lambda_i(t_i|\boldsymbol{E}) \equiv 0$. Equation (6) thus reduces to equation (6-4).

$$\lambda_i(t_i) = 1 - \prod_{j \in \mathbb{N} \setminus i} \left(1 - P_{j \to i}\right), \tag{6-4}$$

Equation (6-4) states that the failure hazard of node *i* at time t_i is a synthesis of failure propagation hazards from all other nodes to node *i*, characterized by the term $P_{j \to i}$. The formulation of $P_{j \to i}$ still follows equation (8), and is a function of $P\left(\tau_{j \to i} = t_i - t_j \middle| j \to i, j^- \nrightarrow i\right)$. And secondly, the Weibull function as specified by equation (16), instead of the geometric function employed in the interdependent infrastructure cascading failures, is adopted for the inference model formulation in congestion cascade and cascading power outages. This setting is to account for the potentially different temporal dependence between congestion cascade and cascading power outages. Therefore, the formulation for $P\left(\tau_{j \to i} = t_i - t_j \middle| j \to i, j^- \nrightarrow i\right)$ in the congestion cascade and cascade power outages is given by equation (16-1).

$$\begin{aligned} P\left(\tau_{j \to i} = t_i - t_j \middle| j \to i, j^- \nrightarrow i\right) &= f_{p,3}\left(\tau_{ji};\, \boldsymbol{\beta^S}, \beta^T, \boldsymbol{\beta^F}\right) \\ &= \exp\left\{-\left[\gamma_{ji,3}(\boldsymbol{\beta^S}, \boldsymbol{\beta^F})\tau_{ji}\right]^{\beta^T}\right\} - \exp\left\{-\left[\gamma_{ji,3}(\boldsymbol{\beta^S}, \boldsymbol{\beta^F})\left(\tau_{ji}+1\right)\right]^{\beta^T}\right\}. \end{aligned} \tag{16-1}$$

The transmission rate $\gamma_{ji,3}(\boldsymbol{\beta^S}, \boldsymbol{\beta^F})$ is parameterized the same way as for $p_{ji,1}(\boldsymbol{\beta^S}, \boldsymbol{\beta^F})$ in interdependent infrastructure cascading failures. This parameterization is based on the consideration that $\gamma_{ji,3}(\boldsymbol{\beta^S}, \boldsymbol{\beta^F})$ and $p_{ji,1}(\boldsymbol{\beta^S}, \boldsymbol{\beta^F})$ have the same meaning for a given node pair $j \to i$ at any single time step. The functional form of $\gamma_{ji,3}(\boldsymbol{\beta^S}, \boldsymbol{\beta^F})$ is thus given by equation (18-1).

$$\gamma_{ji,3}(\boldsymbol{\beta^S}, \boldsymbol{\beta^F}) = \beta_1^S e^{-\beta_2^S d_{ji}} + \beta^F A_{ji}^{null} - \beta_1^S \beta^F A_{ji}^{null} e^{-\beta_2^S d_{ji}}. \quad (18\text{-}1)$$

In the inference model for congestion cascade, d_{ji} is the distance between two road segments *j* and *i*, and A_{ji}^{null} indicates whether there exists a directed link from *j* to *i* in a null model constructed for the congestion cascade following the null model construction rules for failure propagation in transportation networks (section 4.2.2). In the inference model for cascading power outages, d_{ji} is the distance between two power lines *j* and *i*, and A_{ji}^{null} indicates whether there exists a link from *j* to *i* in a null model constructed for the cascading power outages following the null model construction rules for failure propagation in power networks (section 4.2.2). β_1^S, β_2^S and β^F are the parameters associated with co-location dependence, distance-based spatial dependence and functional dependence, respectively, which are explained in detail in section 4.3.1.

4.4. Methodology summary

The purpose of the methodology is to define and quantify all the terms in figure 5, and how their connections can be mathematically described and proven. This serves the ultimate goal of connecting the (general) failure mechanisms with the likelihood of a cascading failure instance, which answers the question of how the (general) failure mechanisms give rise to an observed cascading failure instance. In this procedure, the likelihood of a cascading failure instance is first decomposed into the likelihoods of failures of individual nodes. And the failure likelihood of a given node, through a survival model formulation, can be transformed into failure hazards due to external factors and failure propagations, respectively. The latter can be further described by node-to-node failure propagation likelihoods. And the failure hazards due to external factors and node-to-node failure propagation likelihoods can be formulated directly in terms of the four (general) failure mechanisms.

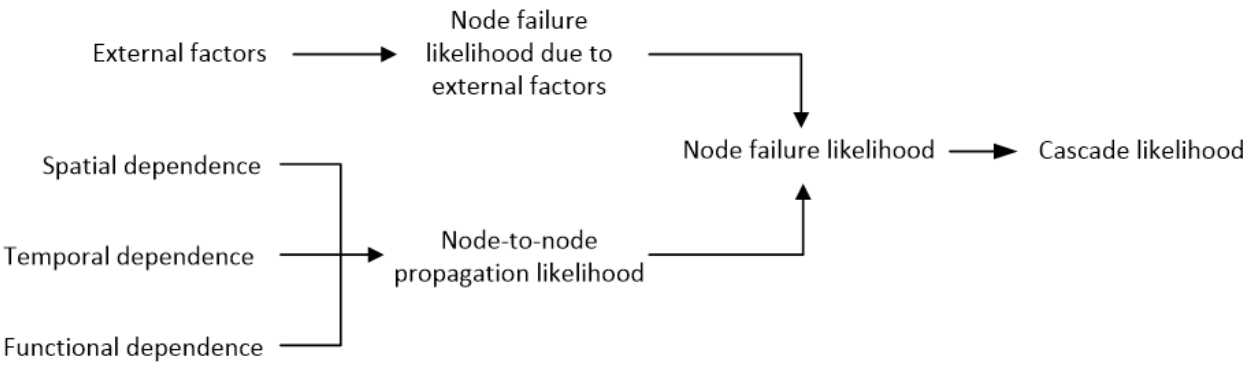

Figure 5: Methodology summary. The key quantities involved in the inference model formulation and how these quantities are connected is presented in this figure. The methodology seeks to mathematically describe this figure.

The inference model consists of a general component based on survival analysis and a specific component built upon the general component. The cascade likelihood, node failure likelihood, failure likelihood due to external factors and node-to-node propagation likelihood as shown in figure 5 are general quantities that apply to any given cascading failure instance. More importantly, their formulations stay unchanged from one type of cascading failures to another type, as shown in the proofs and derivations of their formulations in this section. This part of model is thus generally applicable to all cascading failures. When it comes down to the formulations of the (general) failure mechanisms, however, the model can be either general or specific. A general formulation involves characterizing the failure hazards due to external factors as a function of time, temporal dependence as a function of failure time interval between two nodes, spatial dependence as a function of distance, and functional dependence as generated by null models. This is the case for the inference models in interdependent cascading failures, congestion cascade and cascading power outages. A specific formulation for the failure mechanisms requires domain knowledge in how failures propagate in a given network and integrates the specific mechanisms into the inference model. This is the case for the inference model in influenza epidemics. It is worth noting that most specific failure mechanisms can be categorized into one of the four general failure

mechanisms by definition, as demonstrated by the inference model of influenza epidemics whose specific failure mechanisms fall into either functional dependence or spatial dependence.

This bipartite model formulation of general component versus specific component ensures a balance between the generalizability and precision of the model. While the model can be generalized to provide estimation for an arbitrary cascading failure instance (which may not yet be fully understood) thanks to its general component, its specific component enables precisely modeling a cascading failure instance with known failure mechanisms.

Section 5
Simulation study setups

The methodology described in section 4 is tested and validated through four simulation studies: a) cascading failures in interdependent transportation and power infrastructures in New York City (NYC) during Hurricane Sandy; b) an influenza epidemic in NYC; c) a congestion cascade scenario in the Sioux-Falls benchmark network; and d) cascading power outages in a 6-bus benchmark power system. In each simulation study, a cascading failure process is simulated to generate the required inputs to the model, i.e. the failure time of each node. Using the simulated failure times and the above inference model, the parameters $\boldsymbol{\beta}$ are estimated. Using the estimated parameters $\langle\boldsymbol{\beta}\rangle$**,** the inference model is re-run to obtain the inferred node failure times and node-to-node failure propagation probability.

For the convenience of description, the terms shown in table 3 are used in describing the simulation study setups. The simulation-validation process in every simulation study is illustrated in figure 6.

Table 2: Glossary in simulation studies

Term	Meaning
Infrastructure	"… identifiable industries, institutions, including people and procedures, and distribution capabilities that provide a reliable flow of products and services essential to the defense and economic security of the United States, the smooth functioning of governments at all levels, and society as a whole." [243]
Infrastructure system	A group of connected infrastructures that provide similar products/service to humans and the society.
Infrastructure network	A network representation of an infrastructure system, with individual component as nodes and their connections as links.

Simulation data	The input data that a simulation of cascading failure requires.
Simulation result	The output of a simulation, i.e. the simulated failure time of each node and node-to-node failure propagation patterns.
Inference model	The model that infers $\boldsymbol{\beta}$ from simulation results, as presented in section 4.
Inference result	The parameter estimated $\langle\boldsymbol{\beta}\rangle$ and reconstructed failure time of each node and node-to-node failure propagation patterns using the inference model and $\langle\boldsymbol{\beta}\rangle$.

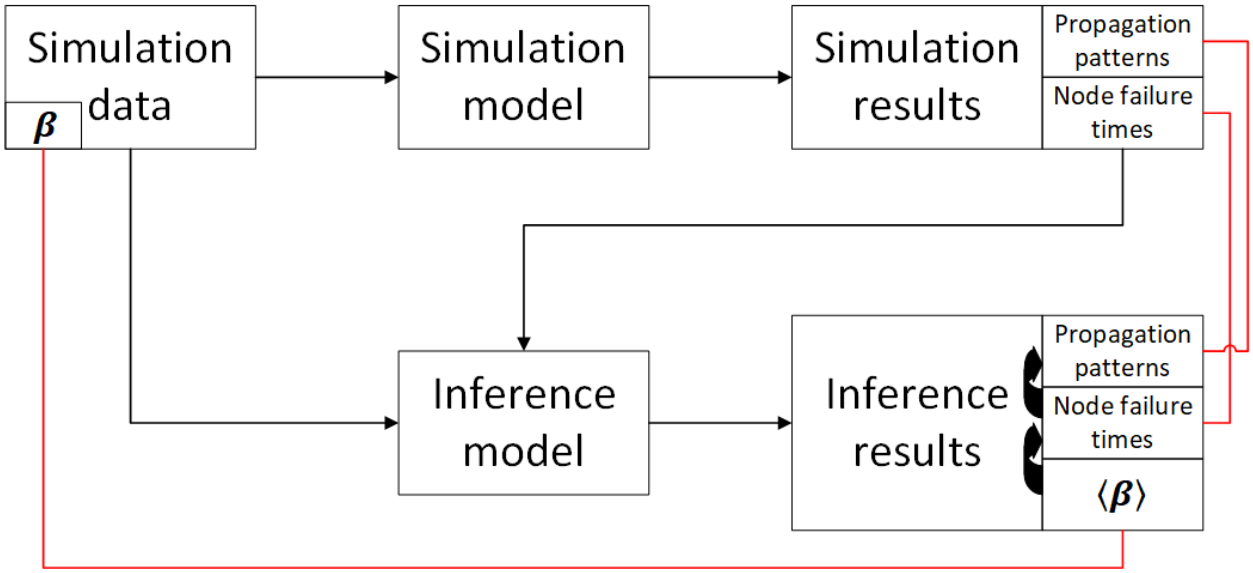

Figure 6: Steps in each of the four simulation studies. Every box represents one step in the simulation study, and arrows represent input-output relation between the steps. A red line connects two results that are compared for the purpose of model validation (which are presented in section 6).

As shown in figure 6, a simulation model takes simulation data as inputs. In two of the four simulation studies, the simulation data also includes the preset parameter values $\boldsymbol{\beta}$ as the "ground truth". The simulation model is then implemented **only once** to simulate a single cascade instance, whose process and outcomes are recorded to be the simulation results which include the failure propagation patterns (process) and the failure time of each node (outcomes) in the simulated

cascade instance. The failure time of each node, as well as part of the simulation data (e.g. the geographical distances between nodes) serves as input to the inference model as presented in section 4, which returns three types of inference results: parameter estimates $\langle \boldsymbol{\beta} \rangle$, (inferred) failure time of each node and (inferred) failure propagation patterns. The parameter estimates $\langle \boldsymbol{\beta} \rangle$ is the direct output of MLE in the inference model. Using $\langle \boldsymbol{\beta} \rangle$ as approximations of the true parameter values $\boldsymbol{\beta}$, the probability of failure at any given time step t_i for any given node *i* can be evaluated through equation (3), (4) or (5). The inferred failure time of node *i* is thus randomly sampled from this probability distribution. With parameter estimates $\langle \boldsymbol{\beta} \rangle$ and sampled failure time of any two given nodes *i* and *j*, the probability of failure propagation from one to the other can be evaluated by equation (11).

The detailed description of the setups for the four simulation studies is presented in the following four subsections, respectively. For each simulation study, the corresponding subsection describes what simulation data is utilized for the study, how the data is collected, what is the cascading process that the simulation model simulates, and how the simulation data and simulation results (node failure times) feed into the inference model as input. As the four simulation studies share similarities in their setups, the simulation study setup of interdependent infrastructure cascading failures is described in detail and the remaining three simulation study setups are presented by emphasizing their similarities and differences to the interdependent infrastructure cascading failure case.

5.1. Setup of the simulation study for interdependent infrastructure cascading failures

The simulation study for infrastructure cascading failures is set in the context of cascading failures

in the interdependent power and transportation systems in NYC. The specific disaster agent that triggers the cascading failures is Hurricane Sandy, which made the landfall on October 29 2012 in the New York City area. New York City is home to 8.3 million residents. Hurricane Sandy caused damages in excess of 50 billion [244]. Sandy's unprecedented storm surge caused widespread power outages and flooding [245]. Approximately 2 million New Yorkers were without power immediately after the storm and public transportation services that the majority of the New Yorkers relied on were dismantled for multiple days after the landfall [245]. Empirical evidence confirms the presence of (type II) cascading failures during the disaster characterized by a high percentage of indirect damages [160], as discussed in section 1.1. Therefore, Hurricane Sandy provides a perfect modeling background for testing if the proposed methodology works in a real-world case. The geographic scope of the simulation study is shown in figure 7a, which covers the entire NYC.

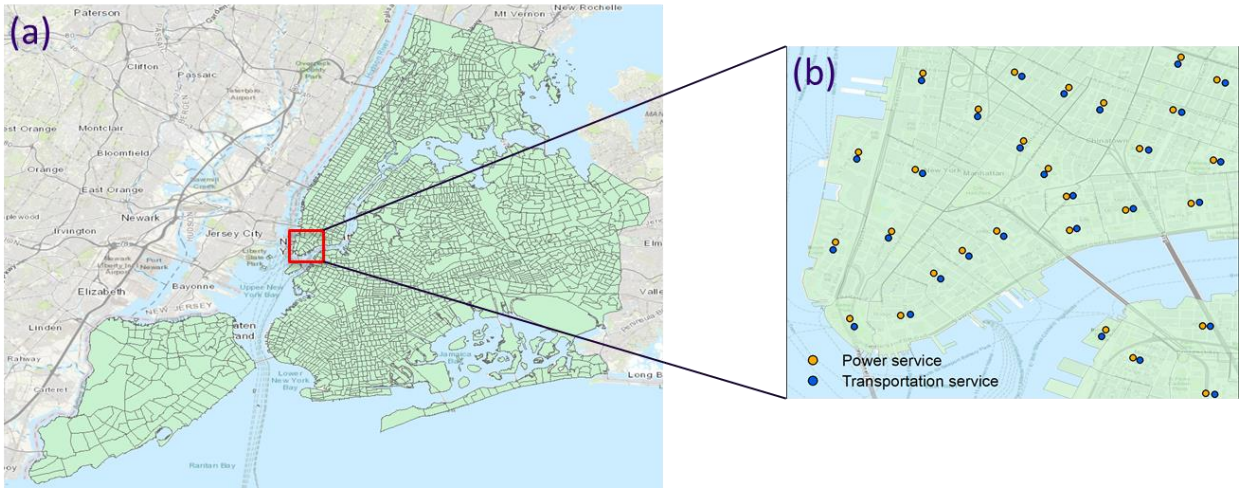

Figure 7: Geographical scope of the simulation study for infrastructure cascading failures. (a) illustrates the study area, i.e. all census tracts in NYC. (b) is a zoom-in of the lower Manhattan to illustrate the layout of the power (service) network and transportation (service) network.

The infrastructure networks used in this simulation study are constructed from a service perspective (see section 2.3): a region is divided into multiple zones, and the power service and transportation service in each zone are abstracted into a node in the power network and

transportation network, respectively. Therefore, the size of the power network and transportation network each is the same as the number of zones. This service perspective avoids tracking the detailed physical infrastructure layouts which are not publicly available while providing a good approximation for them as well [40, 89]. As in the case of NYC, the census tracts are used as the zones. Figure 7b shows that in each census tract, there are a node in the power network and a node in the transportation network, representing the abstracted power service and transportation service in the census tract, respectively. The two nodes in a census tract are located in the geographical center of the census tract, assuming that the power service and transportation service are respectively distributed evenly within the census tract (for convenience of viewing, the two nodes are plotted with a small distance in figure 7b).

The hypothesized topology (due to real-world infrastructure network topologies being unknown) of the infrastructure networks is constructed by generating null models of the two networks and their interdependencies. A null model is a network with some properties predefined while all other properties randomized, and has the flexibility of hypothesizing a network's topology based on different levels of prior knowledge available about the network [177]. In our case particularly, the predefined properties are degree (i.e. number of links attached to a node) distributions of the power and transportation networks respectively. The null models in such a case can be constructed using the uncorrelated configuration model (UCM) [237]. For interdependencies, it is assumed that nodes with a high degree (a.k.a hubs), typically larger than 10, have a function of mutual supporting [147]. Therefore, two hubs in the power network and transportation network respectively are viewed as interdependent.

In the case of a hurricane, external factors in the infrastructure cascading failures refer to the damaging forces of the hurricane, primarily high winds and storm surges, measured by wind speed and flood depth, respectively [238]. Both wind speed and flood depth are node-level quantities. The wind speed at a node is evaluated as the average of the wind speeds measured at various locations within the zone that this node is affiliated with, whose data source is typically publicly available from the aircraft reconnaissance data collected by the National Hurricane Center (NHC) [246]. The flood depth at a node is calculated in a similar manner from the point flooding survey data collected by Federal Emergency Management Agency (FEMA) [247]. The wind speed and flood depth data used in this simulation study is illustrated in figure 8. It can be observed that storm surges hit only coastal areas while high winds were more evenly distributed geographically.

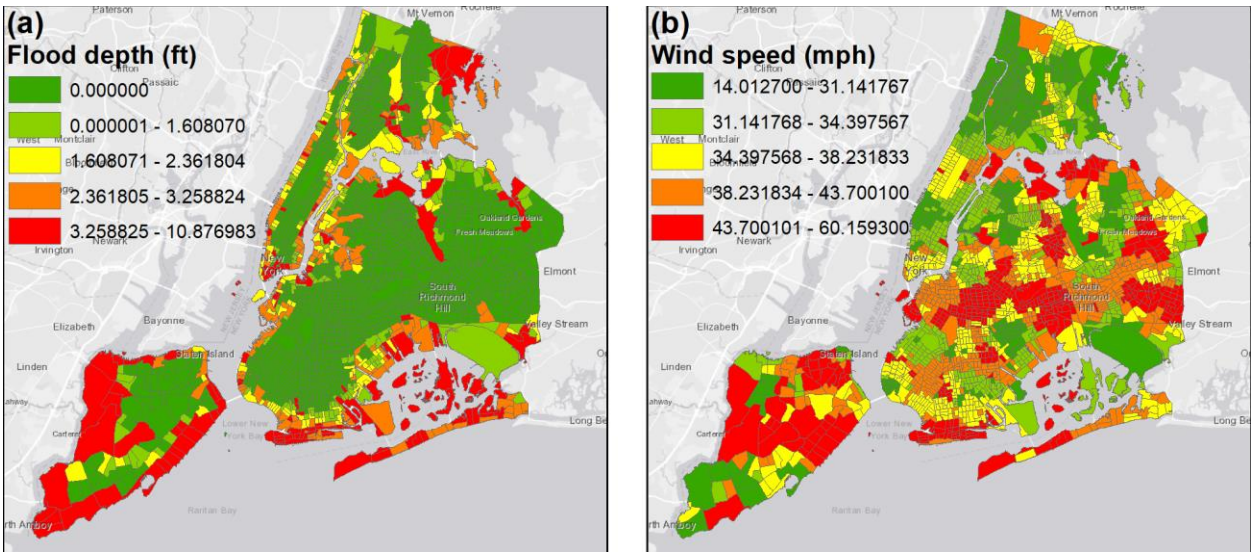

Figure 8: External factors during Hurricane Sandy. (a) and (b) illustrate the (average) surveyed flood depth and wind speed in each census tract, respectively.

Implementing the infrastructure cascading failure simulation requires three types of simulation data: external factors, i.e. flood depth and wind speed, geographical distances between nodes and preset parameter values $\boldsymbol{\beta}$ as the "ground truth". For the geographical distances, if two nodes are in different census tracts, their distance is the Euclidean distance between the geographical centers

of these two census tracts. Otherwise, the distance between two nodes is zero, which happens for the power node and transportation node in the same census tract, a.k.a. co-location. The preset parameter values $\boldsymbol{\beta}$ are randomly generated.

With the required simulation data given, the probability that failure propagates from one node *j* to another node *i* after a time interval $t_i - t_j$ is evaluated as in equation (20).

$$P\left(j \to i, \tau_{j\to i} = t_i - t_j \middle| j^- \nrightarrow i\right) = P\left(\tau_{j\to i} = t_i - t_j \middle| j \to i, j^- \nrightarrow i\right). \quad (20)$$

The probability $P\left(\tau_{j\to i} = t_i - t_j \middle| j \to i, j^- \nrightarrow i\right)$ on the right hand side of equation (20) is quantified later in this section for each of the four simulation studies. It is also one of the two fundamental quantities (the other is $\lambda_i(t_i)$) in formulating the likelihood function (see section 4). Equation (20) conceptually implies that the failure propagation time interval from node *i* to *j* contains all the information about failure propagation from *i* to *j*, e.g. whether the failure propagation happened or not. Proof of equation (20) is provided below.

Proof of equation (20). The probability $P\left(j \to i, \tau_{j\to i} = t_i - t_j \middle| j^- \nrightarrow i\right)$ can be written as in equation (P14).

$$P\left(j \to i, \tau_{j\to i} = t_i - t_j \middle| j^- \nrightarrow i\right) = P\left(\tau_{j\to i} = t_i - t_j \middle| j \to i, j^- \nrightarrow i\right) \cdot P(j \to i | j^- \nrightarrow i). \quad (P14)$$

The first term $P\left(\tau_{j\to i} = t_i - t_j \middle| j \to i, j^- \nrightarrow i\right)$ can be evaluated the same way as in equation (10). The following proof shows how to evaluate the second term $P(j \to i | j^- \nrightarrow i)$. Bringing in the variable of failure propagation time interval $\tau_{j\to i}$ from node *j* to node *i*, the probability $P(j \to i | j^- \nrightarrow i)$ can be written as in equation (P15).

$$P(j \to i | j^- \nrightarrow i) = \sum_{\tau_{j\to i} \in (0,\infty)} P\left(j \to i, \tau_{j\to i} \middle| j^- \nrightarrow i\right)$$

$$= \sum_{\tau_{j\to i}\in(0,\infty)} P\left(j \to i \middle| \tau_{j\to i}, j^- \nrightarrow i\right) \cdot P\left(\tau_{j\to i} \middle| j^- \nrightarrow i\right)$$

$$= \sum_{\tau_{j\to i}\in(0,\infty)} P\left(j \to i \middle| \tau_{j\to i}, j^- \nrightarrow i\right) \cdot \sum_{j\rightsquigarrow i\in\{j\to i, j\nrightarrow i\}} P\left(\tau_{j\to i} \middle| j \rightsquigarrow i, j^- \nrightarrow i\right) \cdot P(j \rightsquigarrow i | j^- \nrightarrow i). \quad \text{(P15)}$$

In the third line of equation (P15), the variable $j \rightsquigarrow i$, denoting whether or not failure propagates from node j to node i, is introduced to decompose the probability $P\left(\tau_{j\to i} \middle| j^- \nrightarrow i\right)$. Applying Bayesian theorem to $P\left(j \to i \middle| \tau_{j\to i}, j^- \nrightarrow i\right)$ and expanding the inner summation leads to equation (P16).

$$P(j \to i | j^- \nrightarrow i) = \sum_{\tau_{j\to i}\in(0,\infty)} a\left(\tau_{j\to i}\right) \cdot P\left(\tau_{j\to i} \middle| j \to i, j^- \nrightarrow i\right) \cdot P(j \to i | j^- \nrightarrow i)$$

$$\cdot \left[P\left(\tau_{j\to i} \middle| j \to i, j^- \nrightarrow i\right) \cdot P(j \to i | j^- \nrightarrow i) + P\left(\tau_{j\to i} \middle| j \nrightarrow i, j^- \nrightarrow i\right) \cdot P(j \nrightarrow i | j^- \nrightarrow i)\right], \quad \text{(P16)}$$

where $a\left(\tau_{j\to i}\right)$ is the scaling factor after applying Bayesian theorem, which is a function of $\tau_{j\to i}$. The probability $P\left(\tau_{j\to i} \middle| j \nrightarrow i, j^- \nrightarrow i\right)$ is constantly zero for $\tau_{j\to i} \in (0, \infty)$. This is because the condition $j \nrightarrow i, j^- \nrightarrow i$ suggests none of the nodes spreads failure to node i, and thus node i can never fail. Therefore, $T_i = \infty$ and thus $\tau_{j\to i} = \infty$ under the condition $j \nrightarrow i, j^- \nrightarrow i$, which suggests $\tau_{j\to i}$ having no finite value. Equation (P17) thus simplifies to equation (P12).

$$P(j \to i | j^- \nrightarrow i) = \sum_{\tau_{j\to i}\in(0,\infty)} a\left(\tau_{j\to i}\right) \cdot P\left(\tau_{j\to i} \middle| j \to i, j^- \nrightarrow i\right)^2 \cdot P(j \to i | j^- \nrightarrow i)^2. \quad \text{(P17)}$$

$\tau_{j\to i}$ having finite value implies that $P(j \to i | j^- \nrightarrow i) \neq 0$, as a feasible path must exist for failure to reach i. Consequently, $P(j \to i | j^- \nrightarrow i)$ can be obtained by solving equation (P18).

$$P(j \to i | j^- \nrightarrow i) = \frac{1}{\sum_{\tau_{j\to i}\in(0,\infty)} a\left(\tau_{j\to i}\right) \cdot P\left(\tau_{j\to i} \middle| j \to i, j^- \nrightarrow i\right)^2}. \quad \text{(P18)}$$

Substituting equation (P18) to (P14) results in equation (P19).

$$P\left(j \to i, \tau_{j\to i} = t_i - t_j \middle| j^- \nrightarrow i\right) = \frac{P\left(\tau_{j\to i} = t_i - t_j \middle| j \to i, j^- \nrightarrow i\right)}{\sum_{\tau_{j\to i}\in(0,\infty)} a\left(\tau_{j\to i}\right) \cdot P\left(\tau_{j\to i} \middle| j \to i, j^- \nrightarrow i\right)^2}$$

$$= \frac{1}{a} \cdot P\left(\tau_{j\to i} = t_i - t_j \middle| j \to i, j^- \nrightarrow i\right), \quad \text{(P19)}$$

where a is a scaling constant. Equation (P19) suggests that the probability $P\left(j \to i, \tau_{j\to i} = t_i - t_j \middle| j^- \nrightarrow i\right)$ is just a scaled version of $P\left(\tau_{j\to i} = t_i - t_j \middle| j \to i, j^- \nrightarrow i\right)$, so that $\sum_{j\rightsquigarrow i}\sum_{\tau_{j\to i}} P\left(j \rightsquigarrow i, \tau_{j\to i} \middle| j^- \nrightarrow i\right) = 1$. In the case where $P\left(\tau_{j\to i} = t_i - t_j \middle| j \to i, j^- \nrightarrow i\right)$ is a probability distribution as in the simulation studies, $a = 1$. This is shown in equation (P20).

$$\sum_{j\rightsquigarrow i}\sum_{\tau_{j\to i}} P\left(j \rightsquigarrow i, \tau_{j\to i} \middle| j^- \nrightarrow i\right) = \frac{1}{a}\sum_{\tau_{j\to i}} P\left(\tau_{j\to i} \middle| j \to i, j^- \nrightarrow i\right) + \frac{1}{a}\sum_{\tau_{j\to i}} P\left(\tau_{j\to i} \middle| j \nrightarrow i, j^- \nrightarrow i\right)$$

$$= \frac{1}{a}\sum_{\tau_{j\to i}} P\left(\tau_{j\to i} \middle| j \to i, j^- \nrightarrow i\right) = \frac{1}{a} = 1. \quad \text{(P20)}$$

Therefore $a = 1$ and $P\left(j \to i, \tau_{j\to i} = t_i - t_j \middle| j^- \nrightarrow i\right) = P\left(\tau_{j\to i} = t_i - t_j \middle| j \to i, j^- \nrightarrow i\right)$. Proof of equation (20) is complete.

The simulation process of infrastructure cascading failures is illustrated in figure 9 using a four-zone example. At the beginning of time step 1, there is no failed node in the infrastructure networks. Therefore, nodes may only fail due to external factors at time step 1. The hazard of failure $\lambda_i(1|\boldsymbol{E})$ due to external factors at time step 1 for every node in the infrastructure networks is evaluated by equation (9), and realizations of failures due to external factors are generated by comparing a uniformly distributed random number on the range [0,1] with the evaluated $\lambda_i(1|\boldsymbol{E})$ for each node. At the end of time step 1, some nodes may fail due to external factors. For the example shown in figure 9, node G (the power node in the lower-right census tract) fails due to external factors at the first time step.

For each subsequent time step *t*, two sets of quantities will be evaluated: the hazard of failure due to external factors at time step t for every surviving node, $\{\lambda_i(t|\boldsymbol{E});\ i \in \mathbb{N}^S\}$, and the failure propagation probability from every failed node to every surviving node, $\{P(j \to i, \tau_{j\to i} = t - t_j | j^- \nrightarrow i);\ j \in \mathbb{N}^F, i \in \mathbb{N}^S\}$, where $\mathbb{N}^S$ is the set of surviving nodes at time step *t*, $\mathbb{N}^F$ is the set of failed nodes at time step *t*, and t_j is the time step at which node *j* is simulated to have failed. For each surviving node *i*, whether it fails due to external factors at time step *t* is determined by a realization of its failure hazard due to external factors at this time step, $\lambda_i(t|\boldsymbol{E})$. This is similar to realizing node failures due to external factors in time step 1. For each pair of failed node *j* and surviving node *i*, failure propagation is realized by comparing a uniform distributed random number on [0,1] with the probability $P(j \to i, \tau_{j\to i} = t - t_j | j^- \nrightarrow i)$. A surviving node *i* will fail at time step *t* if either failure due to external factors is realized for *i* at time step *t*, or failure propagation from any failed node to *i* at time step *t* is realized. In the example shown in figure 9, failure propagation from node G to node B is realized at time step 2, leading node B to fail at time step 2. And at time step 3, failure propagations from node G to node D, from node B to node D, and from node B to node C are realized, respectively, leading node D and C to fail at time step 3. As the time steps move forward, the process of evaluating failure hazard due to external factors and failure propagation probabilities, generating realizations of failure due to external factors and failure propagations, and collecting nodes' failure times will repeat, until the simulation ends (right censoring) or all nodes have failed.

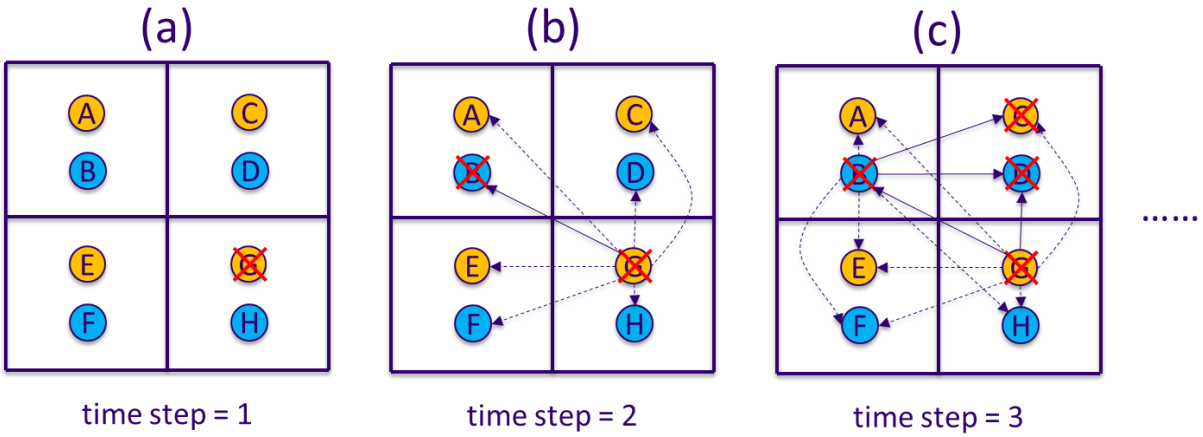

Figure 9: An example illustrating the simulation process of infrastructure cascading failures. Subfigure (a), (b) and (c) show the details at the first three time steps of the simulation. Each square represents a census tract, and the yellow node in it represents the power service in it and the blue node represents transportation service. A dash arrow means there exists a probability of failure propagation from one node to another, and a solid arrow indicates a realized failure propagation. A failed node is marked by a cross.

5.2. Setup of the simulation study for influenza epidemics

A hypothetical influenza outbreak in NYC is set as the context of this simulation study. The geographical scope and temporal scope of this study are the same as those in the study of interdependent infrastructure cascading failures, i.e. the entire NYC (five administrative boroughs including Manhattan, Brooklyn, Queens, Bronx and Staten Island) for 30 days.

The epidemic process is simulated and modeled at individual person level, compared to the construct of infrastructure services at zone-level. Each person (resident) in NYC is a node, and which census tract this person's home is located is known from the 2010 census data [248]. Therefore, the influenza spreading network has 8,175,133 nodes, the same as the population size in NYC by 2010 [248]. However, due to vaccination, a proportion of the population is immune to influenza. This proportion is taken to be the average of vaccine effectiveness for influenza over

the past 10 years (2006-2016), which has a value of 46% [249, 250]. Therefore, the number of susceptible nodes in the influenza spreading network that could potentially be infected and spread influenza is 4,414,610. The susceptible population is assumed to be geographically distributed proportionally to the total population in an area.

The spreading of influenza is viewed as a failure propagation process, where failure of a node refers to an individual getting infected by influenza. As mentioned in section 4.3.2, the simulation study of influenza epidemics adopts a specific failure propagation mechanism – close human contact – in both the simulation process and inference model. The influenza epidemic is simulated following a standard susceptible-infected-recovered (SIR) model. Initially all individuals in the region are susceptible. At time step 0 (the start of the simulation), a group of randomly selected individuals are infected and become the seed for disease transmissions. At every time step, each infected individual has a probability of transmitting influenza to the susceptible individuals based on the transmission (failure propagation) rate $\gamma_{ji,2}(\boldsymbol{\beta^S}, \boldsymbol{\beta^F})$ specified in equation (19). That is, at a given time step *t*, the increase in the number of infections in zone *i* due to disease transmission from zone *j* to zone *i* is evaluated by equation (21).

$$\Delta I_i^j(t) = I_j(t-1) \cdot \gamma_{ji,2}(\boldsymbol{\beta^S}, \boldsymbol{\beta^F}), \tag{21}$$

where $\Delta I_i^j(t)$ is the increase in the number of infection cases in zone *i* at time *t* due to transmission from zone *j*, and $I_j(t-1)$ is the number of infected individuals in zone *j* at time *t*-1. The number $\Delta I_i^j(t)$ of individuals will then be randomly sampled from zone *i* (if $\Delta I_i^j(t) < \text{POP}_i$ where POP_i is the population in zone *i*; otherwise, every susceptible individual in zone *i* turns infected at time *t*). If a sampled individual is in susceptible state, this individual will become infected at time *t*. This process is repeated for every zone *j* (including zone *i* itself) that can transmit influenza to

zone i, in order to identify all the susceptible individuals in zone i who will become infected at time t. After implementing the above process for every zone i, the epidemic simulation moves to time step t+1 with the updated infection status (susceptible, infected or recovered) for every individual. An infected individual stays infective for a fixed period of 6 days [185] and then becomes recovered. The epidemic process stops when no individual is in the infected state (meaning that everyone is either susceptible or recovered) or when the observation ends (which leads the remaining susceptible nodes to being right-censored).

The simulation data used in this simulation study is listed below.

- Trip rate v_{ji}: the number of trips made from zone j to zone i per person in zone j every day. It is evaluated as $v_{ji} = \frac{TR_{ji}}{\mathrm{POP}_j}$ where TR_{ji} is the number of trips traveled from zone j to zone i on a daily basis. The census-tract-level TR_{ji} is not directly available, and is estimated using the method presented in the following subsection "Estimating trip numbers at census tract level".
- Population size POP_i: the number of people living at zone i. The census tract populations are available from the 2010 national census data [251].
- Zone proximity $\mathrm{Prox}(i,j)$: whether zone i and zone j have overlapping borders. $\mathrm{Prox}(i,j) = 1$ if i and j have overlapping borders, and $\mathrm{Prox}(i,j) = 0$ otherwise. This data is obtained by analyzing a GIS map of NYC collected from NYC Department of City Planning [252].
- Zone distance d_{ij}: the Euclidean distance between the geographical centers of two zones i and j. It can also be calculated from the GIS map of NYC.
- Preset parameter values β^T, $\boldsymbol{\beta^S}$ and $\boldsymbol{\beta^F}$: the values of the parameters associated with

temporal dependence, spatial dependence and functional dependence, respectively. These values are randomly generated.

Estimating trip numbers at census tract level. Trip numbers are only available at county-to-county level from the American Community Survey [253], and this section presents how the census-tract-to-census-tract trip numbers can be estimated from the county-to-county trip numbers. Following [254], the gravity model (in its logarithmic form) as shown in equation (21) is fitted to the county-to-county trip data.

$$\log T_{ij} = \text{const} + \alpha_i \cdot \log m_i + \alpha_j \cdot \log m_j - \varphi \cdot \log d_{ij}, \tag{22}$$

where T_{ij} is the number of trips made from county *i* to county *j*, m_i and m_j are the population size in county *i* and county *j* respectively, and d_{ij} is the distance between the geographical centers of county i and j. The const, α_i, α_j and φ are the regression coefficients to be estimated. Their estimated values from the county-level trip numbers are -1.63, 0.24, 1.02 and 2.54, respectively, with an adjusted R^2 value of 0.79.

Assuming the county-level and census-tract-level trip numbers follow the same scaling law with population and distance [255], the above gravity model is applied to the census-tract-level data, as presented by equation (22-1).

$$\log TR_{ij} = -1.63 + 0.24 \cdot \log \text{POP}_i + 1.02 \cdot \log \text{POP}_j - 2.54 \cdot \log d_{ij}, \tag{22-1}$$

where *i* and *j* correspond to two census tracts. Therefore, the number of trips from one census tract to another can be estimated by equation (22-1) using the given simulation data including population sizes and distances between census tracts.

5.3. Setup of the simulation study for congestion cascade

In a roadway network, when a link (i.e. a road segment) gets congested, travelers using this link will choose an alternative route to bypass the congested link(s) [256]. This behavior causes a redistribution of traffic flow from the congested link(s) to other links and could overload other links, resulting in an iterative process of link congestions, flow redistributions and more link congestions. This process is termed congestion cascade in this dissertation.

In this simulation study, a congestion cascade process is viewed as a failure propagation process, where a failure refers to a road segment becoming congested. The Sioux-Falls network, shown in figure 10, is employed as the backdrop of this simulation study. In figure 10, each node (with an index) represents an intersection where two or more roads intersect and every link represents a road segment in the city of Sioux Falls. The Sioux-Falls network is a widely-used case for testing newly developed models in transportation network analysis [131], and thus serves as a benchmark network [257] to test the validity of the inference model.

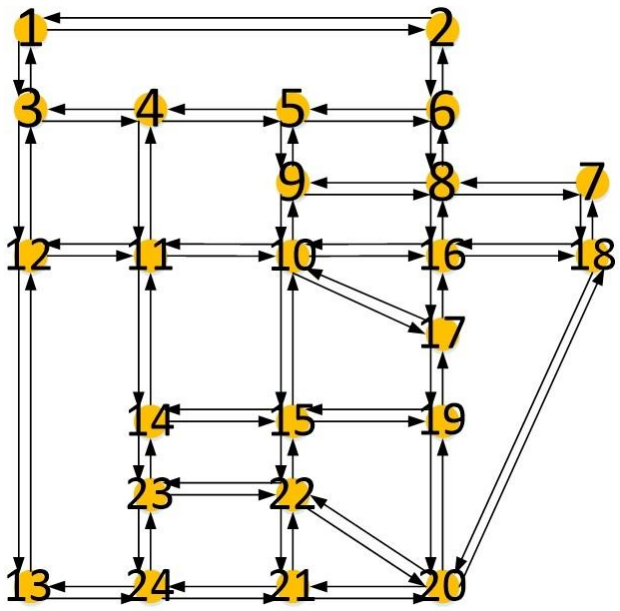

Figure 10: Sioux-Falls network. This diagram is a simplification of the real road network layout

in the city of Sioux Falls. Each node represents a road intersection where two or more roads intersect and every link represents a road segment.

Beside the topology of the Sioux-Falls network presented in figure 10, the simulation data used in this study also includes the following information on the Sioux-Falls network.

- OD matrix: the number of trips per day from every node (origin, or O) to every other node (destination, or D), measure in vehicles/day. The entry in the i^{th} row and j^{th} column of the OD matrix is also called the OD demand from node i to node j. This data is available in [131].
- Link capacity: the maximum number of vehicles that can traverse a link (road segment) every day [258]. It is measured for every link in the unit vehicles/day. This data is available in [131].
- Free-flow travel time: the time (in minutes) required to traverse a link when there is no vehicle on this link [258]. It is measured for every link. This data is available in [131].

The OD demand from one node to another node is assigned to routes in the Sioux-Falls network, which means identifying a sequence of links every traveler needs to traverse in order to get from the origin to the destination. The network is assumed to be initially operating at user equilibrium state [259] in which every traveler chooses the fastest route that has the minimum travel time among all possible routes. It is worth noting that the travel time on a link depends on the traffic flow (i.e. the number of vehicles) on it and therefore reaching user equilibrium is a dynamical process. An algorithm of calculating the link traffic flows at user equilibrium was provided by Frank and Wolfe [260] and is adopted in this simulation study.

The following process simulates how a congestion cascade proceeds. At time step 0 (start of the simulation), the network is at the user equilibrium state as described in the previous paragraph. At time step 1, links 6→8 (meaning the road segment from node 6 to node 8 in figure 9) and 8→6 would fail as they are already overloaded under user equilibrium, and become the seeds for subsequent failure propagations. Starting at time step 2, the following steps are iterated.

1. The travel time on all congested links is set to ∞;
2. If a (used) route from node *i* to node *j* has congested links on it, all travelers taking this route will abandon this route and be redistributed to the current shortest route from *i* to *j*; otherwise, travelers previously on this route remain on this route. The traffic flow on each link is updated;
3. If there is no route available from node *i* to *j*, meaning that all routes from node *i* to *j* have congested links on them, it will be regarded infeasible to travel from node *i* to node *j* and thus the OD demand from *i* to *j* will perish;
4. The travel time on each link is updated using the BPR (Bureau of Public Roads) function [261]: $TT_l = t_l^f \left[1 + 0.15\left(\frac{v_l}{C_l}\right)^4\right]$, where TT_l is the updated travel time on link l, t_l^f is the free-flow travel time on link l, v_l is the updated traffic flow on link l at step 2, and C_l is the capacity of link l;
5. The current link flows and link travel times are replaced by the updated link flows and link travel times, and the iteration moves on to the next time step.

The length of a time step in the congestion cascade process is set to be the time required for the flow redistribution to finish in step 2 of the above iteration. This is assumed to be one day, as the OD demand accounts for only commuting trips, and commuting trips are mostly made on a daily

basis. At every iteration, two features of the congestion cascade are recorded. If there are links getting congested at this iteration, the current time step is recorded as the links' failure time. In addition, the directions of the flow redistributions at this iteration, i.e. to which links the traffic flow has been redistributed from a previously congested link, are recorded. Step 1-5 iterates until all links are congested (a.k.a. gridlock) or no more congestion emerges (i.e. the network reaches a new equilibrium).

5.4. Setup of the simulation study for cascading power outages

The setup of this simulation study is a partial replication of the detailed simulation process on a 6-bus benchmark system [132] as implemented by Hines et al. [136]. Hines et al. [136] took the 6-bus benchmark system originally developed by Wood and Wollenberg [132] as a testing ground for cascading power outages. The original system has 6 buses (i.e. power stations) and 11 branches (i.e. power lines), and is robust against cascading outages. To enable generating outage cascades in the system, Hines et al. [136] proposed the modified version by removing 2 branches, resulting in a 6-bus 9-branch system which is used in both their study and the present simulation study. The original 6-bus system and the modifications made to it are shown in figure 11.

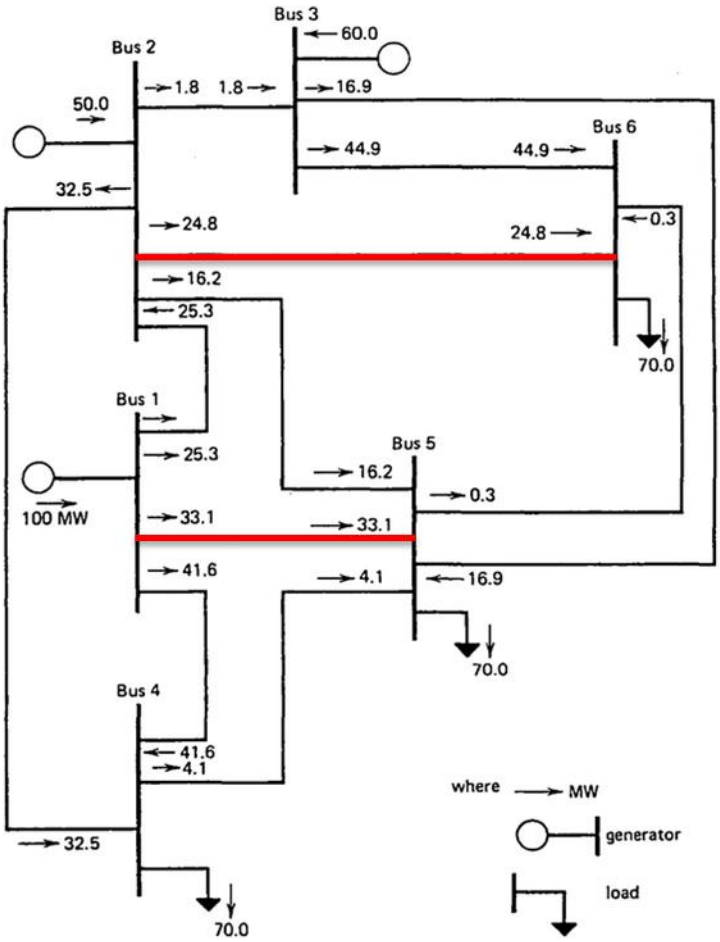

Figure 11: The 6-bus benchmark system. Buses 1, 2 and 3 are power generators that produce electricity, and buses 4,5 and 6 are users who consume electricity. Links between two buses are branches (power lines). Each branch carries a power flow, whose direction is marked by the arrow and the amount marked by the number following the arrow. The two red branches are originally in the system but removed by Hines et al. [136] to make the system vulnerable to cascading outages. This figure is replicated from Wood and Wollenberg [132].

Hines et al. [136] applied a power outage simulator named DCSIMSEP (abbreviation for a DC SIMulator of SEParation in power systems) [134, 135] to the modified 6-bus system. DCSIMSEP simulates multiple complex mechanisms in power outage cascades, including grid separation, load re-balancing, load shedding, flow re-dispatch and overloading failures. It iteratively updates the state of components (i.e. buses and branches) in a power system based on characteristics of electricity flow. At every iteration, it first checks if the network is separated into isolated “islands”.

For each island, electricity from power generators is re-dispatched to users in order to match supply and demand. If the supply is larger than demand after re-dispatching, certain power generators will be shut down; and if the demand is larger than supply, load shedding will take place and user demand for electricity will be scaled down. This process of load re-dispatching, generator tripping and load shedding iterates until a balance between supply and demand is reached. When an island reaches balance, the electricity flow on each of its power lines is calculated. A power line will fail if its flow is at a threshold above the flow limit for a certain amount of time. With the failed power line(s) removed, the simulator checks network separation again and repeats the above process, until no more overloaded power lines are present, or system collapse happens.

In Hines et al.'s study [136], the DCSIMSEP simulator was run 1000 times with random initial branch outages: each of the 9 branches has a probability 0.01 to fail initially. This process generated 1000 cascade instances. Hines et al. [136] proposed and applied an "influence graph" approach to the 1000 cascade instances to evaluate the likelihood of one power line outage causing another power line outage. The influence graph approach empirically quantifies the distribution of the number of outages produced by a branch following its failure and the probability that two branches fail at two consecutive time steps, using the 1000 cascade instances generated by the DCSIMSEP simulator. These two quantities are then combined to derive the probability of outage propagating from one of these two branches to the other.

The simulation process in the present simulation study follows Hines et al.'s study [136], except that the DCSIMSEP simulator is applied only once to the modified 6-bus system to generate only one cascade instance in the present simulation study. The time when each branch fails (i.e. becomes

overloaded and undergoes an outage) during the cascade is recorded. The DCSIMSEP simulates power system dynamics in continuous time. The recorded branch failure times are discretized to time steps of a length of 5 seconds, in order to suit them for the inputs to the inference model which is formulated in discrete time steps. Another input to the inference model is the geographical distance between any two branches in the modified 6-bus system. As this system is not spatially embedded and thus lacks geographical information about the branches, the geographical distance between two branches is estimated by their topological distance in the network, i.e. the minimum number of buses a path has to go through in order to connect the two branches.

Section 6
Simulation study results

The proposed inference model in section 4 is tested by comparing the inferred cascading failure process with the simulated cascading failure process in the four simulation studies described in section 5. The result of each simulation study focuses on the comparison at three aspects, as shown in figure 6. Firstly, the parameter estimates from the inference model are compared to the preset parameter values. This comparison applies only to the simulation studies of cascading failures in interdependent infrastructures and influenza epidemics, as only these two simulation studies have setups with known preset parameter values in the simulation process. Secondly, the temporal and spatial patterns of the cascading failure processes are compared between the simulation result and inference result. The temporal patterns refer to how the failures are distributed over time and the spatial patterns refer to how the failures spread in geographical space. This comparison applies to all the four simulation studies. Thirdly, the simulated node-to-node failure propagation patterns and their inferred counterparts are compared. Quantifying node-to-node failure propagation patterns involves first evaluating the failure propagation likelihood as in equation (11) from every node to every other node, and then identifying every node's most likely failure source as given by equation (23).

$$S(i) = \underset{j: j \in \mathbb{N} \setminus i}{\operatorname{argmax}} P\left(j \to i \middle| T_j = t_j, T_i = t_i\right), \tag{23}$$

where $S(i)$ is the most likely failure source for node i. The node-to-node failure propagation pattern can thus be represented by a "propagation network", in which a node represents a failed component and a directed link from node j to node i indicates that node j is node i's most likely failure source. In other words, a propagation network depicts the most likely paths through which failures propagate from the initial seeds to the rest of the network. Locally it also answers the

question of why a given node fails by identifying the sources responsible for the node's failure. Comparing the node-to-node failure propagation patterns therefore reduces to comparing the propagation networks between the simulation result and inference result. This comparison applies to all the four simulation studies as well. The results described in this section have been published as [262]. The following five sub-sections present the comparison results in the four simulation studies respectively and analysis of the computational complexity of the inference model.

6.1. Results in interdependent infrastructure cascading failures

The four general failure mechanisms are adopted as abstractions of the complex and difficult-to-model (specific) failure mechanisms behind cascading failures of interdependent infrastructures [89]. The external factors include the impacts of high winds and storm surges [263], evaluated by parameter $\beta_1^E \in [0,1]$ and $\beta_2^E \in [0,1]$, respectively. Spatial dependence is associated with parameter $\beta_1^S \in [0,1]$ and $\beta_2^S \in [0,\infty)$, which capture the location-based failure propagation likelihood [119] between two nodes when they are co-located and when they are separated by a distance, respectively. Functional dependence is drawn from null models (see section 4.2.2), and is characterized by β^F, which denotes the likelihood of failure propagation from one node to another if their operations are related (e.g. one providing resources to the other). The parameter estimates, together with their preset values and *t* values from the MLE, are shown in Table 4. A *t* value is the standardized deviation of a parameter estimate from its preset value, evaluated as $t = (\langle\beta\rangle - \beta)/\mathrm{SE}_\beta$, where $\langle\beta\rangle$ is the parameter estimate, β is the parameter's preset value and SE_β is the estimated standard error for this parameter.

Table 3: Parameter estimates for the model of infrastructure cascading failures

Parameter	Preset value	Estimate	t value

β_1^E	0.035	0.037	1.13
β_2^E	0.113	0.113	0.02
β_1^S	0.032	0.032	0.09
β_2^S	1.691	1.691	0.01
β^F	0.065	0.047	-1.81

All parameter estimates have insignificant deviations from their preset values, indicated by t values within the range [-1.96, 1.96]. This demonstrates the capability of the inference model to accurately quantify how the general failure mechanisms contributes to the emergence of cascading failures.

The number of failed nodes due to external factors, failure propagations and a combination of the two at each time step are shown in figure 12. Their temporal patterns show remarkable correspondence between the inferred curves (figure 12b) and the simulated ones (figure 12a). In terms of trends, the total number of failed nodes and failures due to propagations keep increasing until time step 5, before they drop to close to zero around time step 14. This trend is overall consistent with the empirical results on disaster impacts during Hurricane Sandy [263]. The number of failed nodes due to external factors decreases straight to zero at time step 6. The highest numbers of failed nodes per time step for the simulation and inference result are also similar with a value of 1050 and 1037 respectively, both at time step 5. The almost identical temporal patterns of simulation and inference result provide strong evidence that the model can capture the underlying cascading failure process given cascading failure outcomes (node failure times). This is further demonstrated by the comparison of failure hazards in figure 13.

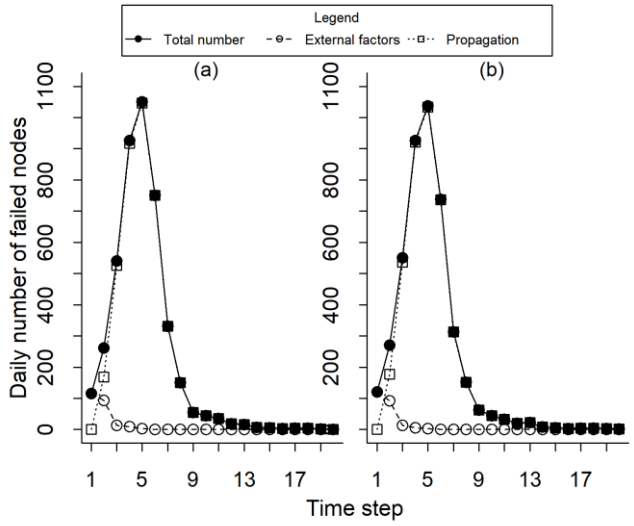

Figure 12: Comparison between simulated cascading process (a) and the inferred one (b). Different curves correspond to different spreading mechanisms. Failure due to external factors represents damages caused by storm surges and high winds. Propagations means failures of certain nodes lead to the failure of a given node. The total number is the sum of the number of failures due to the above two mechanisms.

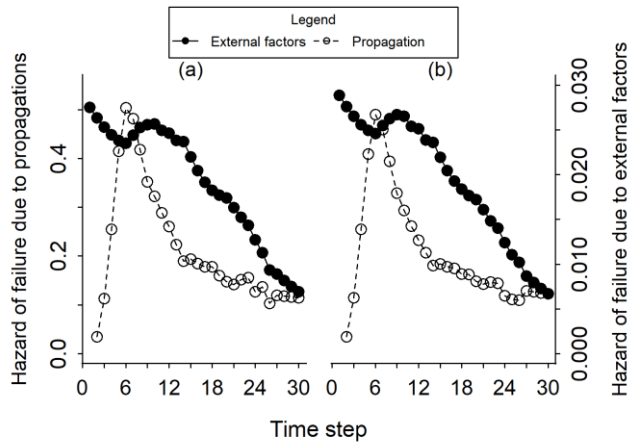

Figure 13: Evolution of failure hazards in the simulated cascading failure process (a) and the inferred one (b). Each figure shows the hazards of failures due to external factors or propagations separately.

Failure hazard is the instantaneous failure likelihood of a given node at a given time step. Failure hazard of node i due to external factors at time t_i is quantified by $\lambda_i(t_i|\boldsymbol{E})$ and the failure hazard of node i due to failure propagations at time t_i is quantified by $1-\prod_{j\in\mathbb{N}\setminus i}\left(1-P_{j\to i}\right)$. Both

quantities can be evaluated using formulations presented in section 4. Figure 13 shows that the inferred hazard functions (figure 13b) present patterns similar to the simulated ones (figure 13a). The hazard of failure due to external factors trends downwards from the beginning of the simulation, while the hazard of failure due to propagations reaches a peak around time step 7, and decreases thereafter. The result suggests that the model is able to recover the dynamics of general failure mechanisms in a scenario where they are constantly evolving. In addition, although the failure hazards due to external factors and due to propagations assume similar functional forms (see section 4.3.1), the differences in their temporal trends suggest that a single functional form in the detailed model formulation could capture different dynamics for the general failure mechanisms. This property suggests our model's versatility to handle diverse types of cascading failure processes.

The spatial patterns of infrastructure cascading failures in the simulation and inference result are presented in figure 14. The inference result (figure 14b and 14d) accurately captures the failure time of power service and transportation service in the majority of the census tracts in NYC when compared to the simulated failure times (figure 14a and 14c). The inferred failures and simulated failures show comparable spatial patterns in terms of how they spread geographically: early-stage failures (at time step 1-3) are scattered across the region, surrounded by failures that occurred later in time. This implies that certain census tracts act as centers that propagate failures of infrastructure service to their surrounding census tracts.

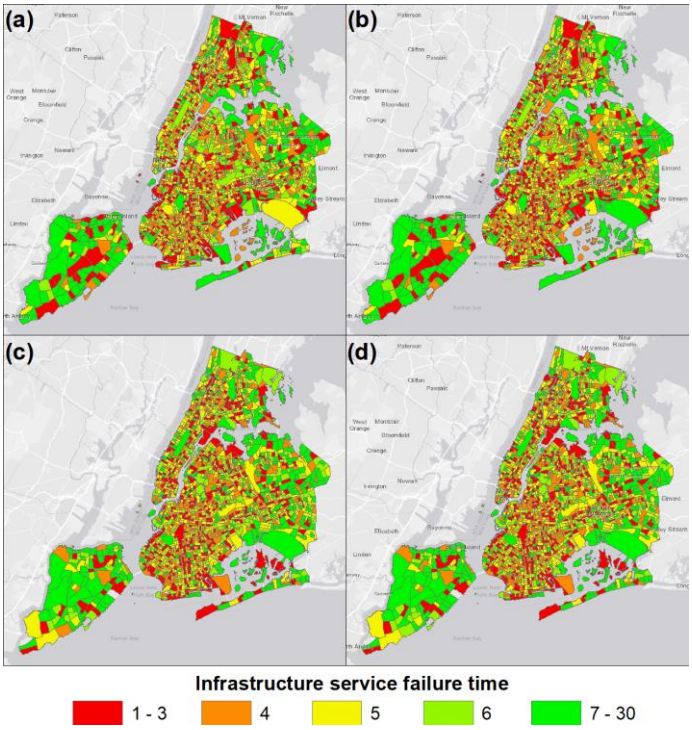

Figure 14: Comparison of the spatial patterns of infrastructure cascading failures between the inferred patterns (b and d) and simulated patterns (a and c). The upper two figures (a and b) show simulated and inferred failure time of transportation service in each census tract. The lower two figures (c and d) show corresponding results for the power service.

In addition to the temporal and spatial patterns of cascading failures, the node-to-node failure propagation patterns are also compared between the simulated patterns (figure 15a) and the inferred patterns (figure 15b) by first visualizing the propagation networks (as shown in the sub-figures of figure 15a and 15b) and then quantifying the degree distributions of the propagation networks. The degree of a node in a propagation network is defined as the number of nodes it is linked with, which include nodes that either propagate failures to it or it propagate failures to.

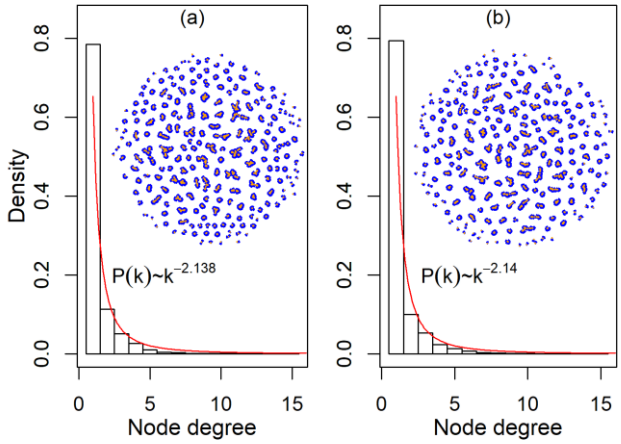

Figure 15: Comparison between the simulated failure propagation network (a) and the inferred one (b). The histograms and the curves in the figures show the degree distributions of the propagation networks and power-law functions fitted to the degree distributions, respectively. The graph inside each figure illustrates the propagation network, with nodes colored orange and links colored blue.

In figure 15, the visualized propagation networks show comparable patterns between simulation (figure 15a) and inference (figure 15b): nodes form tiny clusters among which few links are present. This suggests that in both the simulateion result and the inference result, the node-to-node propagation patterns are “local”, where any single node only influences a few other nodes rather than having a widespread influence over the entire infrastructure networks. This is also implied by the degree distributions shown in figure 15, on which power-law distributions can be fitted. The simulated propagation network and the inferred propagation network have notably matched degree distributions, with both similar densities for each degree category and close values of the fitted power-law coefficients.

6.2. Results in influenza epidemics

The simulation study of influenza epidemics does not consider external factors, as inflow of influenza infection cases from outside the study region is assumed to be controllable through travel

restrictions [241]. Therefore, the parameter $\boldsymbol{\beta^E}$ is not present in this simulation study. In addition, a temporal dependence parameter $\beta^T \in [0, \infty)$ is introduced to account for how the separation of two node failures in time affects the likelihood of failure propagation between these two nodes, as specified in equation (16). For functional dependence which is associated with close human contact (see section 4.3.2), the close-contact rate between two individuals is modeled to be proportional to the travel rate (number of trips per day) with a coefficient $\beta_1^F \in [0,1]$ if these two individuals are located in different zones, and proportional to the population density (population per square mile) with a coefficient $\beta_2^F \in [0,1]$ if the two individuals live in the same zone [239]. The spatial dependence in the epidemic model is not distance-based, but depends on zone proximity: any two individuals living in neighboring zones (which means the two zones share some boundaries) have a likelihood $\beta^S \in [0,1]$ of transmitting influenza between them in addition to the transmission likelihood attributed to close contact. The parameter estimates, along with their preset values and t values, are presented in Table 5.

Table 4: Parameter estimates for the model of epidemics

Parameter	Preset value	Estimate	t value
β_1^F	0.0015	0.0014	-0.07
β^S	0.017	0.017	-0.0001
β_2^F	0.038	0.038	-7×10^{-7}
β^T	3.6	3.6	0.07

All four parameters are accurately estimated, with estimates close to their preset values and deviations being insignificant ($|t|<1.96$). This demonstrates the capability of the inference model to recover the dynamics of a cascading failure process when underlying (specific) failure mechanisms are known and can be integrated into the inference model. The inferred epidemic process, in comparison with the simulated one, is illustrated in figure 16.

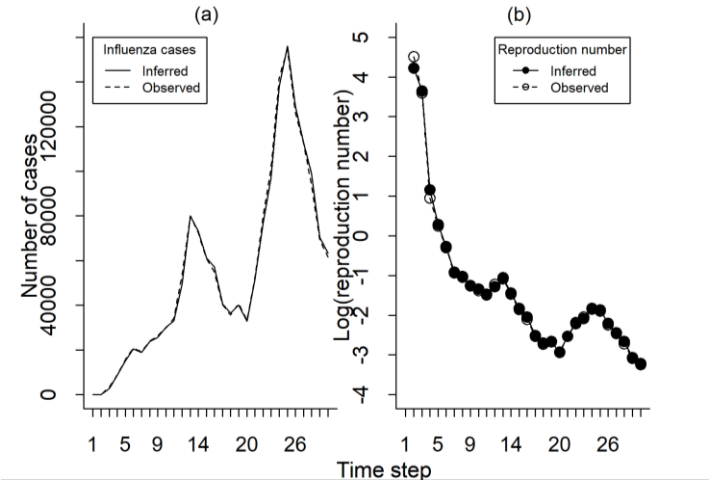

Figure 16: Comparison between inferred epidemic process and the simulated one. (a) illustrates the number of influenza cases per time step throughout the study period, and (b) shows the temporal evolution of reproduction numbers.

The inferred epidemic process and the simulated epidemic process in figure 16 show almost identical patterns. In terms of the number of influenza cases per time step, the curves for the inferred cases and simulated cases almost overlap: the inferred number of cases is within 1% deviation from the simulated number of cases for any time step. Two waves of infection outbreaks, one around time step 13 and the other around time step 25, are noticeable in both the simulated and inferred epidemic process. The reproduction numbers in both the inference result and simulation show decreasing trends, and cross the threshold of 1 (0 at log-scale) at the same time step of 6. These findings demonstrate our model's ability to recover the temporal patterns of an epidemic process. In terms of the spatial patterns, figure 17 illustrates the proportion of infected population in each census tract at time step 10, 20 and 30 for the inferred epidemic process (figure a-c) and the simulation (figure d-f), respectively. It further substantiates the consistency between the inferred epidemic process and the simulated one, as their spatial patterns are highly similar: the disease first emerges and spreads locally in southern Brooklyn, gradually covers the entire borough, and propagates to Manhattan, Queens and Staten Island by the end of the study period.

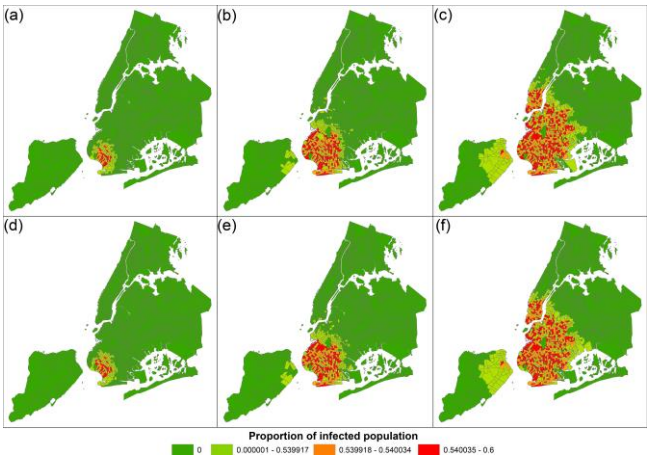

Figure 17: Spatial-temporal evolution of infections. (a)-(c) illustrate the inferred proportion of infected population in each census tract at time step 10, 20 and 30 respectively. And (d)-(f) are the corresponding proportions in the simulation data.

The node-to-node failure propagation patterns are analyzed at both zone level and individual level. The zone-level propagation networks, which indicate whether influenza spreads from one zone (census tract) to another, are illustrated in figure 18. The inferred propagation network (figure 18b) and the simulated propagation network (figure 18a) share a noticeable topological pattern: the network organization evolves from a lattice-like structure observed at early stages to a tree-like structure later in the process. The former pattern is recognizable in the upper part of the networks in figure 18a and 18b, which is characterized by small, overlapping cycles; and the latter is obvious in the lower part of the networks, showing “spikes” that are long branches in the tree structures. This finding adds to the evidence that the proposed model is capable of capturing the failure propagation patterns at network level as well as how the patterns evolve over time.

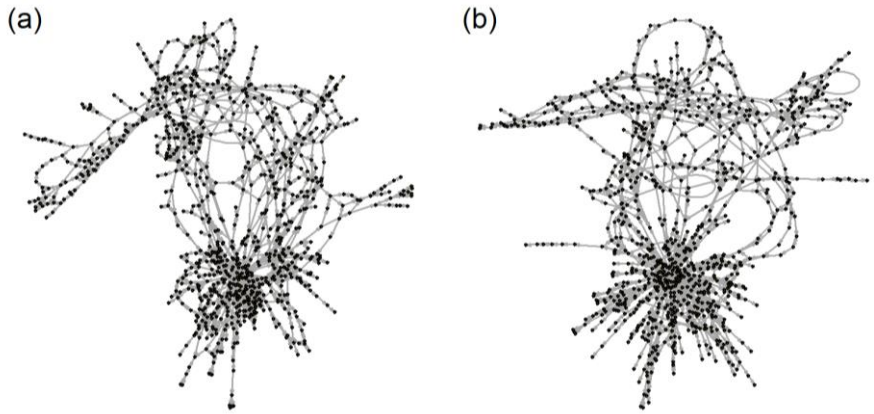

Figure 18: Comparison of the influenza spreading networks (i.e. the propagation networks) at zone level between simulation result (a) and inference result (b). Every node in the networks represents a census tract, and a link from A to B indicates there exist (at least one) cases in which an individual from census tract A infects an individual(s) in census tract B.

The degree distributions of the propagation networks at both zone level and individual level are evaluated in figure 19. At zone level (figure 19a and 19b), the node degrees follow Poisson distributions, which implies that zone-to-zone propagations take place independently of each other, and can be approximated by Bernoulli processes. The degrees of individual people in the propagation networks, on the other hand, are fitted into power-law distributions, suggesting that most people infect only a few others while there exist a small number who may have transmitted influenza to a large group. The inference model successfully reconstructs the simulated degree distributions at the two different scales, with similar shapes of the distributions as well as close Poisson/power-law coefficients between the simulated propagation networks and inferred propagation networks.

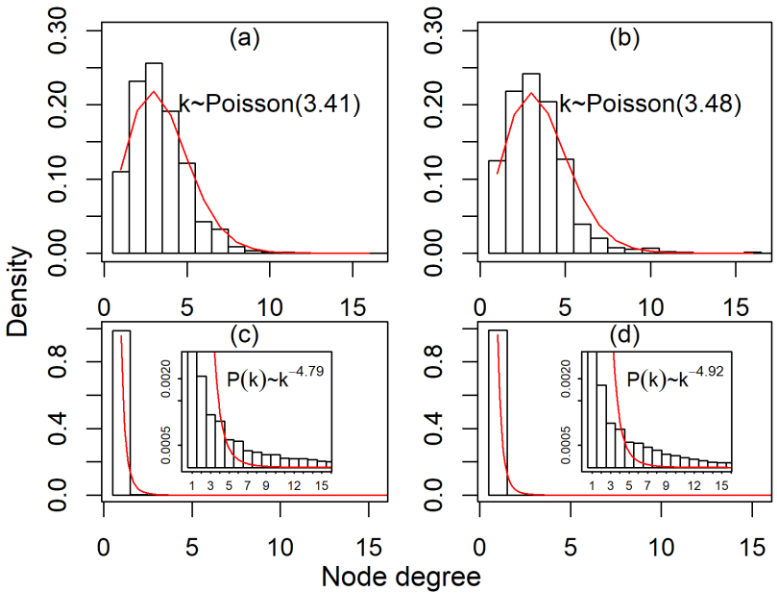

Figure 19: Comparison of degree distributions of influenza spreading networks (i.e. the propagation networks). (a) and (b) show the simulated and inferred degree distributions of the network at zone level. The distributions are fitted to Poisson distributions with similar parameters. (c) and (d) show the corresponding results at individual level. In an individual-level influenza spreading network, nodes represent individual people, and a link from one to the other indicates the former infects the latter. Power-law distributions are fitted for the degree distributions in this case.

6.3. Results in congestion cascade

Different from the previous two simulation studies, the failed (i.e. congested) components in a congestion cascade are links instead of nodes, as shown in figure 20a. The simulated link failure times are illustrated in figure 20a. The number of failed links per time step is shown in figure 20b and 20c for the simulation result and inference result, respectively.

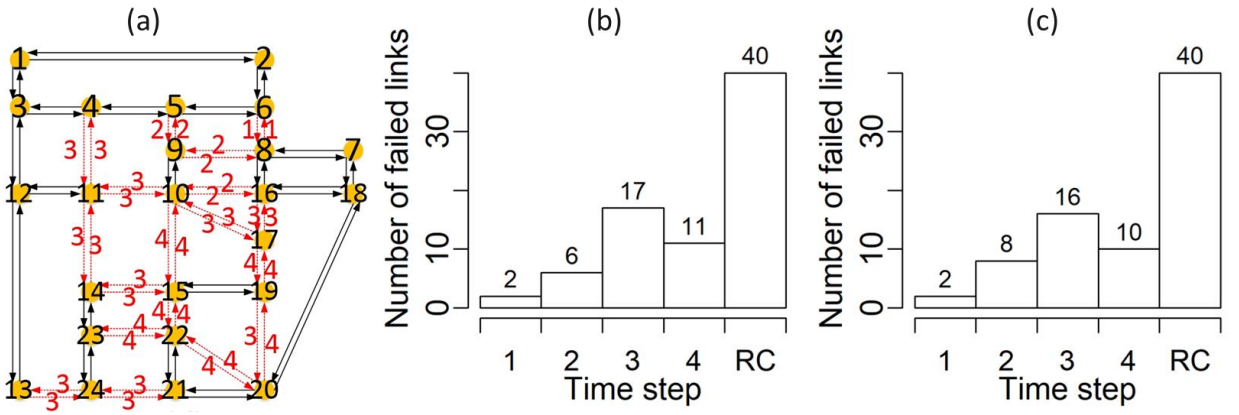

Figure 20: The congestion cascade process in the Sioux-Falls network. The network after the congestion cascade is shown in (a). The red dash links are congested, with the attached numbers denoting the time step when each link becomes congested. The figure (b) and (c) show the simulated number of failed (i.e. congested) links per time step and the inferred number of failed links per time step, respectively. RC means the right censoring period, i.e. when the time step is larger than 4.

The congestion cascade process is concluded in four time steps when the network reaches a new equilibrium, where no new flow redistributions and congestions/failures happen, and the network fragments into separated but functioning clusters of nodes and links. The number of congested/failed links at every time step in the simulation result and inference result demonstrates remarkable similarities, with deviations within ±2. Both numbers increase for three time steps before dropping at the fourth time step. As no more failure happens after time step 4, the surviving links at the end of time step 4 become right-censored, whose numbers are also the same for the simulation result and inference result.

The simulated and inferred failure propagation networks are shown in figure 21a and 21b, respectively. Both propagation networks show a separation of two clusters, one initialized by the failure of link 6→8 (which means the road segment from node 6 to node 8 in figure 10) and the other by the failure of link 8→6. More interestingly, the topologies of the clusters initialized by

link 6→8 in the simulated propagation network and inferred propagation network are exactly the same. For the cluster extending from link 8→6, the model is successful in recovering the hubs for propagating failures. In figure 21a, the link 8→6, 8→9 and 9→5 are identified as hubs, as each of them propagates failures to more than one link. They thus play a more important role in facilitating the failure propagations than other links, and could serve as potential candidates for strengthening in order to inhibit the progress of cascading failures. These three links emerge as hubs in the inferred failure propagation network (figure 21b) as well. A noticeable difference between the simulated propagation network and the inferred one is the overestimation of the number of hubs. The inference model misidentifies link 11→4 and 21→24 as hubs, which does not agree with the simulated propagation network. This difference likely results from the power-law degree distribution assumed for the functional dependence (see section 4.2.2) in the inference model. Due to the fat tail in a power-law distribution, it tends to generate a larger number of high-degree links that have functional dependences with multiple other links, compared to a binomial distribution which suggests more random occurrence of functional dependences. This finding casts doubts on the common belief that power-law distributions are prevalent in transportation systems [264].

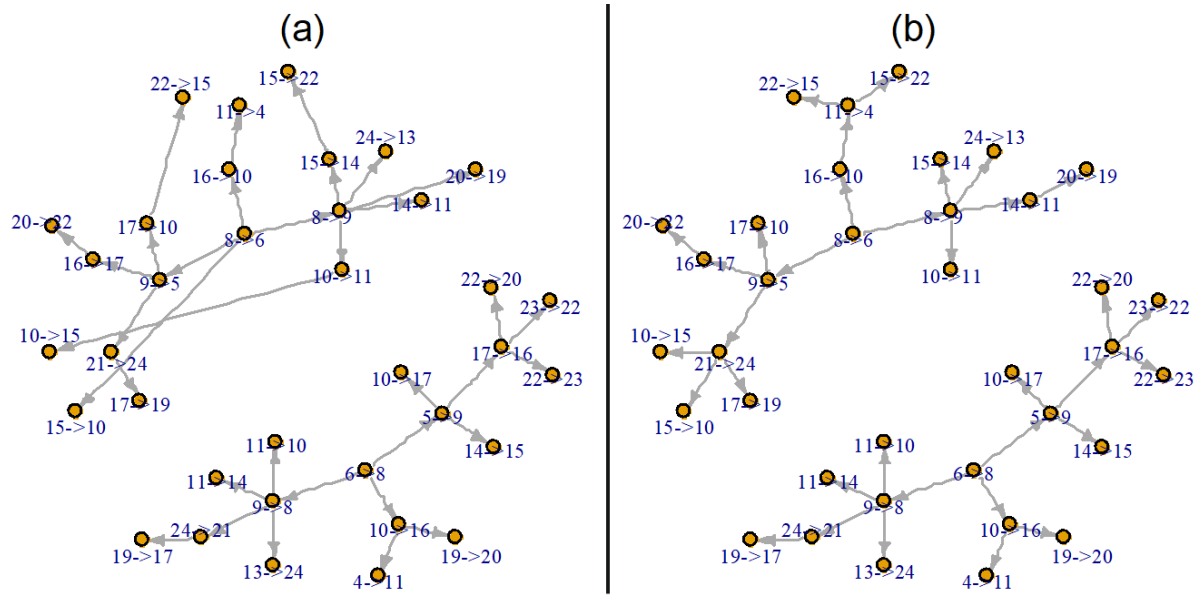

Figure 21: Failure propagation patterns for simulation result (a) and inference result (b). Each node in this figure represents a link (i.e. road segment) in the Sioux-Falls network (figure 10) that fails during the congestion cascade process. Its label A -> B indicates the link (road segment) from A to B in the Sioux-Falls network. Links in this figure represent the directions of failure propagations from one road segment to another.

6.4. Results in cascading power outages

A power outage cascade instance is generated using the DCSIMSEP simulator [134, 135] on the 6-bus benchmark system [132] with the same simulation setting as in Hines et al.'s study [136]. See section 5.4 for the detailed simulation settings. The inference model is applied to this one cascade instance to obtain the inferred power line failure times and inferred failure propagation network. The simulated power line failure times and the inferred power line failure times are illustrated in figure 22 on a simplified diagram of the 6-bus benchmark power system.

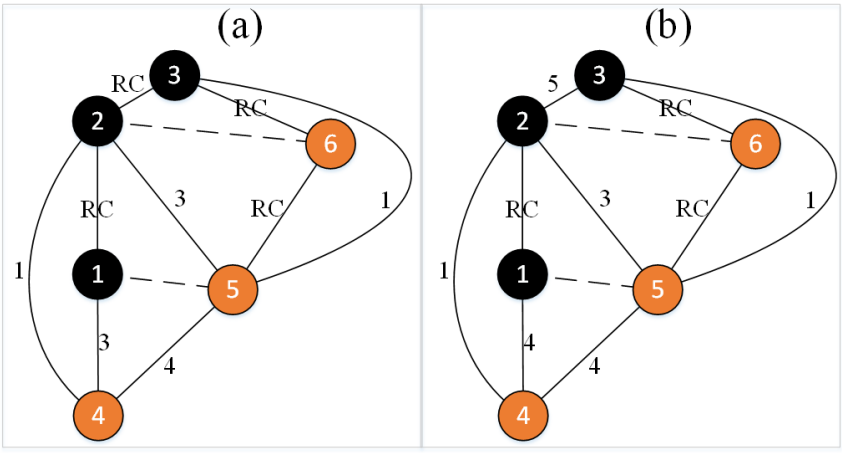

Figure 22: A simplified diagram of the 6-bus benchmark power system, with simulated failure time (a) and inferred failure time (b) of each power line marked. Black-colored nodes are power generators that produce electricity, and orange-colored nodes are users who consume electricity. Links in the networks symbolize power lines. The number attached to each link is the power line's failure time. RC means this link is right censored and does not fail in the simulation or inference model. The dashed two lines are initially removed, and thus regarded non-existent in both the simulation and inference model (see section 5.4).

The simulated failure times and the inferred ones are exactly the same except for two power lines,

namely 1-4 and 2-3. The inferred propagation network, in comparison with the influence graph obtained by Hine et al. [136] are shown in figure 23a and 23b, respectively.

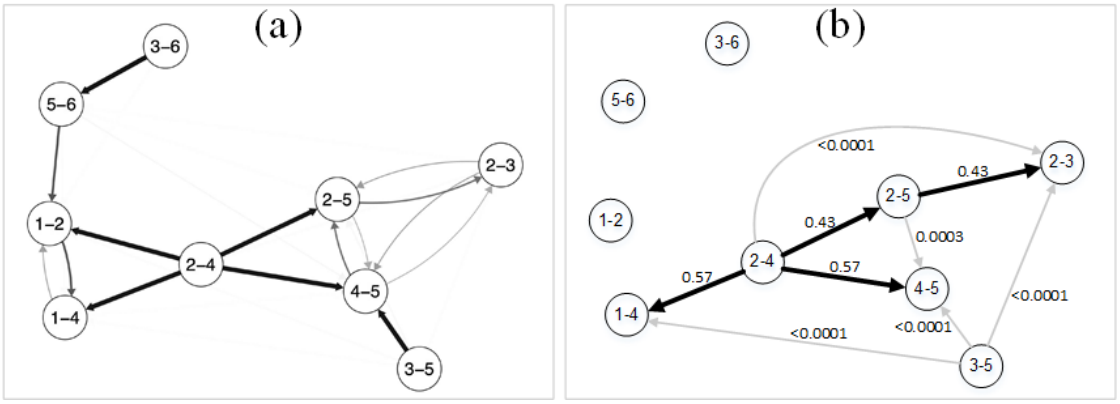

Figure 23: Comparison between the influence graph [136] and propagation network, shown in (a) and (b) respectively. Every node in the two graphs corresponds to a power line (i.e. a link in figure 22), and every link represents a non-zero probability of failure propagating from one power line to another. A darker and bolder link in this figure indicates a higher probability of failure propagation. The number associated with each link in (b) is the failure propagation probability.

The influence graph and the inferred failure propagation network are consistent in two respects. Firstly, for every power line that fails in the simulation, its most likely source of failure in the propagation network coincides with the one in the influence graph. This consistency is evident for the failure propagations from link 2-4 to link 1-4, 2-5 and 4-5, which present high probabilities (marked by dark-bold arrows) in both the influence graph and propagation network. For link 2-3, the propagation network also correctly identifies its most likely source of failure as link 2-5. And secondly, failure propagation probabilities from link 3-5 to link 1-4 and 2-3, and from link 2-5 to 4-5 are all insignificant (<0.05) in the propagation network, which corresponds to the small probabilities of these propagation paths in the influence graph. Two propagation paths, one from link 3-5 to 4-5, and the other from link 2-4 to 2-3, shows differences between the influence graph and propagation network. The failure propagation probability from 3-5 to 4-5 is significantly larger in the influence graph than in the propagation network. This could be attributed to the propagation

network being based on only one cascade instance, which has insufficiently characterized the propagation likelihood from 3-5 to 4-5. The use of only one cascade in obtaining the propagation network is also responsible for another difference between the influence graph and propagation network: the link 1-2, 3-6 and 5-6 are isolated in the propagation network, as no failure happens to them in this single cascade simulation. For the propagation path from link 2-4 to 2-3, its probability is unexpectedly positive (though insignificant) in the propagation network, while the influence graph returns a zero probability for it. A possible reason for this difference is the approximation of the geographical distance between these two links using their topological distance, as the 6-bus benchmark system is not spatially embedded and has no geographical information available for quantifying spatial dependence in the inference model. Assuming figure 11 reflects the real geographical layout of the 6-bus benchmark system, using the topological distance between link 2-4 and 2-3 will underestimate the true geographical distance between them, making them more spatially dependent than they actually are. This will further cause an overestimation of the failure propagation likelihood between them.

6.5. Computational complexity

For a given node i that fails at time t_i, calculating its failure probability $P(T_i = t_i)$ involves evaluating the failure hazard $\lambda_i(t_j)$ for node i at every time step t_j prior to t_i, i.e. $\forall\, t_j: t_j < t_i$, as suggested by equation (3)-(5). This process contributes to the computation time by a factor of $\sum_{t_j \in [1, t_i)} \delta(t_j < t_i)$, where $\delta(t_j < t_i)$ is an indicator function for $(t_j < t_i)$, i.e. $\delta(t_j < t_i) = \begin{cases} 1, & \text{if } t_j < t_i \\ 0, & \text{otherwise} \end{cases}$. Calculating the failure hazard $\lambda_i(t_j)$ for a given node i at a given time step t_j requires evaluating its probability of failure due to failure propagation $P_{k \to i}$ from every other node k that fails before t_j to node i, as suggested by equation (6). This process contributes to the

computation time by a factor of $\sum_{k\in\mathbb{N}\setminus i}\delta(t_k < t_j)$. And calculating the probability of failure due to failure propagation P_{k-i} demands the consideration of all time steps before t_j as possible failure times for node *k*, as suggested by equation (8). Therefore, it contributes to the computation time by a factor of $\sum_{t_k\in[1,t_j)}\delta(t_k < t_j)$. Combing these three key steps in formulating the likelihood function, the total computation time is

$$CT = \sum_{i\in\mathbb{N}}\sum_{t_j\in[1,t_i)}\delta(t_j < t_i)\sum_{k\in\mathbb{N}\setminus i}\delta(t_k < t_j)\sum_{t_k\in[1,t_j)}\delta(t_k < t_j), \tag{24}$$

The outer-most summation has a computational complexity to the order of $O(N)$ where *N* is the number of nodes in the network(s). The computational complexity of the inner three summations however, depends on the distribution of the failure times. The worst scenario is when nodes' failures are distributed evenly through the entire study period (i.e. uniformly distributed), which gives rise to a computational complexity of the inner summations to the order of $O(T_{obs}^2 N)$, where T_{obs} is the length of the study period. In contrast, when node failures are centered around a certain time, the inner three summations lead to a low order of computational complexity. In the extreme case where all nodes fail at the same time, the inner three summations have a computational complexity of $O(1)$. Combining the computation time of the outer summation and the inner three summations, the computational complexity for evaluating the likelihood function has a theoretical range from $O(N)$ to $(T_{obs}^2 N^2)$.

Considering that cascading failures are typically fast processes characterized by large numbers of failures in a short span of time [184, 230], it is expected that when applied to real-world cascading failure instances, the proposed model should demonstrate a performance close to $O(N)$. This result is demonstrated by a numerical analysis of the relationship between computation time and network

size (i.e. the number of individuals) in the influenza epidemic simulations, as depicted in figure 24. In this analysis, the population in every census tract is decreased by a common scaling factor, and the computation time is evaluated as the scaling factor changes. The result in figure 24 supports that the inference model has a computational complexity close to $O(N)$ by demonstrating a close-to-linear relationship between the computation time and the scaling factor.

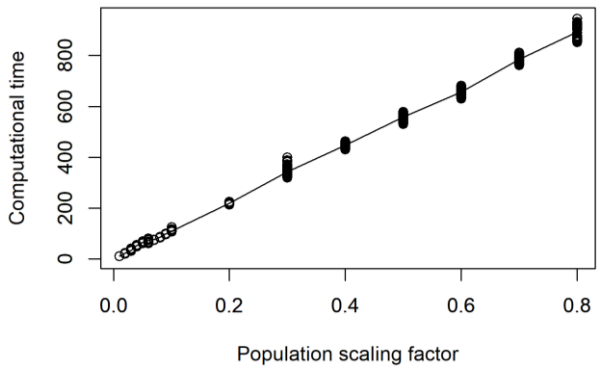

Figure 24: Numerical analysis of computational complexity. The figure shows how computation time for one iteration in solving the MLE changes with varying network sizes. For each network size (corresponding to a population scaling factor in the figure), 100 instances of simulation and inference with randomized population selections are implemented. Each point in the figure represents one instance. The line connects the mean computation time over the 100 instances for every value of the network size.

Section 7
Conclusions and discussion

Modeling cascading failure processes is an active and promising research field across multiple disciplines, considering their ubiquity and many unaddressed challenges in the current state of the art. The ultimate goals along this line of research are to understand and control the spreading of failures. A backward approach modeling framework aimed at these goals is proposed and tested in this dissertation. Four general failure mechanisms, which serve as abstractions of a variety of domain-specific failure mechanisms, are assumed to underlie all cascading failure processes. They are formulated into a survival-analysis-based model formulation that describes how the four general failure mechanisms give rise to a cascade of node failures. MLE is used to estimate the parameters associated with the general failure mechanisms. With the estimated parameters, the cascading failure process and node-to-node failure propagation patterns are reconstructed.

The proposed modeling framework demonstrates good performance both in quantification of the four general failure mechanisms and in reconstructing the cascading failure process temporally and spatially as well as the local node-to-node failure propagation patterns. In the simulation study of interdependent infrastructure cascading failures (a) and influenza epidemic (b) where the parameter values are preset in the simulations, the proposed model accurately infers the parameters in both cases. The temporal-spatial patterns of the cascading failure processes, as well as the node-to-node propagation patterns are compared between the simulation and inference results in all four simulation studies. The simulated and inferred temporal-spatial patterns show remarkable correspondence consistently throughout the four studies. The proposed model is also capable of recovering properties of the simulated failure propagation patterns, such as the degree distributions

of the propagation networks, the clustering of failures, the emergence of hubs in the propagation process, and the most likely failure propagation paths to individual nodes, as demonstrated by all four simulation studies. Particularly in the case of cascading power outages (d), the inferred node-to-node failure propagation probabilities using one cascade instance are consistent with the result from a validated simulation approach using the same power network but 1,000 cascade instances. This further demonstrates the capacity of the proposed approach in inferring cascading failure processes under non-data-intensive circumstances, considering that certain types of cascading failure data such as data on large-scale infrastructure failures are often sparse and difficult to collect.

One challenge in modeling cascading failures is that (specific) failure mechanisms vary from case to case and in different systems. Consequently, the specific failure mechanisms involved in a real-world cascading failure instance are usually not immediately known following the failures, and only knowable after a period of investigations and study [121, 122]. The proposed approach demonstrates potential capacity to address this challenge by using a high-level abstraction of specific failure mechanisms, which are represented by the four general failure mechanisms. Two properties of the proposed approach could be summarized from the four simulation studies. First, the model demonstrates the flexibility of integrating knowledge in specific failure mechanisms. In the influenza epidemic simulation study (b), where the specific failure propagation mechanism (i.e., close human contact) is known, this specific mechanism can be formulated into the model. In other words, the proposed approach can be operational both at an abstract level with the four general failure mechanisms and at a more detailed level with domain-specific failure mechanisms. This provides the proposed approach with the capacity to model both a well-understood cascading failure process (e.g., the spreading of some infectious diseases) as well as an emergent cascading

failure process where there is little knowledge about its underlying mechanisms. Second, the ability of the proposed approach in inferring the dynamics of cascading failure processes can be independent of the specific failure mechanisms underlying the cascading processes in specific systems. This is shown through the simulation study of congestion cascade (c) and cascading power outages (d), where the simulation data are generated by distinct (specific) failure propagation mechanisms. We show that our inference model recovers notably similar cascading failure processes and node-to-node failure propagation patterns with their simulated counterparts that are independently generated using domain-specific simulators. This finding has two implications: (i) the proposed model has general applicability to a variety of systems and cascading failures; and (ii) the model demonstrates robustness against misspecifications of its detailed formulations that quantify the general failure mechanisms.

One limitation of the proposed approach is the approximations made in formulating the likelihood of node failure due to external factors and the likelihood of node-to-node failure propagation, by assuming a probability distribution of node failure time (due to external factors) and a distribution of failure time interval, respectively. The approximations can cause two potential issues. First, it creates an interaction effect among the three failure propagation mechanisms. In particular, temporal dependence is made interactive with spatial dependence and functional dependence. This is because the parameterization of the probability distributions in terms of spatial dependence and functional dependence affects the shape of the distributions which capture temporal dependence. The interaction among the propagation mechanisms is a potential problem when the time dimension has an effect on the node-to-node failure propagations (e.g., periodicity in propagation occurrences) independent from spatial and functional factors. Interpreting the modeling results to

capture the dynamics of each failure propagation mechanism would then be difficult in this case, as their dynamics would confound each other. Second, a predefined and fixed probability distribution may be insufficient to characterize the dynamics of the failure mechanisms under certain circumstances. This is especially the case for a cascading failure process with a long life span, such as a global influenza epidemic which could last for months or even years. In this case, the failure mechanisms themselves could be evolving over time, resulting in shifts in the parameter values or even the type of probability distributions. Addressing this issue would require an inference model formulation that is capable of updating itself, which is a potentially interesting topic for future research.

Section 8
Future research suggestions

Addressing uncertainties in network-level propagation patterns. This dissertation addresses the uncertainties in failure propagation processes (see section 1.3) by solving baseline problem 1 as discussed in section 2.4.2. In other words, evaluating the pairwise failure propagation probability between any two nodes enables the proposed methodology to properly address the existence of multiple possible failure sources for a given failed node. However, when it comes to the failure propagation patterns at network level (e.g. the failure propagation network as analyzed in section 6), this dissertation takes the maximum likelihood approach and considers only the failure source with the highest likelihood to propagate failure to a given node. The concern behind this treatment is the computational complexity of considering all possible failure propagation patterns when dealing with a large network, whose number of possible propagation patterns increases exponentially with the number of nodes in the network. In this case where only the most likely propagation pattern is considered, one way to address the uncertainties in the propagation patterns is to run the model repeatedly. Depending on how many cascade instances are observed, the repeated runs of the model can take the same input or multiple different inputs. Each run of the model produces a most likely propagation pattern. After a sufficiently large number of model runs, the frequency (and thus probability) of each "most likely propagation pattern" can be evaluated. This approach provides a potential way to address the uncertainties in failure propagation patterns at network level.

Integrating the inference problem and reconstruction problem. The relationship between the inference problem and reconstruction problem (see section 2.4.2) in the proposed methodology is

illustrated in figure 25.

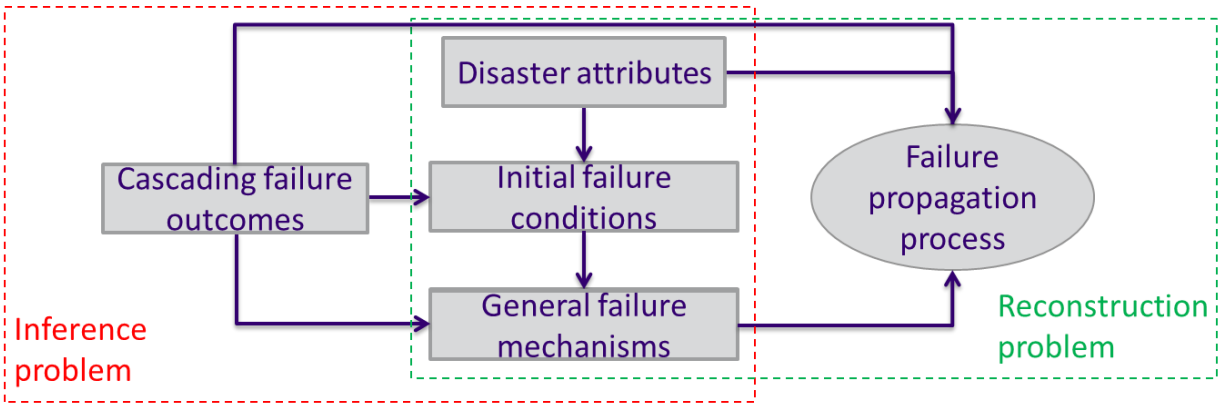

Figure 25: Relationship between the inference problem and reconstruction problem in the methodology framework. In this framework, cascading failure outcomes (i.e. node failure times) and disaster attributes (i.e. external factors) are taken as inputs. The external factors and node failure times combined can be used to infer the initial failures (due to external factors) which serve as seeds. The general failure mechanisms can be quantified by solving the MLE in the inference problem. Then the external factors, node failure times and quantified failure mechanisms are used to reconstruct the failure propagation process, which involves solving the reconstruction problem.

These two problems currently exist in a sequential manner: the inference problem is solved first and provide inputs to the reconstruction problem, and then the reconstruction problem is solved. As described in section 4.2.2, solving the reconstruction problem requires evaluating the *prior* probabilities of certain failure propagation patterns. The present methodology proposes the null models that can be utilized to evaluate these probabilities. A drawback of this approach is that in some cases, prior knowledge may not be available to generate the null models, and consequently the null models would be completely random.

One way to address this issue is to more closely integrate the inference problem and reconstruction problem by adding feedbacks to the sequential procedures. More specifically, instead of using the null models for prior probabilities of failure propagation patterns (in the reconstruction problem) and functional dependence structures (in the inference problem), the output propagation patterns (e.g. the propagation networks) by the model can be used. This would make the model an *iterative*

process. For every iteration, the failure propagation networks (each with a probability of occurrence) outputted from the last iteration are taken in place of the role of the null models in the present methodology, that is, to quantify the prior probabilities of certain failure propagation patterns in the reconstruction problem and the functional dependence structures in the inference problem. The iterative process converges when the propagation patterns obtained for two consecutive iterations stays consistent. Development of the present methodology in this direction could potentially increase the robustness of this methodology against the availability of prior knowledge in cascading failures.

Accounting for human factors. Infrastructure cascading failures in some cases are facilitated by human factors. For example, a human error or mistake in constructing a bridge decades ago could lead to the collapse of this bridge decades later. In this case, failure propagates from a human network (i.e. the network of engineers and construction workers) to an infrastructure system, which happens with a long time span. Modeling similar scenarios requires advancing the present methodology from three aspects. First, it requires the modeling capacity for cascading failures at a changing context. This is because failure propagations involving human factors typically take place with a long time span, and the context when the failure happens in the human network and the context when the failure happens in another system are likely different. Second, it calls for an approach with the ability to account for both short-range propagations and long-range propagations in the geographical space simultaneously. This is because human behaviors and decisions are less spatially constrained than infrastructure failures. A faulty bridge design made at a studio in Chicago, for example, could be responsible for a failed bridge in Seattle. Third, the model should be able to handle incomplete information. This is because human errors in most cases are indiscernible and

not reported. Therefore, modeling failure propagations that involve human errors needs to account for potential failures in the human networks that are not in the observed input data. Extending the modeling capacity to account for human factors in cascading failures is an interesting direction for future research as similar failure mechanisms explain many real-world (physical) infrastructure failures.

Understanding the effects of censoring distribution. Right censoring is common in cascading failure observations, where nodes remain functional at the end of an observation period. In survival analysis, the censoring time C_i of a node i was introduced to denote when this node's survival time becomes right-censored, and its distribution is a key input to formulating the survival likelihood function [265]. The proposed methodology addresses the right-censoring issue by assuming a constant C_i for all nodes. This assumption is typically true for infrastructure cascading failures where observations consist of snapshots of the infrastructure networks at every time step during the observation period. In some other cases, the propagation of rumors in a social network for example, the observations are obtained by tracking the traces of a piece of rumor instead of monitoring individual people's behaviors, and thus C_i may vary for different individuals. Therefore, it is worthwhile for future research to explore how different distributions of censoring time C_i would affect the formulation and performance of the proposed methodology.

Bibliography

1. Commission, F.P., *Report to the President by the Federal Power Commission on the Power Failure in the Northeastern United States and the Province of Ontario on November 9-10, 1965*, 1965, Federal Power Commission: Washington, D.C.
2. Vassell, G.S., *Northeast Blackout of 1965.* IEEE Power Engineering Review, 1991. **11**(1): p. 4.
3. Force, U.S.-C.P.S.O.T., *Final Report on the August 14, 2003 Blackout in the United States and Canada: Causes and Recommendations*, 2004.
4. Group, N.S., *Technical analysis of the August 14, 2003, blackout: What happened, why, and what did we learn*, 2004, North American Electric Reliability Council: Princeton, NJ.
5. Hines, P., K. Balasubramaniam, and E.C. Sanchez, *Cascading failures in power grids.* IEEE Potentials, 2009. **28**(5): p. 24-30.
6. Lu, W., et al. *Blackouts: Description, Analysis and Classification*. in *The 6th WSEAS International Conference on Power Systems*. 2006. Lisbon, Portugal.
7. Neumann, P.G., *Cause of AT&T network failure.* The Risks Digest, 1990. **9**(62).
8. Pertet, S. and P. Narasimhan. *Handling cascading failures: the case for topology-aware fault-tolerance*. in *IEEE First Workshop on Hot Topics in System Dependability*. 2005.
9. Peterson, I., *Fatal Defect: Chasing Killer Computer Bugs*1996, New York, NY: Vintage Books.
10. Wang, J., et al., *Cascading dynamics in congested complex networks.* European Physical Journal B, 2009. **67**(1): p. 95-100.
11. Motter, A.E. and Y.-C. Lai, *Cascade-based attacks on complex networks.* Physical Review E, 2002. **66**(6): p. 065102.
12. Motter, A.E., *Cascade Control and Defense in Complex Networks.* Physical Review Letters, 2004. **93**(9): p. 098701.
13. Zheng, J.-F., Z.-Y. Gao, and X.-M. Zhao, *Modeling cascading failures in congested complex networks.* Physica A: Statistical Mechanics and its Applications, 2007. **385**(2): p. 700-706.
14. Long, J., et al., *Urban traffic congestion propagation and bottleneck identification.* Science in China Series F: Information Sciences, 2008. **51**(7): p. 948-964.
15. Long, J., et al., *Urban Traffic Jam Simulation Based on the Cell Transmission Model.* Networks and Spatial Economics, 2011. **11**(1): p. 43-64.
16. Sun, H., et al., *Spatial distribution complexities of traffic congestion and bottlenecks in different network topologies.* Applied Mathematical Modelling, 2014. **38**(2): p. 496-505.
17. Daganzo, C.F., *The cell transmission model: A dynamic representation of highway traffic consistent with the hydrodynamic theory.* Transportation Research Part B: Methodological, 1994. **28**(4): p. 269-287.
18. Wright, C. and P. Roberg, *The conceptual structure of traffic jams.* Transport Policy, 1998. **5**(1): p. 23-35.
19. Daganzo, C.F., *The cell transmission model, part II: Network traffic.* Transportation Research Part B: Methodological, 1995. **29**(2): p. 79-93.
20. Crucitti, P., V. Latora, and M. Marchiori, *Model for cascading failures in complex networks.* Physical Review E, 2004. **69**(4): p. 045104.
21. Wu, J.J., H.J. Sun, and Z.Y. Gao, *Cascading failures on weighted urban traffic equilibrium networks.* Physica A: Statistical Mechanics and its Applications, 2007.

386(1): p. 407-413.
22. Johnson, C.W., *Analysing the causes of the Italian and Swiss Blackout, 28th September 2003*, in *Proceedings of the twelfth Australian workshop on Safety critical systems and software and safety-related programmable systems*2007, Australian Computer Society, Inc.: Adelaide, Australia. p. 21-30.
23. Corsi, S. and C. Sabelli. *General blackout in italy sunday september 28, 2003, h. 03: 28: 00*. in *Power Engineering Society General Meeting*. 2004. IEEE.
24. Buldyrev, S.V., et al., *Catastrophic cascade of failures in interdependent networks.* Nature, 2010. **464**(7291): p. 1025-1028.
25. Gao, J., et al., *Networks formed from interdependent networks.* Nature Physics, 2012. **8**(1): p. 40-48.
26. Gao, J., et al., *Robustness of a Network of Networks.* Physical Review Letters, 2011. **107**(19): p. 195701.
27. Shao, J., et al., *Cascade of failures in coupled network systems with multiple support-dependence relations.* Physical Review E, 2011. **83**(3): p. 036116.
28. Li, W., et al., *Cascading Failures in Interdependent Lattice Networks: The Critical Role of the Length of Dependency Links.* Physical Review Letters, 2012. **108**(22): p. 228702.
29. Dickison, M., S. Havlin, and H.E. Stanley, *Epidemics on interconnected networks.* Physical Review E, 2012. **85**(6): p. 066109.
30. Dong, G., et al., *Robustness of network of networks under targeted attack.* Physical Review E, 2013. **87**(5): p. 052804.
31. Wang, S., L. Hong, and X. Chen, *Vulnerability analysis of interdependent infrastructure systems: A methodological framework.* Physica A: Statistical Mechanics and its Applications, 2012. **391**(11): p. 3323-3335.
32. D'Agostino, G. and A. Scala, *Networks of networks: the last frontier of complexity*2014: Springer.
33. Cooper, C. and R. Block, *Disaster: Hurricane Katrina and the Failure of Homeland Security*2007, New York, NY: Times Books, Henry Holt and Company.
34. Childs, J.B., *Hurricane Katrina: Response and Responsibilities*2008, Berkeley, CA: North Atlantic Books.
35. Graham, S., *Disrupted Cities: When Infrastructure Fails*2010, New York, NY: Routledge.
36. Radio, N.P. *Timeline: Who Knew When the Levees Broke*. 2006; Available from: http://www.npr.org/templates/story/story.php?storyId=5200940.
37. Kates, R.W., et al., *Reconstruction of New Orleans after Hurricane Katrina: A research perspective.* Proceedings of the National Academy of Sciences, 2006. **103**(40): p. 14653-14660.
38. Reliability, O.O.E.D.a.E., *Hurricane Katrina Situation Report #11*, U.S.D.o. Energy, Editor 2005.
39. Benfield, K., et al., *After Katrina: New Solutions for Safe Communities and a Secure Energy Future*, 2005, Natural Resources Defense Council.
40. O'Rourke, T.D., *Critical infrastructure, interdependencies, and resilience.* The Bridge 2007. **37**(1): p. 22-29.
41. Chow, E. and J. Elkind, *Hurricane Katrina and US Energy Security.* Survival, 2005. **47**(4): p. 145-160.
42. Hamilton, R. *Lessons in emergency power preparedness: Planning in the wake of Katrina*. 2007; Available from:

http://power.cummins.com/sites/default/files/literature/technicalpapers/PT-7006-Standby-Katrina-en.pdf.
43. Kwasinski, A., et al., *Telecommunications Power Plant Damage Assessment for Hurricane Katrina– Site Survey and Follow-Up Results.* IEEE Systems Journal, 2009. **3**(3): p. 277-287.
44. Reed, D.A., M.D. Powell, and J.M. Westerman, *Energy Supply System Performance for Hurricane Katrina.* Journal of Energy Engineering, 2010. **136**(4): p. 95-102.
45. Bloomberg, M., *A stronger, more resilient New York*, in *The City of New York Special Initiative for Rebuilding and Resilience*2013, The City of New York: New York, NY.
46. Kolker, R., *How Did the MTA Restore Subway Service in Time for Monday's Rush Hour?*, in *New York Magazine*2012.
47. Comes, T. and B. Van de Walle. *Measuring disaster resilience: the impact of Hurricane Sandy on critical infrastructure systems*. in *Proceedings of the eleventh international ISCRAM conference*. 2014. University Park, PA.
48. Kaufman, S., et al., *Transportation During and After Hurricane Sandy*, 2012, New York University: New York, NY.
49. Sharkey, T.C., et al., *Identification and Classification of Restoration Interdependencies in the Wake of Hurricane Sandy.* Journal of Infrastructure Systems, 2016. **22**(1): p. 04015007.
50. Yusta, J.M., G.J. Correa, and R. Lacal-Arántegui, *Methodologies and applications for critical infrastructure protection: State-of-the-art.* Energy Policy, 2011. **39**(10): p. 6100-6119.
51. Scheffer, M., et al., *Early-warning signals for critical transitions.* Nature, 2009. **461**(7260): p. 53-59.
52. Rosato, V., et al., *Modelling interdependent infrastructures using interacting dynamical models.* International Journal of Critical Infrastructures, 2008. **4**(1-2): p. 63-79.
53. Kröger, W., *Critical infrastructures at risk: A need for a new conceptual approach and extended analytical tools.* Reliability Engineering & System Safety, 2008. **93**(12): p. 1781-1787.
54. Dokic, J., B. Müller, and G. Meyer, *European roadmap smart systems for automated driving*, 2015, European Technology Platform on Smart Systems Integration.
55. Wei, W., et al., *Expansion Planning of Urban Electrified Transportation Networks: A Mixed-Integer Convex Programming Approach.* IEEE Transactions on Transportation Electrification, 2017. **3**(1): p. 210-224.
56. Fagnant, D.J. and K. Kockelman, *Preparing a nation for autonomous vehicles: opportunities, barriers and policy recommendations.* Transportation Research Part A: Policy and Practice, 2015. **77**: p. 167-181.
57. Emanuel, K., *Increasing destructiveness of tropical cyclones over the past 30 years.* Nature, 2005. **436**(7051): p. 686-688.
58. Emanuel, K.A., *Downscaling CMIP5 climate models shows increased tropical cyclone activity over the 21st century.* Proceedings of the National Academy of Sciences, 2013. **110**(30): p. 12219-12224.
59. Diffenbaugh, N.S. and C.B. Field, *Changes in Ecologically Critical Terrestrial Climate Conditions.* Science, 2013. **341**(6145): p. 486-492.
60. Rosenzweig, C., et al., *Developing coastal adaptation to climate change in the New York City infrastructure-shed: process, approach, tools, and strategies.* Climatic Change,

2011. **106**(1): p. 93-127.
61. Obama, B., *Executive Order 13636: Improving Critical Infrastructure Cybersecurity*, T.W. House, Editor 2013: Washington, D.C.
62. President, T., *Presidential policy directive–critical infrastructure security and resilience*, T.W. House, Editor 2013: Washington, D.C.
63. Friedlander, G.D., *The Northeast power failurea – blanket of darkness.* IEEE Spectrum, 1966. **3**(2): p. 54-73.
64. Farrell, A.E., H. Zerriffi, and H. Dowlatabadi, *Energy infrastructure and security.* Annual Review of Environment and Resources, 2004. **29**(1): p. 421-469.
65. Farmer, R.G. and E.H. Allen. *Power System Dynamic Performance Advancement From History of North American Blackouts*. in *2006 IEEE PES Power Systems Conference and Exposition*. 2006. Atlanta, GA.
66. Pourbeik, P., P.S. Kundur, and C.W. Taylor, *The anatomy of a power grid blackout - Root causes and dynamics of recent major blackouts.* IEEE Power and Energy Magazine, 2006. **4**(5): p. 22-29.
67. Makarov, Y.V., et al., *Blackout Prevention in the United States, Europe, and Russia.* Proceedings of the IEEE, 2005. **93**(11): p. 1942-1955.
68. Parrilo, P.A., et al. *Model reduction for analysis of cascading failures in power systems*. in *Proceedings of the 1999 American Control Conference (Cat. No. 99CH36251)*. 1999.
69. Watts, D.J., *A simple model of global cascades on random networks.* Proceedings of the National Academy of Sciences, 2002. **99**(9): p. 5766-5771.
70. Albert, R. and A.-L. Barabási, *Statistical mechanics of complex networks.* Reviews of Modern Physics, 2002. **74**(1): p. 47-97.
71. Ben-Naim, E., H. Frauenfelder, and Z. Toroczkai, *Complex Networks*2004: Springer Science & Business Media.
72. Gao, J., B. Barzel, and A.-L. Barabási, *Universal resilience patterns in complex networks.* Nature, 2016. **530**(7590): p. 307-312.
73. Moreno, Y., J. Gómez, and A. Pacheco, *Instability of scale-free networks under node-breaking avalanches.* EPL (Europhysics Letters), 2002. **58**(4): p. 630-636.
74. Goh, K.I., et al., *Sandpile on Scale-Free Networks.* Physical Review Letters, 2003. **91**(14): p. 148701.
75. Rinaldi, S.M., J.P. Peerenboom, and T.K. Kelly, *Identifying, understanding, and analyzing critical infrastructure interdependencies.* IEEE Control Systems, 2001. **21**(6): p. 11-25.
76. Newman, M.E.J., *The Structure and Function of Complex Networks.* SIAM Review, 2003. **45**(2): p. 167-256.
77. Dueñas-Osorio, L. and S.M. Vemuru, *Cascading failures in complex infrastructure systems.* Structural Safety, 2009. **31**(2): p. 157-167.
78. Hernandez-Fajardo, I. and L. Dueñas-Osorio, *Probabilistic study of cascading failures in complex interdependent lifeline systems.* Reliability Engineering & System Safety, 2013. **111**: p. 260-272.
79. Johansson, J. and H. Hassel, *An approach for modelling interdependent infrastructures in the context of vulnerability analysis.* Reliability Engineering & System Safety, 2010. **95**(12): p. 1335-1344.
80. Wang, Z., et al., *Failure risk propagation and protection schemes in coupled systems.* Chaos, Solitons & Fractals, 2015. **80**: p. 62-75.

81. Parshani, R., S.V. Buldyrev, and S. Havlin, *Interdependent Networks: Reducing the Coupling Strength Leads to a Change from a First to Second Order Percolation Transition.* Physical Review Letters, 2010. **105**(4): p. 048701.
82. Baxter, G.J., et al., *Avalanche Collapse of Interdependent Networks.* Physical Review Letters, 2012. **109**(24): p. 248701.
83. Cellai, D., et al., *Percolation in multiplex networks with overlap.* Physical Review E, 2013. **88**(5): p. 052811.
84. Gao, J., D. Li, and S. Havlin, *From a single network to a network of networks.* National Science Review, 2014. **1**: p. 346-356.
85. Gao, J., et al., *Recent Progress on the Resilience of Complex Networks.* Energies, 2015. **8**(10): p. 12187-12210.
86. Barabási, A.L., *Network Science*2016, Cambridge, UK: Cambridge University Press.
87. Dueñas-Osorio, L., J.I. Craig, and B.J. Goodno, *Seismic response of critical interdependent networks.* Earthquake Engineering & Structural Dynamics, 2007. **36**(2): p. 285-306.
88. Robert, B., *A method for the study of cascading effects within lifeline networks.* International Journal of Critical Infrastructures, 2004. **1**(1): p. 86-99.
89. Ouyang, M., *Review on modeling and simulation of interdependent critical infrastructure systems.* Reliability Engineering & System Safety, 2014. **121**: p. 43-60.
90. Cuadra, L., et al., *A Critical Review of Robustness in Power Grids Using Complex Networks Concepts.* Energies, 2015. **8**(9): p. 9211.
91. Guo, H., et al., *A critical review of cascading failure analysis and modeling of power system.* Renewable and Sustainable Energy Reviews, 2017. **80**: p. 9-22.
92. Liao, H., J. Apt, and S. Talukdar. *Phase transitions in the probability of cascading failures*. in *Electricity Transmission in Deregulated Markets: Challenges, Opportunities, and Necessary R&D Agenda*. 2004. Pittsburgh, PA.
93. Hines, P., et al. *Autonomous agents and cooperation for the control of cascading failures in electric grids*. in *Proceedings. 2005 IEEE Networking, Sensing and Control, 2005.* 2005. Tucson, AZ.
94. Talukdar, S.N., et al., *Cascading Failures: Survival versus Prevention.* The Electricity Journal, 2003. **16**(9): p. 25-31.
95. Dobson, I. *Where is the edge for cascading failure?: challenges and opportunities for quantifying blackout risk*. in *2007 IEEE Power Engineering Society General Meeting*. 2007. Tampa, FL.
96. Dorogovtsev, S.N., A.V. Goltsev, and J.F.F. Mendes, *Critical phenomena in complex networks.* Reviews of Modern Physics, 2008. **80**(4): p. 1275-1335.
97. Barrat, A., M. Barthelemy, and A. Vespignani, *Dynamical processes on complex networks*2008, Cambridge, UK: Cambridge university press.
98. Cohen, R. and S. Havlin, *Complex Networks: Structure, Robustness and Function*2010, Cambridge, UK: Cambridge University Press.
99. Simonsen, I., et al., *Transient Dynamics Increasing Network Vulnerability to Cascading Failures.* Physical Review Letters, 2008. **100**(21): p. 218701.
100. Dobson, I., et al., *Complex systems analysis of series of blackouts: Cascading failure, critical points, and self-organization.* Chaos: An Interdisciplinary Journal of Nonlinear Science, 2007. **17**(2): p. 026103.
101. DeMarco, C.L., *A phase transition model for cascading network failure.* IEEE Control

Systems, 2001. **21**(6): p. 40-51.
102. Kübler, D. and G. Weizsäcker, *Limited Depth of Reasoning and Failure of Cascade Formation in the Laboratory.* The Review of Economic Studies, 2004. **71**(2): p. 425-441.
103. Gross, T., C.J.D. D'Lima, and B. Blasius, *Epidemic Dynamics on an Adaptive Network.* Physical Review Letters, 2006. **96**(20): p. 208701.
104. Bakken, D., *Smart Grids: Clouds, Communications, Open Source, and Automation*2014, Boca Raton, FL: CRC Press.
105. Nicholls, J.G., et al., *From neuron to brain*. Vol. 271. 2001, Sunderland, MA: Sinauer Associates, Inc.
106. Wei, Y., D. Tsigankov, and A. Koulakov, *The molecular basis for the development of neural maps.* Annals of the New York Academy of Sciences, 2013. **1305**(1): p. 44-60.
107. Corrêa Alegria, F., *Measurement challenges in trying to understand our brain.* Measurement, 2013. **46**(8): p. 2950-2962.
108. Power, Jonathan D., et al., *Functional Network Organization of the Human Brain.* Neuron, 2011. **72**(4): p. 665-678.
109. Forstmann, B.U., et al., *Multi-modal ultra-high resolution structural 7-Tesla MRI data repository.* Scientific Data, 2014. **1**: p. 140050.
110. Bumiller, G., L. Lampe, and H. Hrasnica, *Power line communication networks for large-scale control and automation systems.* IEEE Communications Magazine, 2010. **48**(4): p. 106-113.
111. Erseghe, T., S. Tomasin, and A. Vigato, *Topology Estimation for Smart Micro Grids via Powerline Communications.* IEEE Transactions on Signal Processing, 2013. **61**(13): p. 3368-3377.
112. McDaniels, T., et al., *Empirical Framework for Characterizing Infrastructure Failure Interdependencies.* Journal of Infrastructure Systems, 2007. **13**(3): p. 175-184.
113. Kuhn, F., N. Lynch, and R. Oshman. *Distributed computation in dynamic networks*. in *Proceedings of the forty-second ACM symposium on Theory of computing*. 2010. Cambridge, MA: ACM.
114. Vaiman, et al., *Risk Assessment of Cascading Outages: Methodologies and Challenges.* IEEE Transactions on Power Systems, 2012. **27**(2): p. 631-641.
115. Carreras, B.A., et al. *Initial evidence for self-organized criticality in electric power system blackouts*. in *Proceedings of the 33rd Annual Hawaii International Conference on System Sciences*. 2000. Maui, Hawaii.
116. Xianzhong, D. and S. Sheng, *Self-Organized Criticality in Time Series of Power Systems Fault, Its Mechanism, and Potential Application.* IEEE Transactions on Power Systems, 2010. **25**(4): p. 1857-1864.
117. Ma, R., X. Ban, and J.-S. Pang, *Continuous-time dynamic system optimum for single-destination traffic networks with queue spillbacks.* Transportation Research Part B: Methodological, 2014. **68**: p. 98-122.
118. Gentile, G., L. Meschini, and N. Papola, *Spillback congestion in dynamic traffic assignment: A macroscopic flow model with time-varying bottlenecks.* Transportation Research Part B: Methodological, 2007. **41**(10): p. 1114-1138.
119. Daqing, L., et al., *Spatial correlation analysis of cascading failures: Congestions and Blackouts.* Scientific Reports, 2014. **4**: p. 5381.
120. Lorenz, J., S. Battiston, and F. Schweitzer, *Systemic risk in a unifying framework for cascading processes on networks.* The European Physical Journal B, 2009. **71**(4): p. 441.

121. Dobson, I., J. Kim, and K.R. Wierzbicki, *Testing Branching Process Estimators of Cascading Failure with Data from a Simulation of Transmission Line Outages.* Risk Analysis, 2010. **30**(4): p. 650-662.
122. U.S.-Canada Power System Outage Task Force, *Final Report on the August 14th Blackout in the United States and Canada: Causes and Recommendations*, 2004, U.S. Department of Energy and National Resources Canada.
123. Narasimhan, H., D.C. Parkes, and Y. Singer. *Learnability of influence in networks*. in *Advances in Neural Information Processing Systems*. 2015. Montreal, Quebec.
124. Dahleh, M.A., J.N. Tsitsiklis, and S.I. Zoumpoulis. *The Value of Temporally Richer Data for Learning of Influence Networks*. in *Web and Internet Economics: 10th International Conference, WINE 2014*. 2014. Beijing, China: Springer.
125. Dahleh, M.A., J.N. Tsitsiklis, and S.I. Zoumpoulis. *The value of temporal data for learning of influence networks: A characterization via Kullback-Leibler divergence*. in *54th IEEE Conference on Decision and Control (CDC)*. 2015. Osaka, Japan: IEEE.
126. Boccaletti, S., et al., *Complex networks: Structure and dynamics.* Physics Reports, 2006. **424**(4): p. 175-308.
127. Netrapalli, P. and S. Sanghavi. *Learning the graph of epidemic cascades*. in *Proceedings of the 12th ACM SIGMETRICS/PERFORMANCE joint international conference on Measurement and Modeling of Computer Systems*. 2012. London, UK: ACM.
128. Gomez-Rodriguez, M., et al., *Uncovering the structure and temporal dynamics of information propagation.* Network Science, 2014. **2**(1): p. 26-65.
129. Dueñas-Osorio, L., et al., *Interdependent Response of Networked Systems.* Journal of Infrastructure Systems, 2007. **13**(3): p. 185-194.
130. Haydon, D.T., et al., *The construction and analysis of epidemic trees with reference to the 2001 UK foot–and–mouth outbreak.* Proceedings of the Royal Society B: Biological Sciences, 2003. **270**(1511): p. 121-127.
131. LeBlanc, L.J., E.K. Morlok, and W.P. Pierskalla, *An efficient approach to solving the road network equilibrium traffic assignment problem.* Transportation Research, 1975. **9**(5): p. 309-318.
132. Wood, A.J. and B.F. Wollenberg, *Power Generation, Operation, and Control*2012, New York, NY: John Wiley & Sons.
133. Hines, P., E. Cotilla-Sanchez, and S. Blumsack, *Do topological models provide good information about electricity infrastructure vulnerability?* Chaos: An Interdisciplinary Journal of Nonlinear Science, 2010. **20**(3): p. 033122.
134. Eppstein, M.J. and P.D.H. Hines, *A “Random Chemistry” Algorithm for Identifying Collections of Multiple Contingencies That Initiate Cascading Failure.* IEEE Transactions on Power Systems, 2012. **27**(3): p. 1698-1705.
135. Rezaei, P., P.D.H. Hines, and M.J. Eppstein, *Estimating Cascading Failure Risk With Random Chemistry.* IEEE Transactions on Power Systems, 2015. **30**(5): p. 2726-2735.
136. Hines, P.D.H., I. Dobson, and P. Rezaei, *Cascading Power Outages Propagate Locally in an Influence Graph That is Not the Actual Grid Topology.* IEEE Transactions on Power Systems, 2017. **32**(2): p. 958-967.
137. Vázquez, A., *Causal Tree of Disease Transmission and The Spreading of Infectious Diseases*, in *Discrete Methods in Epidemiology*, J. Abello and G. Cormode, Editors. 2006, American Mathematical Society. p. 163-180.
138. Gomez-Rodriguez, M., J. Leskovec, and A. Krause, *Inferring Networks of Diffusion and*

Influence. ACM Transactions on Knowledge Discovery from Data, 2012. **5**(4): p. 1-37.
139. Wang, W.-X., Y.-C. Lai, and D. Armbruster, *Cascading failures and the emergence of cooperation in evolutionary-game based models of social and economical networks.* Chaos: An Interdisciplinary Journal of Nonlinear Science, 2011. **21**(3): p. 033112.
140. Smart, A.G., L.A.N. Amaral, and J.M. Ottino, *Cascading failure and robustness in metabolic networks.* Proceedings of the National Academy of Sciences, 2008. **105**(36): p. 13223-13228.
141. Dudenhoeffer, D.D., M.R. Permann, and M. Manic, *CIMS: a framework for infrastructure interdependency modeling and analysis*, in *Proceedings of the 38th conference on Winter simulation*2006, Winter Simulation Conference: Monterey, California. p. 478-485.
142. Fritz, C.E., *Disasters*, in *Contemporary Social Problems: An Introduction to the Sociology of Deviant Behavior and Social Disorganization*, R.K. Merton and R.A. Nisbet, Editors. 1961, University of California Press: Riverside, CA. p. 651–694.
143. Cromwell, J.E., *Costs of Infrastructure Failure*2002, Denver, CO: AWWA Research Foundation and American Water Works Association.
144. Sporns, O., *Structure and function of complex brain networks.* Dialogues in Clinical Neuroscience, 2013. **15**(3): p. 247-262.
145. Rubinov, M. and O. Sporns, *Complex network measures of brain connectivity: Uses and interpretations.* NeuroImage, 2010. **52**(3): p. 1059-1069.
146. Bell, M.G.H. and Y. Iida, *Transportation Network Analysis*1997, Hoboken, NJ Wiley (John) & Sons.
147. Dueñas-Osorio, L., J.I. Craig, and B.J. Goodno. *Probabilistic response of interdependent infrastructure networks*. in *2nd annual meting of the Asian-pacific network of centers for earthquake engineering research (ANCER)*. 2004. Honolulu, Hawaii.
148. Zhang, P. and S. Peeta, *A generalized modeling framework to analyze interdependencies among infrastructure systems.* Transportation Research Part B: Methodological, 2011. **45**(3): p. 553-579.
149. Setola, R. and M. Theocharidou, *Modelling Dependencies Between Critical Infrastructures*, in *Managing the Complexity of Critical Infrastructures: A Modelling and Simulation Approach*, R. Setola, et al., Editors. 2016, Springer International Publishing: Cham, Switzerland. p. 19-41.
150. Zhou, T., L. Lü, and Y.-C. Zhang, *Predicting missing links via local information.* The European Physical Journal B, 2009. **71**(4): p. 623-630.
151. Yook, S.-H., H. Jeong, and A.-L. Barabási, *Modeling the Internet's large-scale topology.* Proceedings of the National Academy of Sciences, 2002. **99**(21): p. 13382-13386.
152. Barthélemy, M., *Spatial networks.* Physics Reports, 2011. **499**(1): p. 1-101.
153. Rinaldi, S.M. *Modeling and simulating critical infrastructures and their interdependencies*. in *Proceedings of the 37th Annual Hawaii International Conference on System Sciences, 2004.* . 2004. Big Island, HI.
154. Reed, D.A., K.C. Kapur, and R.D. Christie, *Methodology for Assessing the Resilience of Networked Infrastructure.* IEEE Systems Journal, 2009. **3**(2): p. 174-180.
155. Ibáñez, E., et al., *Interdependencies between Energy and Transportation Systems for National Long Term Planning*, in *Sustainable and Resilient Critical Infrastructure Systems: Simulation, Modeling, and Intelligent Engineering*, K. Gopalakrishnan and S. Peeta, Editors. 2010, Springer-Verlag Berlin Heidelberg: Berlin, Germany. p. 53-76.

156. Selva, J., et al. *Seismic performance of a system of interdependent lifeline and infrastructure components*. in *8th International Conference on Urban Earthquake Engineering*. 2011. Tokyo, Japan.
157. Fu, G., et al., *Interdependent networks: vulnerability analysis and strategies to limit cascading failure.* The European Physical Journal B, 2014. **87**(7): p. 148.
158. Heller, M. *Interdependencies in civil infrastructure systems*. in *Frontiers of Engineering: Reports on Leading-Edge Engineering from the 2001 NAE Symposium on Frontiers of Engineering*. 2002. Washington, D.C.: National Academies Press.
159. Leavitt, W.M. and J.J. Kiefer, *Infrastructure Interdependency and the Creation of a Normal Disaster: The Case of Hurricane Katrina and the City of New Orleans.* Public Works Management & Policy, 2006. **10**(4): p. 306-314.
160. Haraguchi, M. and S. Kim, *Critical infrastructure interdependence in New York City during Hurricane Sandy.* International Journal of Disaster Resilience in the Built Environment, 2016. **7**(2): p. 133-143.
161. Dawson, R., *Handling Interdependencies in Climate Change Risk Assessment.* Climate, 2015. **3**(4): p. 1079-1096.
162. Ouyang, M., et al., *A methodological approach to analyze vulnerability of interdependent infrastructures.* Simulation Modelling Practice and Theory, 2009. **17**(5): p. 817-828.
163. Buzna, L., K. Peters, and D. Helbing, *Modelling the dynamics of disaster spreading in networks.* Physica A: Statistical Mechanics and its Applications, 2006. **363**(1): p. 132-140.
164. Chen, C., D. Neal, and M. Zhou, *Understanding the evolution of a disaster—a Framework for Assessing Crisis in a System Environment (FACSE).* Natural Hazards, 2013. **65**(1): p. 407-422.
165. Cimellaro, G.P., A.M. Reinhorn, and M. Bruneau, *Framework for analytical quantification of disaster resilience.* Engineering Structures, 2010. **32**(11): p. 3639-3649.
166. Faturechi, R. and E. Miller-Hooks, *Measuring the Performance of Transportation Infrastructure Systems in Disasters: A Comprehensive Review.* Journal of Infrastructure Systems, 2015. **21**(1): p. 04014025.
167. Mattsson, L.-G. and E. Jenelius, *Vulnerability and resilience of transport systems – A discussion of recent research.* Transportation Research Part A: Policy and Practice, 2015. **81**: p. 16-34.
168. Little, R.G., *Controlling Cascading Failure: Understanding the Vulnerabilities of Interconnected Infrastructures.* Journal of Urban Technology, 2002. **9**(1): p. 109-123.
169. Britton, N.R., *Developing an Understanding of Disaster.* Journal of Sociology, 1986. **22**(2): p. 254-271.
170. Quarantelli, E., *What should we study? Questions and suggestions for researchers about the concept of disasters.* International Journal of Mass Emergencies and Disasters, 1987. **5**(1): p. 7-32.
171. Mieler, M., et al., *A Framework for Linking Community-Resilience Goals to Specific Performance Targets for the Built Environment.* Earthquake Spectra, 2015. **31**(3): p. 1267-1283.
172. Bruneau, M., et al., *A Framework to Quantitatively Assess and Enhance the Seismic Resilience of Communities.* Earthquake Spectra, 2003. **19**(4): p. 733-752.
173. Chang, S.E. and M. Shinozuka, *Measuring Improvements in the Disaster Resilience of Communities.* Earthquake Spectra, 2004. **20**(3): p. 739-755.

174. Francis, R. and B. Bekera, *A metric and frameworks for resilience analysis of engineered and infrastructure systems.* Reliability Engineering & System Safety, 2014. **121**: p. 90-103.
175. McAllister, T., *Research Needs for Developing a Risk-Informed Methodology for Community Resilience.* Journal of Structural Engineering, 2016. **142**(8): p. C4015008.
176. McAllister, T.P., *Community Resilience: The Role of the Built Environment*, in *Multi-hazard Approaches to Civil Infrastructure Engineering*, P. Gardoni and J.M. LaFave, Editors. 2016, Springer International Publishing. p. 533-548.
177. Newman, M.E.J. and M. Girvan, *Finding and evaluating community structure in networks.* Physical Review E, 2004. **69**(2): p. 026113.
178. Gong, H., et al., *A GPS/GIS method for travel mode detection in New York City.* Computers, Environment and Urban Systems, 2012. **36**(2): p. 131-139.
179. Páez, A., D.M. Scott, and C. Morency, *Measuring accessibility: positive and normative implementations of various accessibility indicators.* Journal of Transport Geography, 2012. **25**(Supplement C): p. 141-153.
180. Grassly, N.C. and C. Fraser, *Mathematical models of infectious disease transmission.* Nat Rev Micro, 2008. **6**(6): p. 477-487.
181. Budak, C., D. Agrawal, and A.E. Abbadi, *Limiting the spread of misinformation in social networks*, in *Proceedings of the 20th international conference on World Wide Web*2011, ACM: Hyderabad, India. p. 665-674.
182. Kempe, D., J. Kleinberg, and É. Tardos, *Maximizing the spread of influence through a social network.* Theory of Computing, 2015. **11**(4): p. 105-147.
183. Newman, M.E.J., *Spread of epidemic disease on networks.* Physical Review E, 2002. **66**(1): p. 016128.
184. Newman, D.E., et al. *Risk Assessment in Complex Interacting Infrastructure Systems*. in *Proceedings of the 38th Annual Hawaii International Conference on System Sciences*. 2005. Big Island, HI.
185. Earn, D.J.D., J. Dushoff, and S.A. Levin, *Ecology and evolution of the flu.* Trends in Ecology & Evolution, 2002. **17**(7): p. 334-340.
186. Kleinberg, J., *Cascading behavior in networks: Algorithmic and economic issues*, in *Algorithmic Game Theory*, N. Nisan, et al., Editors. 2007, Cambridge University Press. p. 613-632.
187. Kempe, D., J. Kleinberg, and É. Tardos, *Maximizing the spread of influence through a social network*, in *Proceedings of the ninth ACM SIGKDD international conference on Knowledge discovery and data mining*2003, ACM: Washington, D.C. p. 137-146.
188. Rodriguez, M.G., J. Leskovec, and A. Krause, *Inferring networks of diffusion and influence*, in *Proceedings of the 16th ACM SIGKDD international conference on Knowledge discovery and data mining*2010, ACM: Washington, DC, USA. p. 1019-1028.
189. Venables, M., *Surviving sandy - smart technologies help the recovery.* Engineering & Technology, 2012. **7**(11): p. 20-21.
190. Comes, T. and B. Van de Walle. *Measuring disaster resilience: The impact of hurricane sandy on critical infrastructure systems*. in *Proceedings of the 11th International ISCRAM Conference*. 2014. University Park, PA.
191. Abur, A. and A.G. Expósito, *Power System State Estimation: Theory and Implementation*2004, New York, NY: CRC Press.
192. Litman, T., *Lessons From Katrina and Rita: What Major Disasters Can Teach*

Transportation Planners. Journal of Transportation Engineering, 2006. **132**(1): p. 11-18.
193. Bono, F. and E. Gutiérrez, *A network-based analysis of the impact of structural damage on urban accessibility following a disaster: the case of the seismically damaged Port Au Prince and Carrefour urban road networks.* Journal of Transport Geography, 2011. **19**(6): p. 1443-1455.
194. Cutter, S.L., et al., *A place-based model for understanding community resilience to natural disasters.* Global Environmental Change, 2008. **18**(4): p. 598-606.
195. Handy, S.L., *Regional Versus Local Accessibility: Neo-Traditional Development and its Implications for Non-work Travel.* Built Environment (1978-), 1992. **18**(4): p. 253-267.
196. Farthing, S., J. Winter, and T. Coombes, *Travel behaviour and local accessibility to services and facilities*, in *The Compact City: A sustainable urban form*, E. Burton, M. Jenks, and K. Williams, Editors. 1996, Spon Press: London, UK. p. 181-189.
197. Colten, C.E., *Vulnerability and Place: Flat Land and Uneven Risk in New Orleans.* American Anthropologist, 2006. **108**(4): p. 731-734.
198. Wright, B. and R.D. Bullard, *Washed away by Hurricane Katrina: Rebuilding a 'new' New Orleans*, in *Growing smarter: Achieving livable communities, environmental justice, and regional equity*, R.D. Bullard, Editor 2007, The MIT Press: Cambridge, MA. p. 198-212.
199. Di Muro, M.A., et al., *Recovery of Interdependent Networks.* Scientific Reports, 2016. **6**: p. 22834.
200. Parshani, R., S.V. Buldyrev, and S. Havlin, *Critical effect of dependency groups on the function of networks.* Proceedings of the National Academy of Sciences, 2011. **108**(3): p. 1007-1010.
201. Myers, S.A., C. Zhu, and J. Leskovec, *Information diffusion and external influence in networks*, in *Proceedings of the 18th ACM SIGKDD international conference on Knowledge discovery and data mining*2012, ACM: Beijing, China. p. 33-41.
202. Barrett, C., et al. *Cascading failures in multiple infrastructures: From transportation to communication network*. in *2010 5th International Conference on Critical Infrastructure (CRIS)*. 2010. Beijing, China.
203. Brummitt, C.D., R.M. D'Souza, and E.A. Leicht, *Suppressing cascades of load in interdependent networks.* Proceedings of the National Academy of Sciences, 2012. **109**(12): p. E680-E689.
204. Sachtjen, M.L., B.A. Carreras, and V.E. Lynch, *Disturbances in a power transmission system.* Physical Review E, 2000. **61**(5): p. 4877-4882.
205. Fronczak, P., A. Fronczak, and J.A. Hołyst, *Self-organized criticality and coevolution of network structure and dynamics.* Physical Review E, 2006. **73**(4): p. 046117.
206. Szabó, G. and G. Fáth, *Evolutionary games on graphs.* Physics Reports, 2007. **446**(4): p. 97-216.
207. Sun, K., Z.-X. Han, and Y.-J. Cao, *Review on models of cascading failure in complex power grid.* Power System Technology, 2005. **13**: p. 1-9.
208. Shi, L., et al., *A review of mechanism of large cascading failure blackouts of modern power system.* Power System Technology, 2010. **34**(3): p. 48-53.
209. Pouget-Abadie, J. and T. Horel. *Inferring Graphs from Cascades: A Sparse Recovery Framework*. in *The 32nd International Conference on Machine Learning*. 2015. Lille, France.
210. Farajtabar, M., et al. *Back to the Past: Source Identification in Diffusion Networks from*

Partially Observed Cascades. in *The 18th International Conference on Artificial Intelligence and Statistics (AISTATS)* 2015. San Diego, CA.
211. Anderson, R.M. and R.M. May, *Infectious diseases of humans: dynamics and control*1991, New York: Oxford University Press.
212. Lloyd, A.L., *The dependence of viral parameter estimates on the assumed viral life cycle: limitations of studies of viral load data.* Proceedings of the Royal Society B: Biological Sciences, 2001. **268**(1469): p. 847-854.
213. Woolhouse, M.E.J., et al., *Heterogeneities in the transmission of infectious agents: Implications for the design of control programs.* Proceedings of the National Academy of Sciences, 1997. **94**(1): p. 338-342.
214. Lloyd, A.L., *Realistic Distributions of Infectious Periods in Epidemic Models: Changing Patterns of Persistence and Dynamics.* Theoretical Population Biology, 2001. **60**(1): p. 59-71.
215. Ferguson, N.M., C.A. Donnelly, and R.M. Anderson, *The Foot-and-Mouth Epidemic in Great Britain: Pattern of Spread and Impact of Interventions.* Science, 2001. **292**(5519): p. 1155-1160.
216. Keeling, M.J. and K.T.D. Eames, *Networks and epidemic models.* Journal of The Royal Society Interface, 2005. **2**(4): p. 295-307.
217. Wallinga, J. and P. Teunis, *Different Epidemic Curves for Severe Acute Respiratory Syndrome Reveal Similar Impacts of Control Measures.* American Journal of Epidemiology, 2004. **160**(6): p. 509-516.
218. Keeling, M.J., *The effects of local spatial structure on epidemiological invasions.* Proceedings of the Royal Society B: Biological Sciences, 1999. **266**(1421): p. 859-867.
219. Hampson, K., et al., *Transmission Dynamics and Prospects for the Elimination of Canine Rabies.* PLOS Biology, 2009. **7**(3): p. e1000053.
220. Myers, S. and J. Leskovec. *On the convexity of latent social network inference*. in *Advances in Neural Information Processing Systems*. 2010. Vancouver, Canada.
221. Du, N., et al. *Learning networks of heterogeneous influence*. in *Advances in Neural Information Processing Systems*. 2012. Lake Tahoe, NV.
222. Du, N., et al. *Uncover topic-sensitive information diffusion networks*. in *Proceedings of the sixteenth international conference on artificial intelligence and statistics*. 2013. Scottsdale, AZ.
223. Wang, L., S. Ermon, and J.E. Hopcroft, *Feature-Enhanced Probabilistic Models for Diffusion Network Inference*, in *Machine Learning and Knowledge Discovery in Databases: European Conference, ECML PKDD 2012, Bristol, UK, September 24-28, 2012. Proceedings, Part II*, P.A. Flach, T. De Bie, and N. Cristianini, Editors. 2012, Springer Berlin Heidelberg: Berlin, Heidelberg. p. 499-514.
224. Chowell, G., H. Nishiura, and L.M.A. Bettencourt, *Comparative estimation of the reproduction number for pandemic influenza from daily case notification data.* Journal of The Royal Society Interface, 2007. **4**(12): p. 155-166.
225. Danon, L., et al., *Networks and the Epidemiology of Infectious Disease.* Interdisciplinary Perspectives on Infectious Diseases, 2011. **2011**: p. 28.
226. Saito, K., R. Nakano, and M. Kimura, *Prediction of Information Diffusion Probabilities for Independent Cascade Model*, in *Knowledge-Based Intelligent Information and Engineering Systems: 12th International Conference, KES 2008, Zagreb, Croatia, September 3-5, 2008, Proceedings, Part III*, I. Lovrek, R.J. Howlett, and L.C. Jain,

Editors. 2008, Springer Berlin Heidelberg: Berlin, Heidelberg. p. 67-75.
227. Gomez-Rodriguez, M., J. Leskovec, and B. Schölkopf. *Modeling information propagation with survival theory*. in *International Conference on Machine Learning*. 2013. Atlanta, GA.
228. Zhou, G., et al., *Association between climate variability and malaria epidemics in the East African highlands.* Proceedings of the National Academy of Sciences of the United States of America, 2004. **101**(8): p. 2375-2380.
229. Koski, T. and J. Noble, *Bayesian networks: an introduction*. Vol. 924. 2011, Chichester, UK: John Wiley & Sons.
230. Zonghua, L. and H. Bambi, *Epidemic spreading in community networks.* EPL (Europhysics Letters), 2005. **72**(2): p. 315-321.
231. Albert, R., I. Albert, and G.L. Nakarado, *Structural vulnerability of the North American power grid.* Physical Review E, 2004. **69**(2): p. 025103.
232. Strogatz, S.H., *Exploring complex networks.* Nature, 2001. **410**(6825): p. 268-276.
233. Sienkiewicz, J. and J.A. Hołyst, *Statistical analysis of 22 public transport networks in Poland.* Physical Review E, 2005. **72**(4): p. 046127.
234. Von Ferber, C., V. Palchykov, and Y. Holovatch, *Scaling in public transport networks.* Condens. Matter Phys., 2005. **8**(225): p. 1-9.
235. von Ferber, C., et al., *Public transport networks: empirical analysis and modeling.* The European Physical Journal B, 2009. **68**(2): p. 261-275.
236. Amaral, L.A.N., et al., *Classes of small-world networks.* Proceedings of the National Academy of Sciences, 2000. **97**(21): p. 11149-11152.
237. Catanzaro, M., M. Boguñá, and R. Pastor-Satorras, *Generation of uncorrelated random scale-free networks.* Physical Review E, 2005. **71**(2): p. 027103.
238. Kryvasheyeu, Y., et al., *Rapid assessment of disaster damage using social media activity.* Science Advances, 2016. **2**(3): p. e1500779.
239. Belik, V., T. Geisel, and D. Brockmann, *Natural Human Mobility Patterns and Spatial Spread of Infectious Diseases.* Physical Review X, 2011. **1**(1): p. 011001.
240. Beigel JH et al., *Avian Influenza A (H5N1) Infection in Humans.* New England Journal of Medicine, 2005. **353**(13): p. 1374-1385.
241. Germann, T.C., et al., *Mitigation strategies for pandemic influenza in the United States.* Proceedings of the National Academy of Sciences, 2006. **103**(15): p. 5935-5940.
242. Rizzo, A., M. Frasca, and M. Porfiri, *Effect of individual behavior on epidemic spreading in activity-driven networks.* Physical Review E, 2014. **90**(4): p. 042801.
243. Clinton, W.J., *William Jefferson Clinton*, T.W. House, Editor 1996, Office of the Federal Register: Washington, D.C. p. 37347-37350.
244. Abramson, D.M. and I. Redlener, *Hurricane Sandy: Lessons Learned, Again.* Disaster Medicine and Public Health Preparedness, 2012. **6**(4): p. 328-329.
245. Gibbs, L. and C. Holloway, *Hurricane sandy after action: report and recommendations to Mayor Michael R Bloomberg*, in *Bloomberg. The City of New York, New York, NY*2013, City of New York: New York, NY.
246. NHC, *NHC Aircraft Reconnaissance*, N.H. Center, Editor 2012: Miami, FL.
247. FEMA Modeling Task Force, *FEMA MOTF Hurricane Sandy Impact Analysis*, F.E.M. Agency, Editor 2012: Washington, D.C.
248. NYC Department of City Planning, *Decennial Census - Census 2010*, 2010: New York, NY.

249. Gany, F., R. Rau-Murthy, and I. Mujawar, *Increasing influenza vaccination in New York City taxi drivers: A community driven approach.* Vaccine, 2015. **33**(22): p. 2521-2523.
250. Centers for Disease Control and Prevention, *Seasonal Influenza Vaccine Effectiveness, 2005-2017*, 2017: Atlanta, GA.
251. United States Census Bureau, *TIGER/Line® with Selected Demographic and Economic Data*, U.S.C. Bureau, Editor 2016: Suitland, MD.
252. NYC Department of City Planning, *Political and Administrative Districts - Download and Metadata*, N.D.o.C. Planning, Editor 2018: New York, NY.
253. United States Census Bureau, *2009-2013 5-Year American Community Survey Commuting Flows*, U.S.C. Bureau, Editor 2017: Suitland, MD.
254. Simini, F., et al., *A universal model for mobility and migration patterns.* Nature, 2012. **484**(7392): p. 96-100.
255. Bettencourt, L. and G. West, *A unified theory of urban living.* Nature, 2010. **467**: p. 912.
256. Scott, D.M., et al., *Network Robustness Index: A new method for identifying critical links and evaluating the performance of transportation networks.* Journal of Transport Geography, 2006. **14**(3): p. 215-227.
257. Bialek, J., et al., *Benchmarking and Validation of Cascading Failure Analysis Tools.* IEEE Transactions on Power Systems, 2016. **31**(6): p. 4887-4900.
258. Transportation Research Board, *Highway Capacity Manual (HCM2010)*, 2010, National Research Council: Washington, DC.
259. Wardrop, J.G., *Some Theoretical Aspects of Road Traffic Research.* Proceedings of the Institution of Civil Engineers, 1952. **1**(3): p. 325-362.
260. Marguerite, F. and W. Philip, *An algorithm for quadratic programming.* Naval Research Logistics Quarterly, 1956. **3**(1-2): p. 95-110.
261. The Bureau of Public Roads, *Traffic Assignment Manual*, U.P.D. U.S. Department of Commerce, Editor 1964: Washington, D.C.
262. Guan, X. and C. Chen, *General methodology for inferring failure-spreading dynamics in networks.* Proceedings of the National Academy of Sciences, 2018.
263. Guan, X. and C. Chen, *Using social media data to understand and assess disasters.* Natural Hazards, 2014. **74**(2): p. 837-850.
264. Akbarzadeh, M., S. Memarmontazerin, and S. Soleimani, *Where to look for power Laws in urban road networks?* Applied Network Science, 2018. **3**(1): p. 4.
265. Tian, L. *Lecture Notes on Survival Analysis: Likelihood Construction, Inference for Parametric Survival Distributions*. 2017 [cited 2018 June 27]; Available from: https://web.stanford.edu/~lutian/coursepdf/unit2.pdf.